ERDA CONTRACT NO. E(04-3)-1109

SOLAR PILOT PLANT

Phase I

CONCEPTUAL DESIGN REPORT

Thermal Storage Subsystem Research Experiment

CDRL Item No. 5

17 December 1975

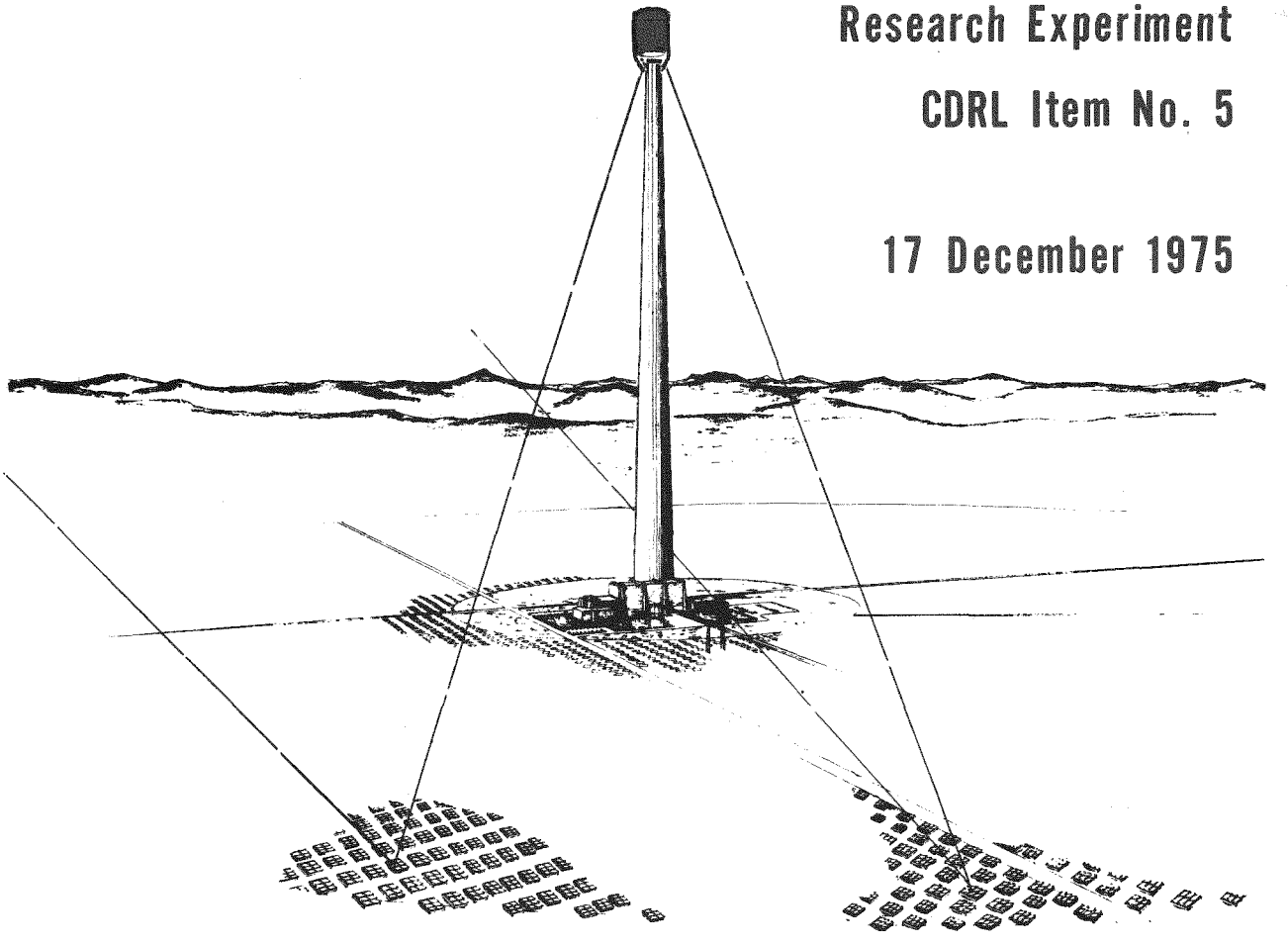

HONEYWELL INC.

BLACK & VEATCH

F3419-DR-104

Honeywell

ERDA Contract No. E(04-3)-1109

17 December 1975

SOLAR PILOT PLANT
PHASE I

CONCEPTUAL DESIGN REPORT

Thermal Storage Subsystem Research Experiment

CDRL Item No. 5

Systems & Research Center
2600 RIDGWAY PARKWAY
MINNEAPOLIS, MINNESOTA 55413

40284

Printed in U.S.A.

F3419-DR-104

AGENDA

SOLAR POWER PLANT PROGRAM

CONCEPTUAL DESIGN REVIEW -
THERMAL STORAGE SUBSYSTEM SRE

17 December 1975

Minneapolis, Minnesota

Wednesday, 17 December 1975		Honeywell SRC G&APD Executive Conference Room
1:00 PM	CONCEPTUAL DESIGN REVIEW - THERMAL STORAGE SRE	
	• Introduction/Summary	D. Lefrois
	• Experiment Conceptual Design	D. Lefrois
	• Experiment Conceptual Design Analysis	D. Lefrois
	• Test Conceptual Design	D. Lefrois
	• Plans and Schedules	D. Lefrois
	• Engineering Model Program	A. Severson/R. Beale
3:30 PM	ERDA COMMENTS/APPROVAL	

FOREWORD

This is the first submittal of the Solar Pilot Plant Thermal Storage Conceptual Design Report per CDRL No. 5 under ERDA Contract No. E(04-3)1009. This design report was prepared in written form and documents the oral presentation delivered concurrently. This report is submitted for review and approval by ERDA.

The conceptual designs delineated in this report were configured around parameters contained in the ERDA approval version of the Preliminary Design Baseline Report (CDRL No. 1) originally submitted 30 September 1975.

Included as part of the foreword is an outline summary of the oral presentation.

CONTENTS

		Page
SECTION I	INTRODUCTION AND SUMMARY	1-1
	Overview	1-2
	Pilot Plant Baseline Design	1-4
	Thermal Storage Subsystem Research Experiment	1-6
	Pilot Plant and SRE Similarity	1-8
	Experiment Configuration and Design	1-12
SECTION II	EXPERIMENT CONCEPTUAL DESIGN	2-1
	Tank and Foundation: General Description	2-2
	Tank and Foundation: Tank Design Pressure	2-6
	Tank and Foundation: Tank Structure Design	2-8
	Insulation and Heat Loss	2-12
	Vaporizer	2-14
	Mechanisms	2-18
	Condenser	2-20
	Phase Change Material	2-24
	Phase Change Material: Thermal Cycling	2-26
	Phase Change Material: Nucleation and Crystallization	2-28
	Steam Drum Separator	2-30
	Recirculation Control	2-34
	Steam Drum Level Control	2-37
	Steam Trap	2-38
	Steam Charge Control	2-40
	Temperature Measurements	2-42
	Thermal Capacity	2-44
	Heat Loss	2-46
	Salt Buildup on Tank Walls	2-47
	Safety and Equipment Design	2-48
SECTION III	EXPERIMENTAL CONCEPTUAL DESIGN ANALYSIS	3-1
	Design Scaling - Vaporizer	3-2
	Design Scaling - Thermal Storage Condenser	3-10
	Tank Design Tradeoff	3-16
SECTION IV	TEST CONCEPTUAL DESIGN	4-1
	Test Objectives	4-2
	Test Parameters	4-4
	Schedule of Sources/Sinks	4-8
	Relative Locations: Test Areas, Sources, Sinks	4-10
	Plan of Test Installation: Thermal Storage	4-12

	Conceptual Configuration	4-14
	SRE Control Panel Configuration	4-16
	Set Point/Indicating Controller Description	4-20
	Requirements - Operational	4-22
	Requirements - Size	4-24
	Concept Configuration	4-26
	Test Control Rationale	4-28
	Thermal Storage Control (Discharge Mode)	4-30
	Thermal Storage Control (Charge Mode)	4-32
	Procedures	4-34
	Support Equipment	4-36
	Test Schedule	4-38
SECTION V	PLANS AND SCHEDULES	5-1
	Long-Lead-Time Items: Thermal Storage (SRE) and Test Item Installation	5-2
	Schedule	5-4
	Supplier Information	5-6
APPENDIX A	THERMAL ENERGY STORAGE (TES) SUBSYSTEMS RESEARCH EXPERIMENT (SRE) DESIGN SPECIFICATION	
APPENDIX B	TEST SPECIFICATION, THERMAL ENERGY STORAGE (TES), SUBSYSTEMS RESEARCH EXPERIMENT (SRE)	
APPENDIX C	ENGINEERING MODEL PROGRAM	
APPENDIX D	VAPORIZER DESIGN/HEAT TRANSFER ANALYSIS	
APPENDIX E	SRE CONDENSER DETAIL DESIGN CALCULATIONS	

SECTION I
INTRODUCTION

Introduction

OVERVIEW

This report is a summary of the effort to establish the conceptual design of the Thermal Storage Subsystem Research Experiment (TS/SRE).

The TS/SRE consists of a Thermal Storage Unit containing a salt phase change material, Steam Generator System, Steam Condensing System, Instrumentation with associated controls, valves, piping and support equipment.

The design basis, scaling rationale and overall experiment configuration is summarized in Section I.

The conceptual design of each significant element of the test item is described in Section II.

Experiment design tradeoff scaling rationale is analyzed and discussed in some detail in Section III.

Section IV summarizes the conceptual design of the tests for the experiment from objectives through test data analysis and utilization.

An overview of the detail design and test phase is presented in Section V.

The appendices contain the preliminary design and test specifications, summarize the Engineering Model Test Program results used in support of the concept design, and record the significant detail design calculations.

This page intentionally left blank

Summary

PILOT PLANT BASELINE DESIGN

The purpose of the Thermal Storage Conceptual Design activity was to synthesize a design concept for the subsystem research experiment that will, when tested, provide the necessary data to prepare preliminary design specifications. The Pilot Plant Baseline Design was used as the basis for establishing requirements for the subsystem research experiment.

The basic features of the Pilot Plant Thermal Storage Subsystem include:

Design	Performance
• 255 MWH(t) capacity	• Deliver 7 MW(e) net - 6 hours
• Salt phase change materials (including superheater)	• Provide 50°F superheat
• Battery of 12 unit cells	• 575 psig/534°F discharge cycle
• Below ground storage	• Handle 49 MW(t) - 4 hours
• Self-regulating control system	• 1450 psig/950°F charge cycle
• Modular heat exchangers	• Heat loss < 0.1%/hr
• One out main storage capability	
• 40-year storage life	

The basic main storage concept proposed at the preliminary design baseline review and presented herein for the basis for the start of detail design consists of the following:

- Thermal Energy Storage Material -- Mixture of $NaNO_3$, Na_2SO_4 and NaCl phase change material.

- Thermal Storage Charging -- Transfer of latent heat of condensing steam inside circular tubes to the salts outside the tubes as latent heat of fusion. Use of convection and thermosyphon effects for bulk heat transfer.

- Thermal Storage Discharging -- Transfer of heat from the freezing salts surrounding circular tubes to water forced-circulated through these tubes. The water, receiving heat of vaporization generates steam vapor and is supplied to a steam drum separator where saturated steam is withdrawn. The crystallized salt is removed from the outside of the tubes by mechanical means.

  The basic objective of conducting the Thermal Storage Subsystem Research Experiment Program is to confirm and/or extend the Pilot Plant Preliminary Design mechanization to permit preliminary design specifications to be prepared.

  With this objective in mind, and based on the foregoing concept design, performance and operating requirements on SRE Program are outlined on the succeeding pages.

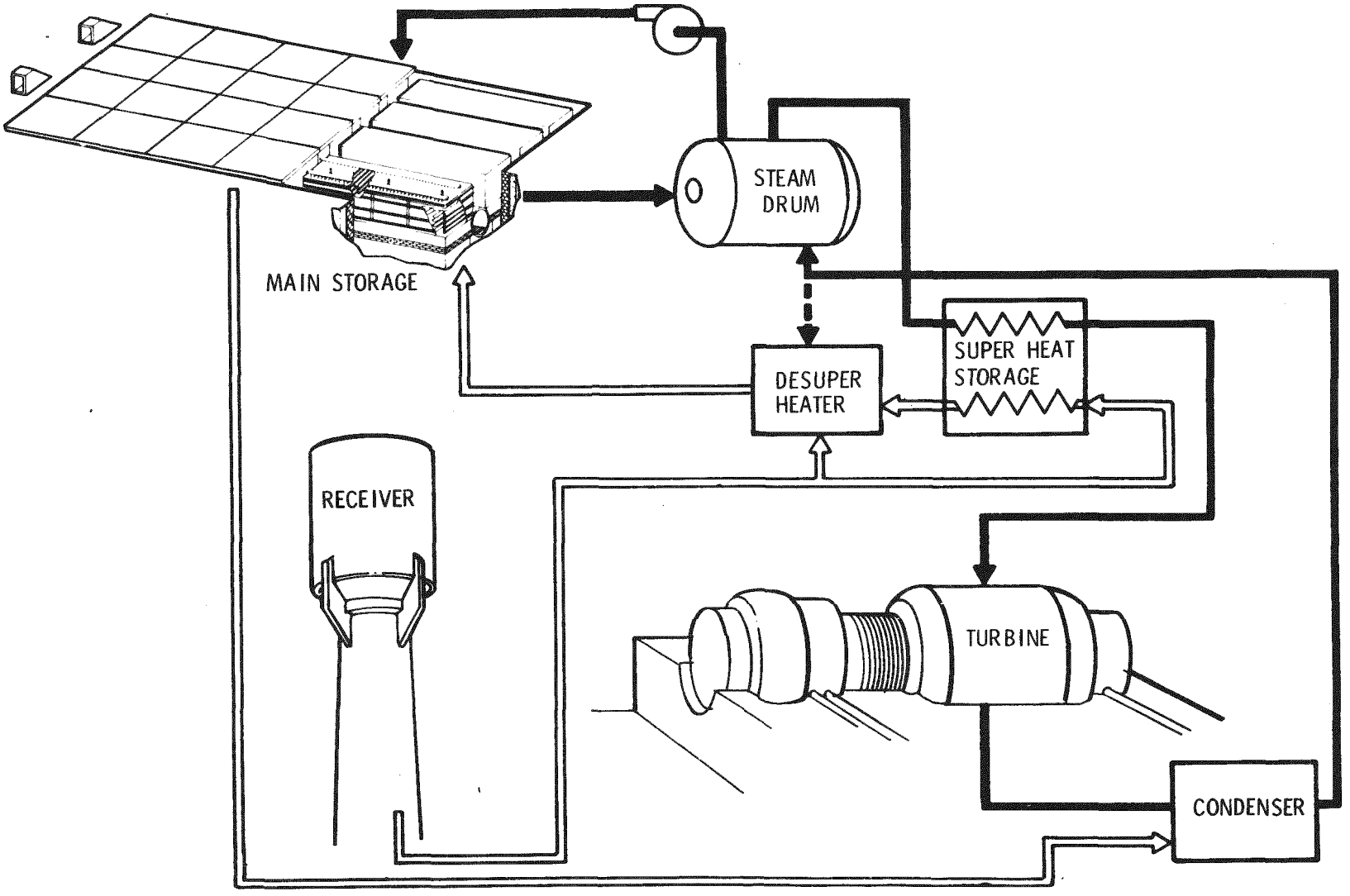

Figure 1-1. Thermal Storage Concept

Summary

THERMAL STORAGE SUBSYSTEM RESEARCH EXPERIMENT

The Thermal Storage Subsystem Research Experiment (TS/SRE) is designed to give maximum information for evaluating the design, performance and operating parameters of the proposed pilot plant configuration.

The requirements for the research experiment dictate that a scale model of the pilot plant main storage unit cell be designed, constructed and tested. The model will contain the same salt mixture as the pilot plant and will exchange heat with scale models of the vaporizer and condenser heat transfer surfaces. The identical control system will be implemented on the model and will operate on the same basic charge and discharge cycle conditions. The performance of the SRE model can be evaluated and the operating characteristics defined and extrapolated to the pilot plant design. The operating experience gained during the testing phases will permit a realistic assessment of equipment reliability and maintenance. This will enable expected subsystem availabilities to be determined as a function of the key plant operating parameters.

PILOT PLANT CHARACTERISTICS	CHARACTERISTICS REQUIRED IN SRE PROGRAM
Design	
• 240 MWH(t) main storage capacity	• 1/4 scale model of quarter unit cell
• Salt PCM	• Same salt PCM
• Battery of 12 unit cells	• 1/4 scale model of quarter unit cell
• 15 MWH(t) superheater capacity	• Based on test results and analysis
• Self-regulating control system	• Same control system
• Below ground storage	• Above ground with insulation/variable heat loss measurements and analysis
• Modular heat exchangers	• 1/4 scale model of quarter unit cell
Performance	
• Deliver 7 MW(e) net or 30 MW(t) net -- 6 hours	• 1/4 scale model of quarter unit cell -- 270 KW(t) - 4.6 hours
• Provide 50°F superheat	• Based on test results and analysis
• 575 psig/534°F discharge cycle	• Same discharge cycle
• Handle 49 MW(t) -- 4 hours	• 1/4 scale model of quarter unit cell -- 282 KW(t) - 4.4 hours
• 1450 psig/950°F charge cycle	• Same charge cycle
• Heat loss 0.1%/hr	• Heat loss rate-variable
Operating	
• Parallel superheat units	• Based on test results and analysis
• One out main storage capability	• Storage fill/drain capability demonstrated
• Storage life	• Salt and material compatibility assessments

Summary

PILOT PLANT AND SRE SIMILARITY

The Thermal Storage SRE should be a scale model of the Pilot Plant Unit Cell to derive a maximum of design and performance information.

Geometric and dynamic similarity must be considered to achieve proper scaling. Geometric similarity is a necessary condition for modeling thermal and fluid dynamic phenomena. The basic elements under consideration for scaling include the storage tank, vaporizer and condenser heat exchanger assemblies. The phase change material, steam and water remain the same.

The Pilot Plant Unit Cell consists of four quarter-capacity cells in parallel. Consquently, a quarter-capacity cell of the Pilot Plant can be considered the "full scale" configuration. The SRE model is a 1/4 capacity scale of this quarter unit cell. The 1/4 scale model magnitude is determined by available resources.

For geometric similarity, the characteristic linear dimensions of the pilot plant and SRE are in proportionate ratios as their respective volumes. This may be expressed as:

$$\frac{Lc/SRE}{Lc/pp} = \left[\left(\frac{\text{SRE Thermal Capacity}}{\text{1/4 Cell PP Thermal Capacity}}\right)\left(\frac{\text{PP Energy Density of Salt}}{\text{SRE Energy Density}}\right)\right]^{1/3}$$

where

Lc = characteristic length

For the same salt the geometric scale factor is:

$$\frac{Lc/SRE}{LC/pp} = 63\%$$

This requires:

- 37% reduction in quarter unit cell size
- 37% reduction in heat exchanger size and lengths
- 37% decrease in tolerances

Dynamic similarity parameters were selected as a result of analysis of the thermal and fluid phenomena taking place. These phenomena include such things as high pressure water boiling inside horizontal tubes; salt crystallizing, growing and being removed from the outside of these tubes; salt particles settling to the bottom of the tank; high-pressure steam condensing inside tubes; salt crystals melting outside these tubes, rising and exchanging heat with the surroundings. The physical laws describing these phenomena were written (Ref. Section III) to gain insight into determining the relative importance of scaled parameters or parameter groupings.

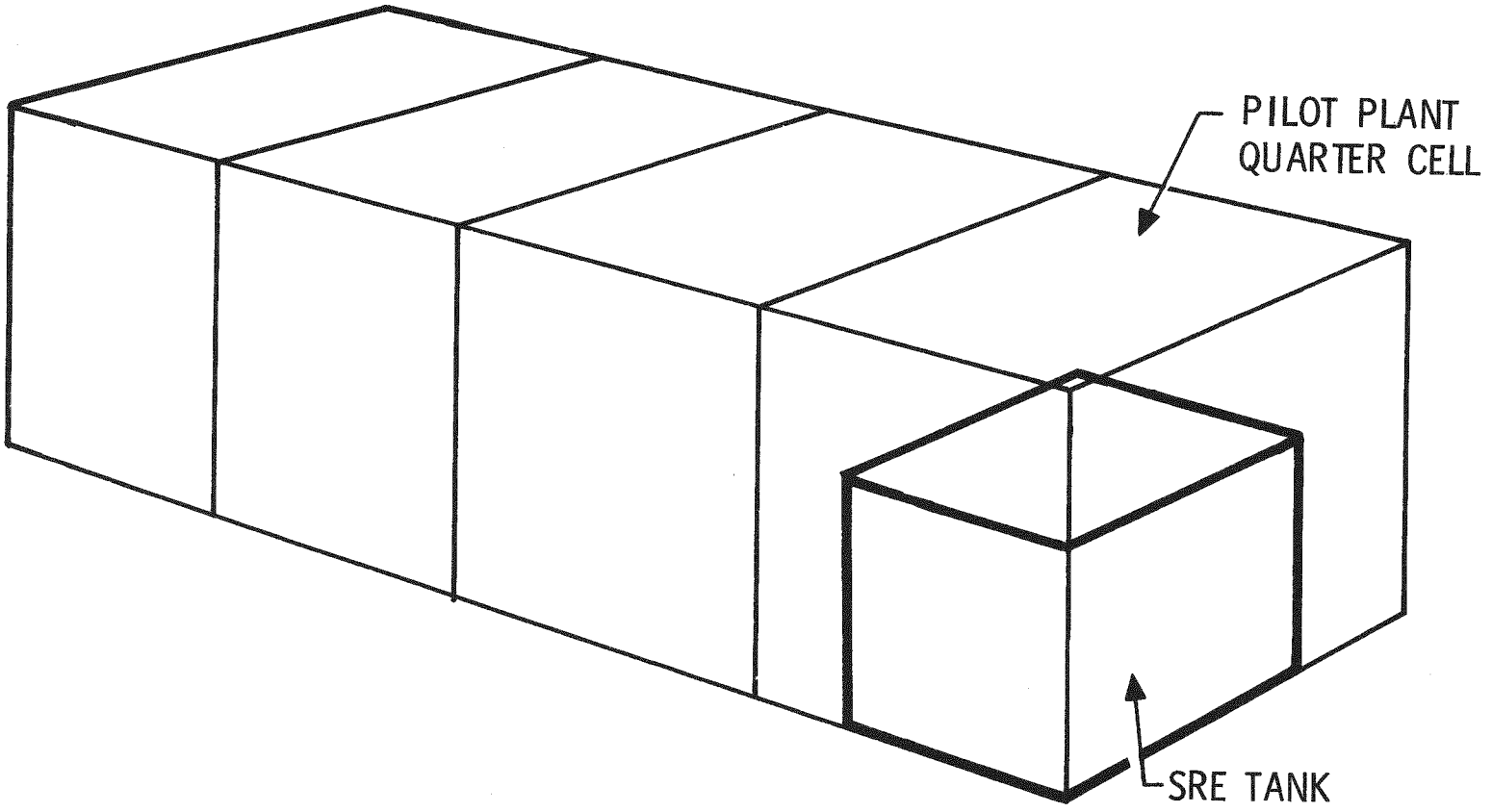

Figure 1-2. Storage SRE Tank Scaling

Preliminary results, when placed in context with the project resources and current test plans, indicate that:

1) Geometric scaling to 1/4 capacity is reasonable assuming that scaling must be done.

2) Dynamic similarity should consider both the macro-thermal phenomena in the tank at large as well as the micro-thermal phenomena occurring at the salt boundaries on the outside of the vaporizer and condenser tubes and on the tank walls.

3) Scaling analysis is an iterative process and is required in the early part of detail design to ensure that the scaled up version of the Pilot Plant Unit Cell will accommodate the real world constraints determined by detail design of the SRE.

The intended scaling and dynamic similarity conditions for testing the SRE consist of the following:

1) Provide geometric similarity on all significant characteristic dimensions

2) Test at both constant heat flux and ΔT for vaporizer performance

3) Test at both constant heat flux and ΔT for condenser performance

4) Test at constant heat flux for tank thermal performance

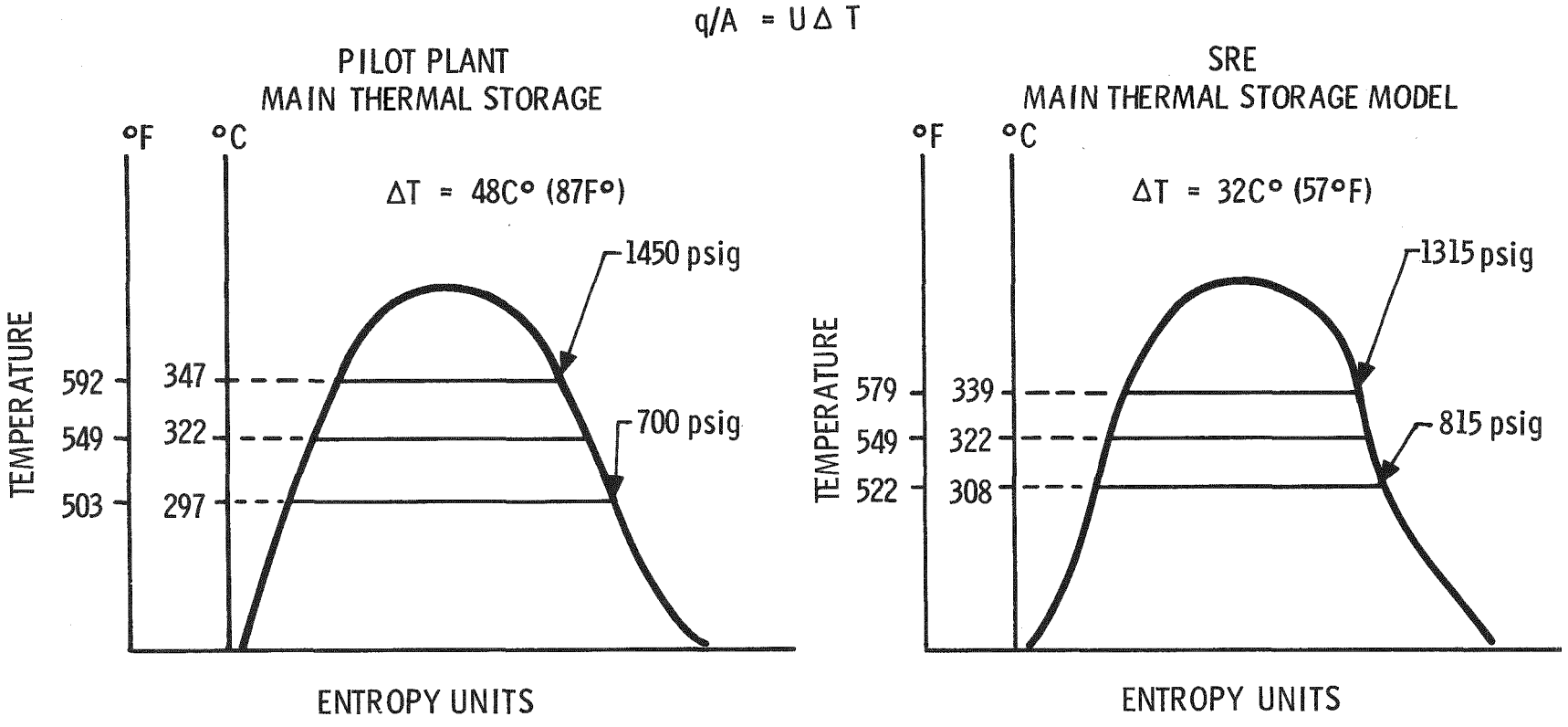

Figure 1-3. Thermodynamic Cycle

Summary

EXPERIMENT CONFIGURATION AND DESIGN

The SRE consists of a Thermal Storage Unit, a Steam Generating System, Steam Condensing System and Instrumentation.

The Thermal Storage Unit is an insulated rectangular tank containing the salt phase change material. The tank supports the vaporizer and condenser modules, as well as the mechanisms and instrumentation.

The Steam Generating System consists of the vaporizer, steam drum separator, pump, controls, valves and piping. Feedwater is pumped through the vaporizer and saturated steam is withdrawn from the steam drum. The steam throttle valve places the same type of demand on the system as the turbine throttle valve.

The Steam Condensing System consists of a condenser module, desuperheater, steam trap, with control valves and piping. The desuperheater provides saturated steam to the condenser module and the condensed steam is discharged from the condensate receiver. The steam throttle valve loads the system in the same manner as the Receiver Steam Generator supply valve.

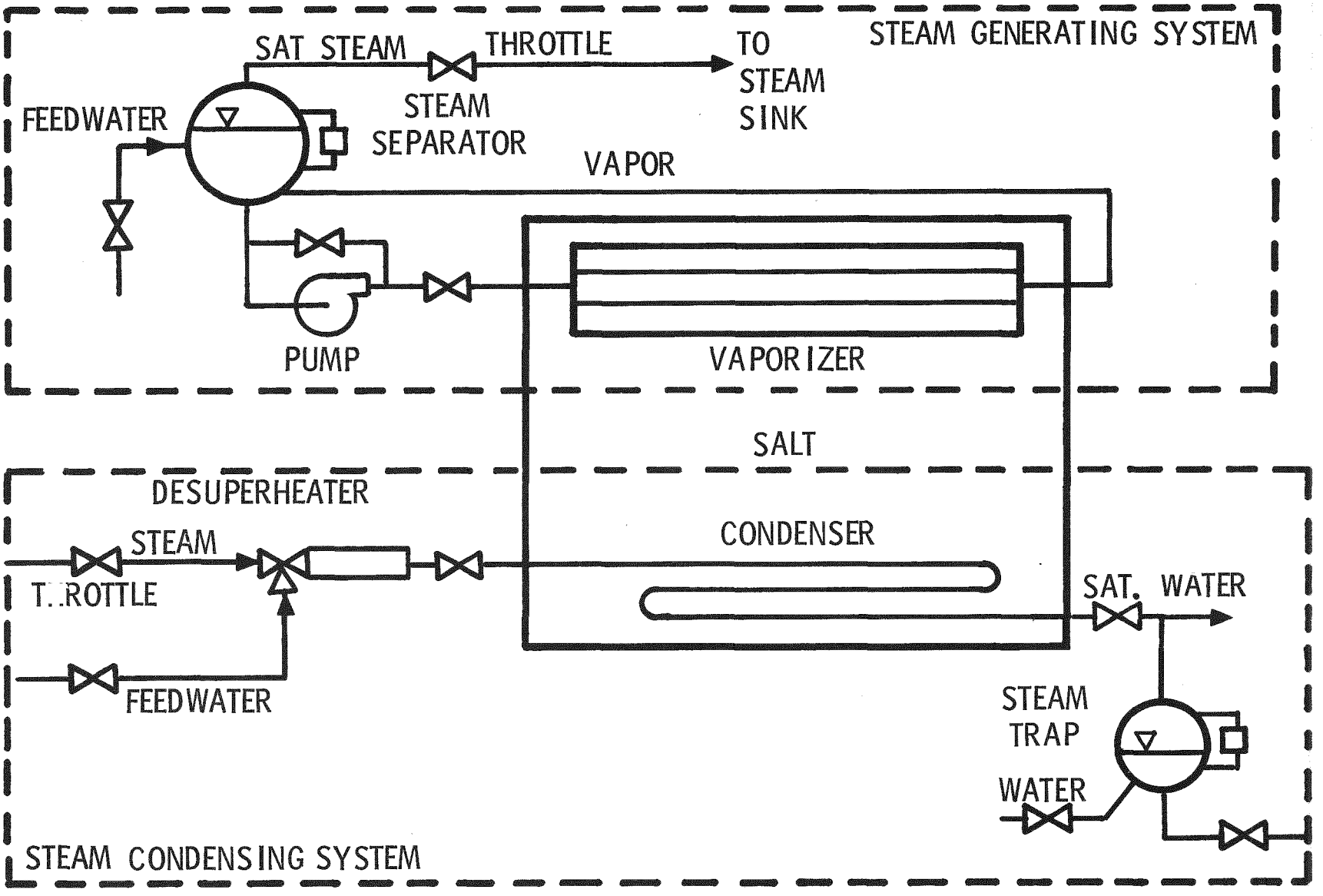

Figure 1-4. SRE Schematic

Table 1-1. SRE Design Summary

	SI Units	English Engineering
Tank Size - Nominal	2.4 m x 2.4 m x 3 m	8 ft x 8 ft x 10 ft
Tank Weight	5,440 kgs	12,000 lb
Boiler Weight	3,630 kgs	8,000 lb
Condenser Weight	2,730 kgs	6,000 lb
Salt Weight	23,200 kgs	51,000 lb
Tank Weight	35,000 kgs	77,000 lb
Thermal Storage Capacity	1.25 MWH(t)	4.3×10^6 Btu
Charge Rate	282 KW(t)	9.6×10^5 Btu/hr
Charge Time	4.4 hr	4.4 hr
Discharge Rate	270 KW(t)	9.2×10^5 Btu/hr
Discharge Time	4.6 hr	4.6 hr
Condenser		
Charge Steam Rate	754 kg/hr	1664 lb/hr
Charge Steam Conditions	9500 KPa/307°C	1375 psi/585°F
Condensate Loading, W/L	3.05 kg/hr-m	2.05 lb/hr-ft
Pipe Size	1.91 cm O.D./1.47 cm I.D.	3/4 in. O.D./14 gauge
Configuration	4-28-leg serpentines with 1.18 fins/cm	4-28 leg serpentines with 3 fins/inch
Total Pipe Length	244 m	800 ft
Vaporizer		
Discharge Steam Rate	590 kg/hr	1300 lb/hr
Discharge Steam Conditions	5722 KPa/272°C	830 psi/522°F
Recirculation Rate	2/1	2/1
Pipe Size	1.59 cm O.D./1.4 cm I.D.	5/8 in./15 gauge
Configuration	1-44 leg serpentine with scrapers on	1-44 leg serpentine with scrapers on
Total Pipe Length	94 m	308 ft

SECTION II
EXPERIMENT CONCEPTUAL DESIGN

Experiment Conceptual Design

Thermal Storage Unit

TANK AND FOUNDATION: GENERAL DESCRIPTION

The SRE Thermal Storage Tank will be insulated reinforced rectangular steel container, mounted on an insulating base and closed by a sealed removable cover. A steam vaporizer and steam condenser will be mounted inside the tank. The condenser supplies heat to melt salt and the vaporizer removes the heat from the salt to generate vapor.

A rectangular tank is readily manufactured and presents a simple shape for design, insulation, handling and transport. A rectangular shape appears to be a logical choice from a standpoint of both vaporizer and condenser design.

The thermo-syphon and convection currents appear the most straight-forward in a rectangular pattern and the deposit of solidified salt from the vaporizer on the condenser would be more uniform. Since a number of tanks are planned for the pilot plant, a good packing array from rectangular tanks may be achieved.

The tank measures 2.32 M high x 2.32 M wide x 2.90 M long (7.6 ft high x 7.6 ft wide x 9.5 ft long) which will hold sufficient molten salt 11.85 m^3 (418.4 ft^3) or 22,930 kg (50550 lb) to provide 1.25 MWH(t) of stored latent heat of fusion. An ullage space of 0.5 m (1.7 ft) is provided for above the liquid level in which the mechanical vaporizer tube scrapers can be suspended.

The tank will be equipped with external "I" beam reinforcements, a sealed cover with four sealable ports for sectional vaporizer design and a bottom-mounted condenser. The tank will be mounted on double grid of 18 cm (7 in.) beams to provide both support and thermal isolation from the lower concrete base. Insulation between five upper cross beams and three longitudinal lower beams will serve to reduce bottom heat loss. The upper I-beams will be welded to the tank to form a rigid base easily able to withstand static, dynamic and seismic loads. The lower I-beams will be fastened to the concrete base to provide firm footing. Anchoring will be arranged to permit the base frame to expand and contract without stress build-up. The base unit loading will be less than 422 gms/cm^6 (6 lbs/$in.^2$). The primary foundation consists of a large 3.35 M x 2.74 M (11 ft x 9 ft) concrete pad.

The pad protrudes 59 cm (1.83 ft above grade). A recessed area around the foundation is adequate in volume to contain the entire molten salt volume in the event of serious leakage.

Mild steel-type A285 GrB, is selected for material since the salts do not appear to attack it. It is also an easily weldable, readily available standard material sold in a wide variety of shapes. For the SRE, use of mild steel will permit substantiating the use of this material on the full-scale Pilot Plant. The application of block insulation and also the thermal heat loss studies will be facilitated by this tank design.

The upper reinforcement will also serve as a seal groove. A cover designed to carry the vaporizer elements will be supported on this I-beam and the vertical edge of this cover will be sealed from leaking by the use of Fe_2O_3 powder. This material is used for this type of service in heat treating furnaces.

Tank Cover Seals

A low-pressure supply of nitrogen will be used to exclude atmospheric air from the bath above the salt storage. A simple trough filled with iron oxide powder around the upper edge of the tank will serve to act as an easily broken seal and may also be used to hydrostatically test the tank after manufacture. If the cover is designed with hold-down bolts which will withstand the designed over-pressure for testing, the sealing of the trough with a low melting point material such as wax or low melting point metals will permit hydrostatic testing. After testing, the sealant may be readily removed by heating. The system described avoids accurate machined joints for the sealing operation.

Tank Drainage

A controlled drain line is planned for routine or emergency drainage. A heatable quick-opening valve on an adequately sized drain line is planned to permit controlled drainage of the tank. This feature will be installed on one end of the tank.

Tank Corrosion

Corrosion of the mild steel is expected to be minimal. At the temperature levels expected, corrosion rates of less than 0.2 nm (0.8 mil) per year under operating conditions will assure adequate system life. The use of the NaCl, $NaNO_3$, and Na_2SO_4 salts will limit corrosive attack since the sulfate acts as a corrosion inhibitor. External surfaces not protected by insulation will require special paints or other coatings. The high external temperatures of the tank will eliminate thenormal operating problems encountered by mild steel in rusting due to condensation.

Tank Temperatures

After charging, the thermal storage system will be exposed to only a limited range of temperatures. The salt eutectic temperature of 288°C (550°F) will be a strong leveling function. Salt temperatures of approximately 310°C (590°F) may be reached only on prolonged charging since most of the energy will be absorbed in the latent heat of fusion of the material. Higher temperatures due to sensible heat charging can only approach the steam charging temperature 316°C (600°F). Minimum temperatures will be represented by the solidified eutectic as exposed to external heat losses. The walls and bottom of the

tank will be cooled by heat loss to the outside through the insulation. The temperature of the walls will be at some level below the solidification temperature 288°C (550°F), depending on tank charging state and heat loss status.

Generally, the tank walls and bottom will be restricted to temperatures below the eutectic point.

Storage Tank Heat Exchangers

The lower part of the tank will be equipped with an extended surface heat exchanger consisting of four serpentine flow paths and the upper section will contain the multiple tube single-pass vaporizer.

The operation of the thermal cycle of the storage systems utilizes the charging steam to melt the salts surrounding the condenser located on the tank bottom. The high-temperature steam melts the salt immediately around the heat exchanger. If the salts are completely solid, a liquid relief path to the upper surface of the salt will be necessary to avoid severe pressures from building up since the frozen salt is denser than the liquid. The steam supply lines will be brought into the tank down through the salt to provide such a path. In addition, a special heating coil, installed just above the condenser, will provide an emergency source of heat and additional liquid paths to the salt surface.

With the salts completely molten, the volume increase will bring the salt level well above the vaporizer tube structure.

The vaporizer will consist of four clusters of 11 tubes each. The tubes will be connected in series to form a single serpentine path. To maintain heat transfer rates during generation of steam, a scraper system driven by external motors on each cluster will be provided. The scrapers surrounding the tubes will be driven through a chain drive system. Each cluster will have its own motor drive independently mounted on the tank cover. This will permit removal of sections of the vaporizer for servicing and experimental work.

The entire structure will be insulated with a high-temperature block type of insulation. A sheet metal casing will be provided around the tank external to the insulation. The cover will be insulated with blocks which can be removed in sections for testing, servicing or observation.

The cover will be arranged with proper seals for each boiler section. At the center of the cover, access parts for observation, sampling, etc., will be provided. The center section of the cover will also be arranged to provide space for the necessary condenser plumbing.

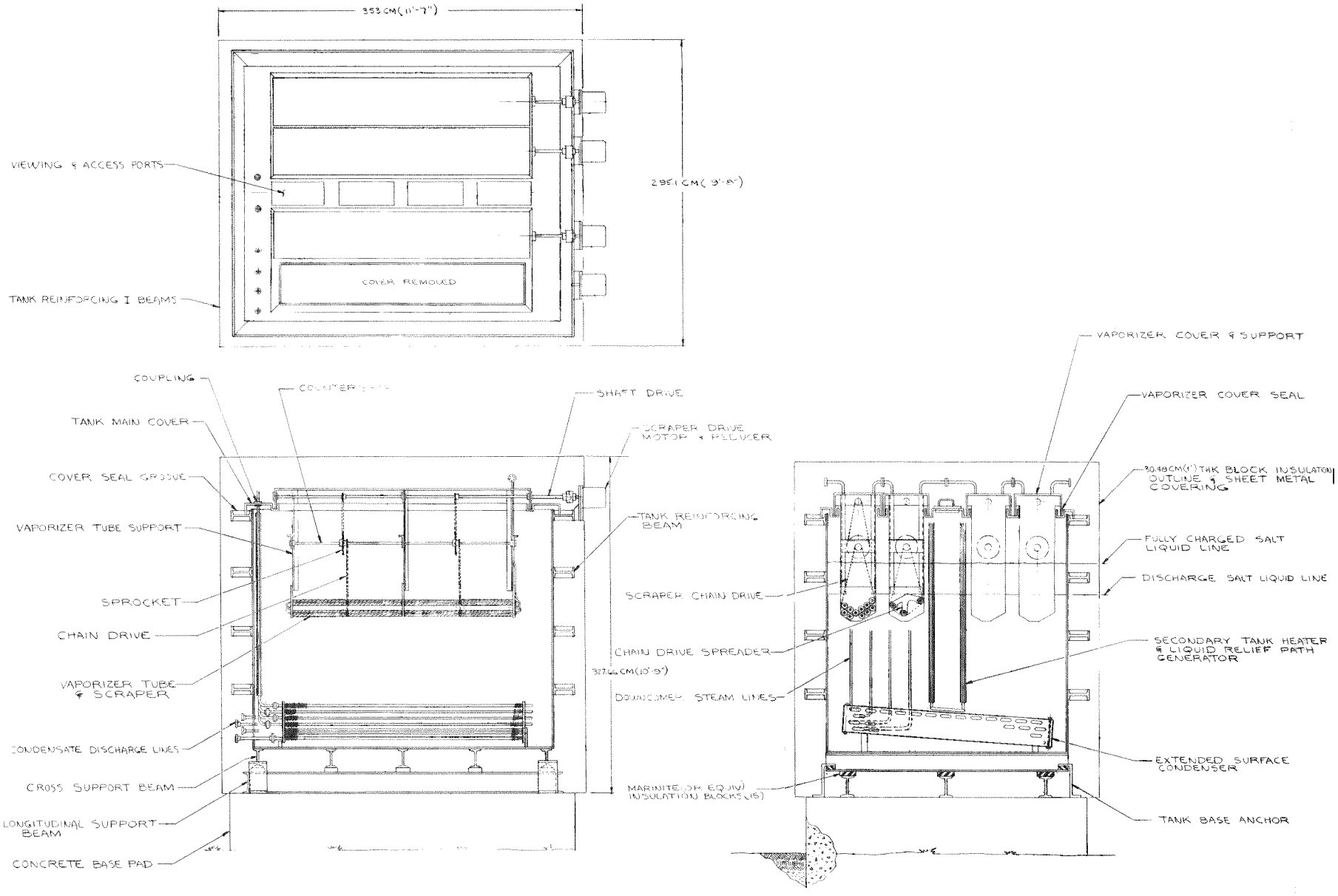

Figure 2-1. Thermal Storage SRE Tank

TANK AND FOUNDATION: TANK DESIGN PRESSURE

The maximum tank pressure is determined by the hydrostatic test requirements.

The tank will be designed to meet the ASME hydrostatic test requirements. The hydrostatic test pressure (HTP) is given by the equation:

$$HTP = 1.5\,(1.1 \times W.P.) \times \frac{(T_{ambient})}{(T_{operating})}$$

where:

W.P. = the working hydrostatic pressure

1.1 = a design working allowance

$(T_{ambient})$ = working stress of steel at test conditions

$(T_{operating})$ = working stress of steel at the actual operating conditions

Figure 2-2 is a plot of the working design and the hydrostatic test pressures.

The hydrostatic test will be performed by filling the tank and a special stand pipe with water and pressurizing the unit. This gives a higher pressure distribution at the tank top than will be observed with the tank filled with molten salt. Consequently, the reinforcing of the tank was designed with uniform spacing of stiffeners to meet the hydrostatic test rather than to meet the load requirements imposed by the molten salt.

The SRE storage tank will be designed in accordance with ASME Sections I and VIII. Construction and certification will be in accordance with API 6-20 and traceability will be maintained on all pertinent materials via mill stamps.

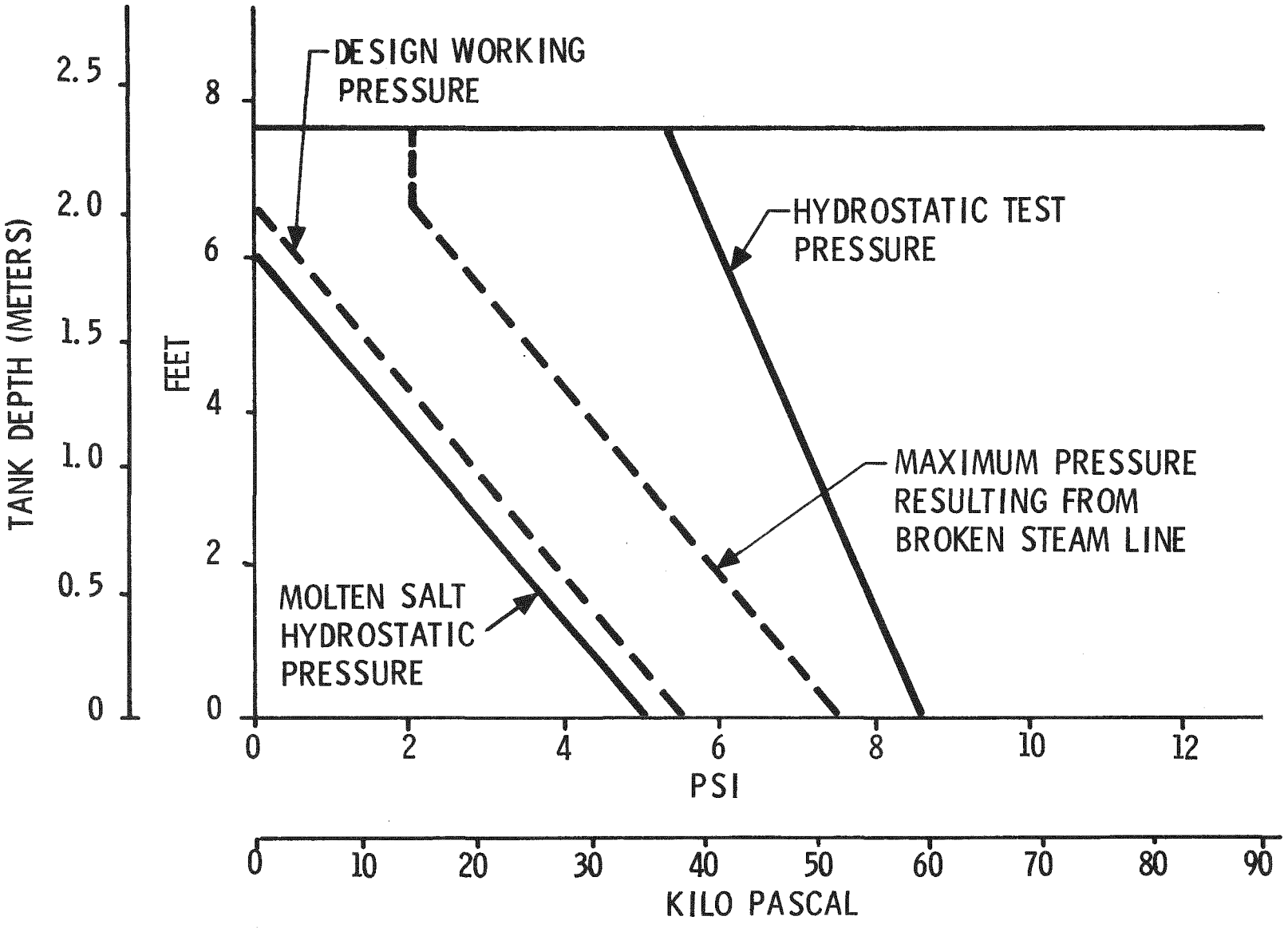

Figure 2-2. Thermal Storage Tank Design Pressure

Experiment Conceptual Design

Thermal Storage Unit

TANK AND FOUNDATION: TANK STRUCTURE DESIGN

The molten salt storage tank for the SRE was designed with adequate size and strength for all anticipated operating conditions.

A structural design was chosen which permits easy construction with reasonable total weight, cost and thermal losses.

For ease of construction the tank could consist of heavy plate walls with no external reinforcing. This would be the easiest to insulate but would be very heavy. The other extreme would be a thin-skinned structure with many reinforcements which increases the cost of construction and makes the apparent outside surface larger and more difficult to thermally insulate. The compromise was to use four horizontal I-beams as stiffeners for 1.27 cm (0.5 in.)-thick side walls and five transverse I-beams supporting a 1.59 cm (5/8 in.)-thick bottom (Figure 2-3).

With four equally spaced horizontal and five equally spaced transverse I-beams under the bottom of the tank, the side and bottom plate thickness was obtained using ASME code data and allowing for corrosion, taking the nearest thicker standard thickness plate steel (see Figure 2-4).

The horizontal stiffeners are I-beams 0.203M by 34.2 kg/m (8 in. x 23 lb/ft) which will be welded together at the corners and welded to the outside of the tank. With tie rods across the middle of the tank, these beams will pass a hydrostatic test pressure of 83 kPa (12 psi). To meet the test pressure of 59 kPa (8.6 psi), only the bottom I-beam reinforcement will be cross tied.

Preliminary calculations indicate that seismic loading on the tank will not pose any serious problem. The increase in wall loading due to translational movement would be less than 7 kPa (1 psi).

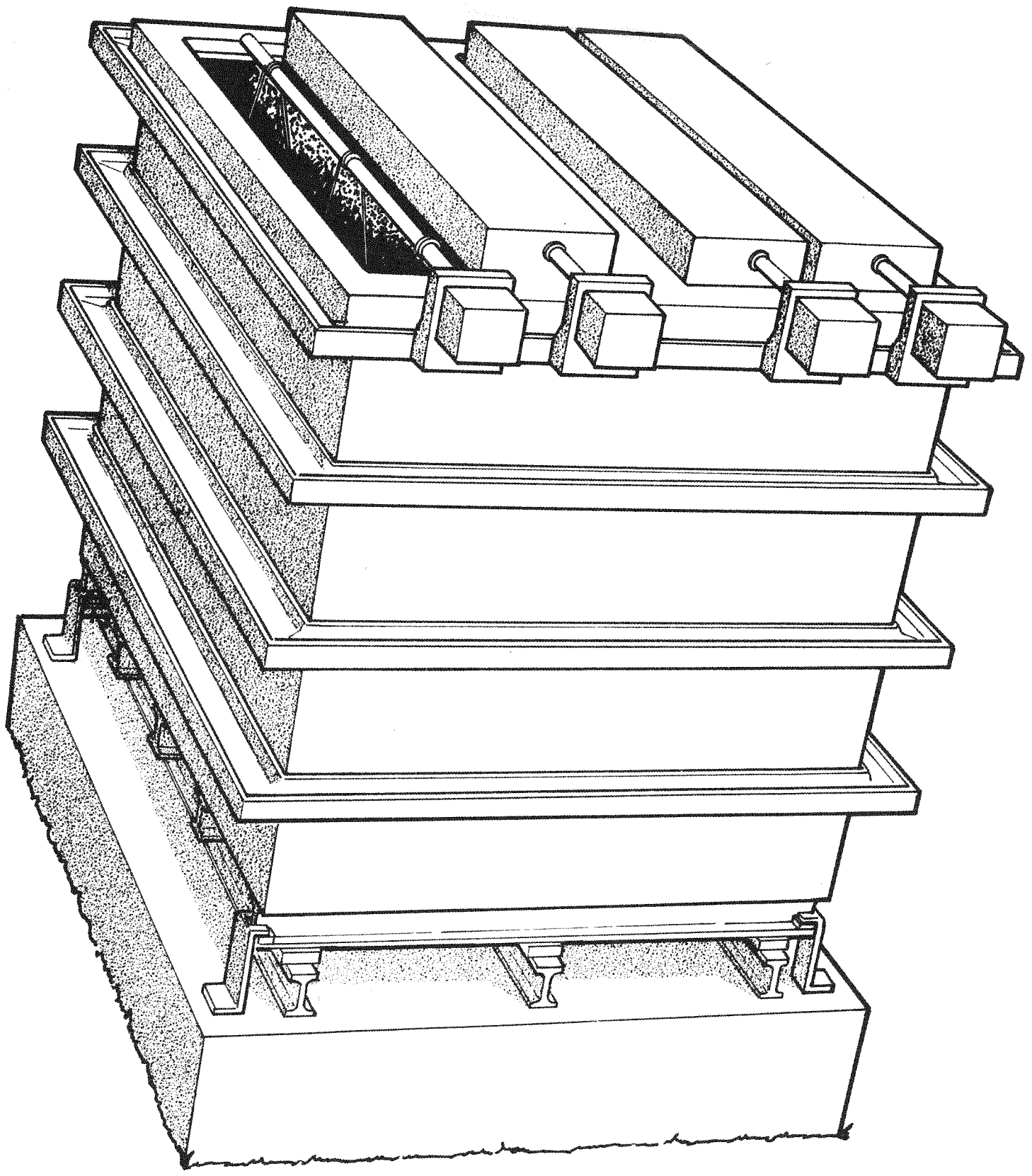

Figure 2-3. Thermal Storage Tank

40284

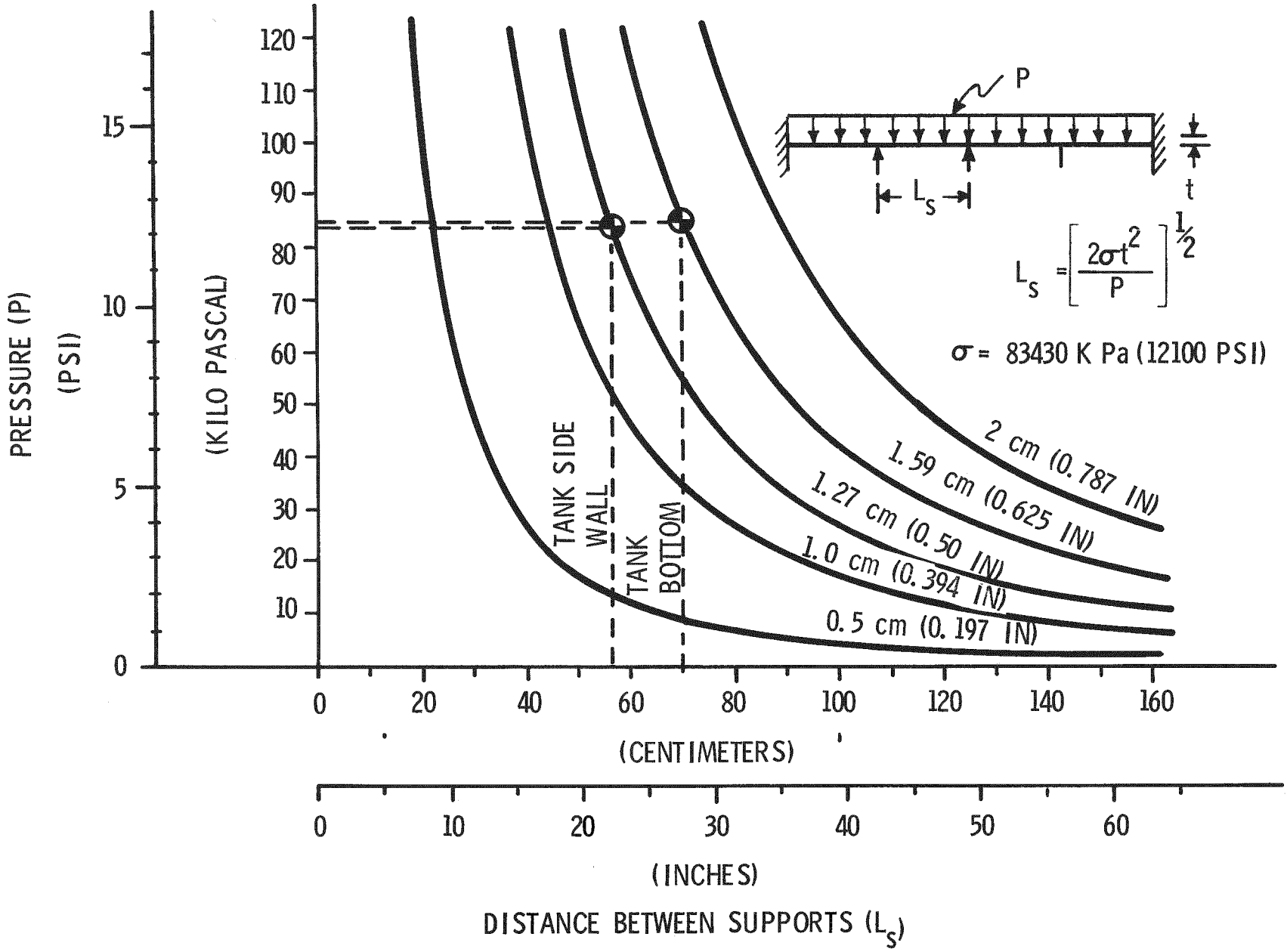

Figure 2-4. Tank Wall Design Point

This page intentionally left blank.

Experiment Conceptual Design

Thermal Storage Unit

INSULATION AND HEAT LOSS

In the melting and freezing of salt in the storage container, salt buildup on the wall may be an important variable. This can be most easily studied with a variable conductivity thermal insulation around the tank.

The storage tank walls will build up a solid layer of frozen salt at the rate of approximately 0.2 mm/hr (0.008 in./hr) per 1000 watts (3414 Btu/hr) of heat loss from the tank. To prevent the salt buildup, heat must be added to the tank. The salt buildup on the walls can be reduced with increased amounts of insulation.

To study the effects of the buildup of salt on the tank walls on the internal convection flow patterns, it is desirable to be able to vary the buildup rate or to reduce it to minimum. This can be achieved by placing guard heaters on the tank walls and using a thinner insulation than that necessary to simulate the heat loss expected in the pilot plant-size storage field.

Figure 2-5 shows that the insulation required to achieve the heat loss rate of 0.1 percent per hour for the SRE-size tank becomes excessive both in size and cost.

The insulation design chosen was to place 30 cm (12 in.) of mineral wool block insulation around the sides and cover of the tank. The base of the tank, which has 5 transverse I-beams, will be placed on top of three longitudinal I-beams, each point of contact being insulated with a 5 cm (2 in.) of Maronite insulation.

The remaining void space between the I-beams will be filled with mineral wool block insulation. The total heat loss from the bottom of the tank will be approximately 500 watts (1700 Btu/hr) and surface temperature of the concrete pad could reach 105°C (221°F). Because of the concrete pad depth no serious heating of the surrounding floor is expected.

The total heat loss with 30 cm (12 in.) of insulation is expected to be approximately 4500 watts (15,000 Btu/hr).

To simulate a variable conductivity insulation, 9000 watts of electrical resistance heating will be installed over the surface of the tank. Provision will be made to vary the heating rate over different zones of the tank and to vary the total power input. To determine the correct power input, heat flux gauges will be mounted on the outside of the tank insulation to determine the amount of heat being lost to the environment, and thermocouples will be attached to the tank walls to measure wall-to-salt temperature differences.

Heating tapes cost approximately $35 per kilowatt of power. With variable transformers and installation this may reach $140 per kilowatt. Figure 2-5 shows that in order to cut the heat loss in half (down to 2250 watts) by adding insulation the cost would be about $6000 as opposed to approximately $1300 for heaters and the ability to change the rate of heat loss would be lost.

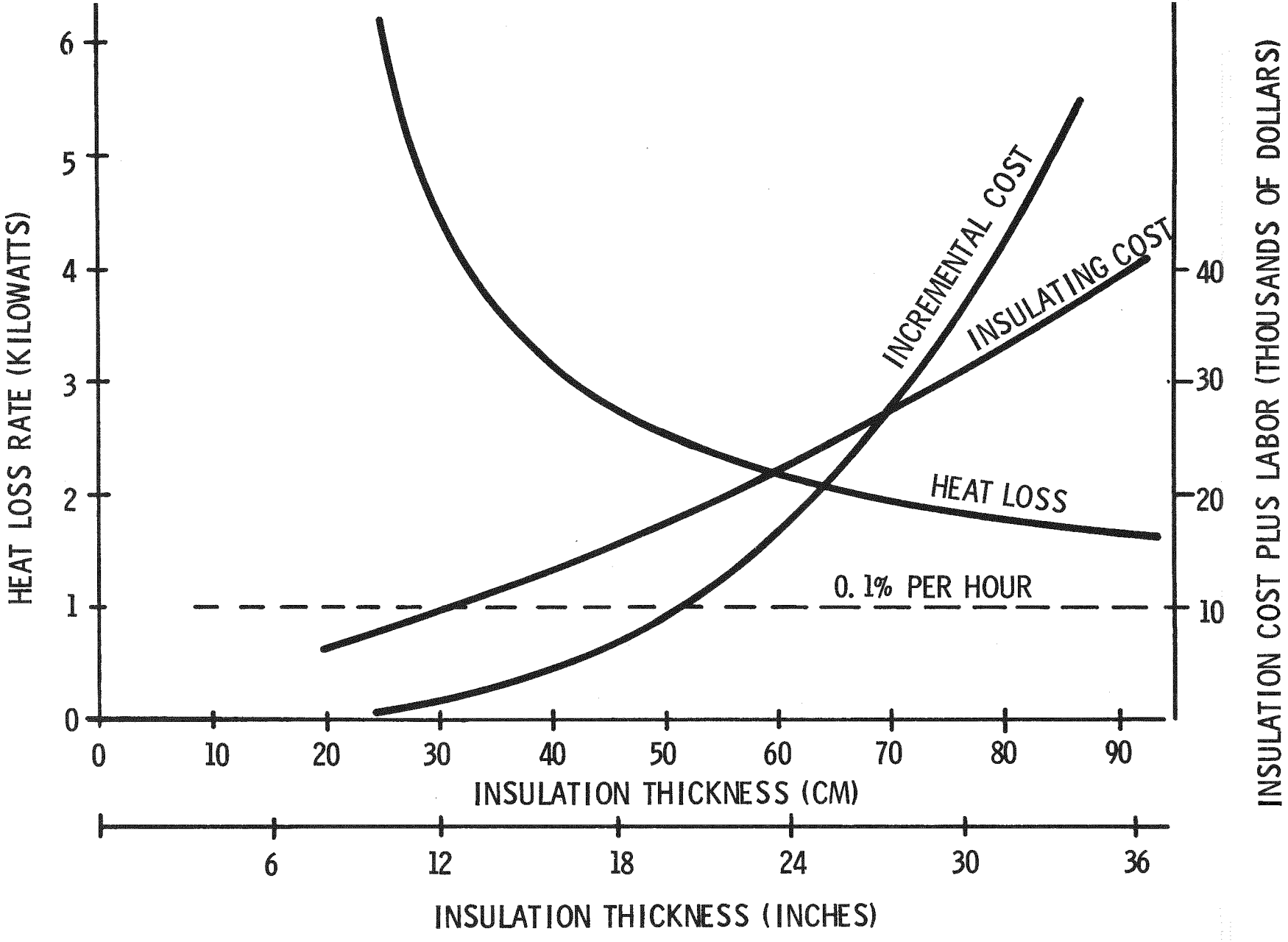

Figure 2-5. Heat Loss and Tank Insulation

Experiment Concept Design

Thermal Storage Unit

VAPORIZER

Heat energy can be extracted from the thermal storage salt to vaporize water using forced-circulation scheme inside pipes and mechanical salt removal on outside pipes.

The vaporizer unit of SRE is a scale model of the vaporizer unit of the one-quarter pilot plant cell. Based on a same heat flux criteria in SRE and pilot plant, the steam output rate from the vaporizer unit is 390 kg/hr (1300 lb/hr). For this condition, the over all temperature difference between salt temperature and steam required is 15°C (27°F), with steam conditions of 5722 kPa/272°C (830 psi/522°F). The vaporizer consists of four identical modules connected in series. Each module is a single serpentine of 1.59 cm OD/1.4 cm ID (5/8 in./14 gauge) tubing 94 in. long (308 ft). Each module serpentine has 11 legs, 2.1 m (7 ft) each with 10 cm (4 in.) between centers. The design parameters are listed in Table 3-1 of vaporizer unit design scaling section and design details in Appendix D. Figure 2-6 shows the arrangement of one of the four modules. Table 2-1 shows the input parameters to be considered for vaporizer design and the corresponding pilot plant values.

Table 2-1. Input Parameters to Vaporizer Design

Input Parameters	Factor For Selection of Value	Value for PP
Steam Rate and Quality	Thermal Output	13,000 lb/hr 0.4
Inlet Velocity	Flow Distribution	Approximately 10 ft/sec
Overall Heat Transfer Coefficient	Scraper Clearance Pipe Size	550 Btu/hr ft^2 °F
Pipe Size Choices	ANSI Code and Available Sizes	1.0 OD/0.870 ID 0.065 wall
Module Size and Number	Tank Size Scrapers Mechanization	16 modules, 44 legs 11 ft long

The piping design is compatible with the ASME and ANSI code.

The tube wall thickness is calculated from the empirical formulae and tables given in the pressure code book (Ref. Appendix D). The tube material selected is A106B carbon steel. Using a corrosion allowance of 16 mils, the pipe wall is determined to be 0.1 cm (0.04 in.) and a standard pipe wall 0.165 cm (0.165 in. or 15 gauge) is selected.

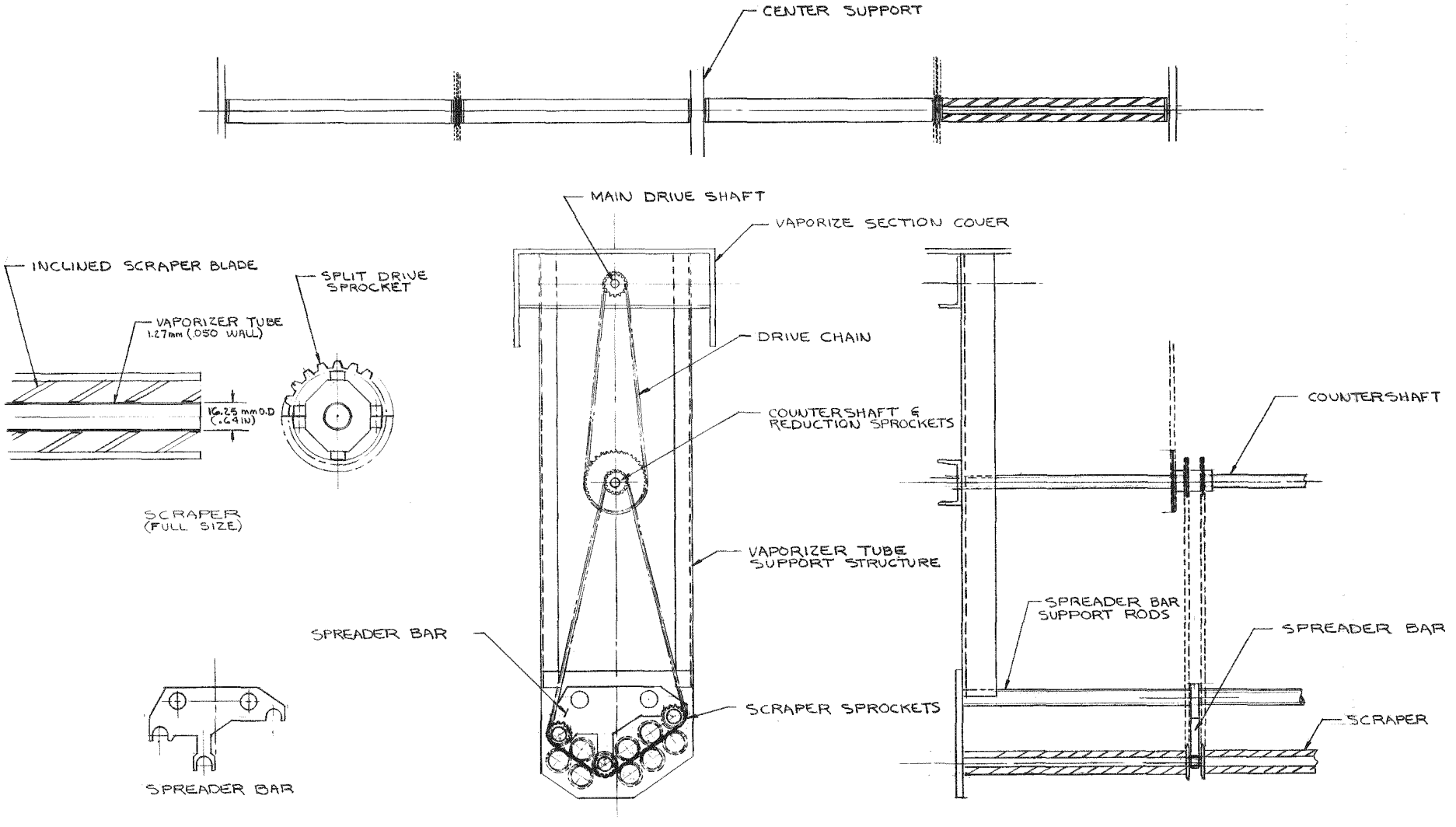

Figure 2-3. Thermal Storage Tank

Small-scale experiments have been successfully conducted with the proposed spiral-type scrapers. However, different scraper configurations and mechanizations will be tested as part of detail design. Also, different salt removal techniques have to be evaluated. Design changes which occur during the detail design of the SRE will be reflected back to the pilot plant to assure that similarity is being maintained.

This page intentionally left blank.

Experiment Concept Design

Thermal Storage Unit

MECHANISMS

Mechanical scraping devices and drives are required for operation of the thermal storage subsystem.

Vaporizer Tube Scrapers

Tests of the vaporizer tube salt buildup during heat removal show that continuous removal of the salt is necessary to maintain satisfactory heat transfer rates. A special scraper design has been developed and is shown in Figure 2-7. The scraper elements consist of elliptical steel half sections which fit closely over the vaporizer tube. A series of these plates are welded into a retaining frame. Two of these frames with half sections of a roller chain sprocket are arranged to fit together over a tube and when rotated, scrape the entire length of the tube during each rotation. The design is such as to avoid bearings and other closed nonscrapeable surfaces. Each vaporizer section consists of 11 of these tubes arranged in "V" shaped double rows, with the drive sprockets arranged in parallel rows so that one double chain will drive both rows of scrapers. The chain drive is tensioned by a spreader bar and finally is driven by a sprocket mounted above the salt surface on a counter shaft. The tubes are supported at their centers and each tube half is scraped by a separate unit.

A special characteristic of the scraper is the lack of normal bearings. The entire tube is scraped and the scraper blades act as bearings as well as scrapers. A relatively close fit, approximately 0.0127 cm (0.005 inch) clearance assures good heat transfer. An interesting characteristic appears to be the formation of a thin film of salt under the scrapers which prevents rapid wear of the assembly. Preliminary tests seem to confirm that the bearing material is being formed by salt. The scraper blades themselves are sharp edged to reduce scraping power.

Rotation of the scraper blades around the tubes increases turbulence and heat transfer due to agitation of the salt. Together with the thin films, this acts to provide relatively high heat transfer coefficients.

Chain-sprocket drives were selected since problems with bearings, gears and shafts are minimized. Chains are positive drives and when lightly loaded, serve well under hostile environments. Chains of stainless or carbon steel are available for this application. The system design is such to minimize interface problems by using a countershaft system for the final drive. A counter-shaft just above the melt keeps the chain which goes into the melt warm and also allows the transfer chain from the motor drive shaft to remain clean.

An electric motor and gear reducer mounted on the tank outside the insulation for each vaporizer section serves to drive the scrapers. The power source

is arranged to be readily disconnected from the vaporizer section so that the vaporizer elements may be removed without disturbing the electric motor and reducer. The location of the motor also facilitates cooling and servicing.

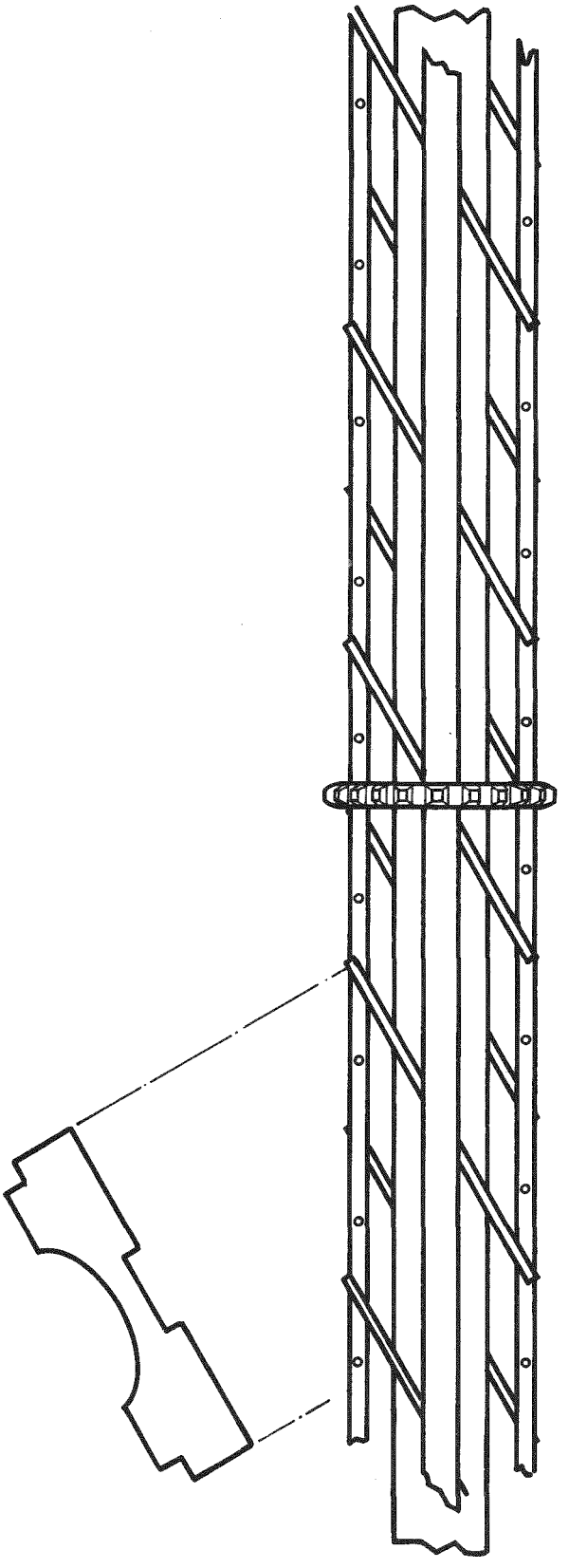

Figure 2-7 Split Design Inclined Plate Rotary Scraper

Experiment Concept Design

Thermal Storage Unit

CONDENSER

Heat energy from condensing steam can be charged into thermal storage salt by using a finned tube exchanger located at bottom of the tank, with natural convection heat transfer to molten salt, with steam condensing on the inside of condenser pipe.

The SRE Condenser is designed for a steam rate of 756 kg/hr (1664 lb/hr) which would give a heat flux (q/A) identical to that in the pilot plant condenser module. For this condition, the design ΔT is 19.5°C (35°F) and the steam conditions, 9480 kPa/863C (1375 psi/585°F). Finned tubes, 1.91 cm O.D. by 1.47 cm I.D. by 246 m (808 ft of 3/4 in./14 gauge), with external helical fins spaced three per inch, with a fin height of 1.22 cm (0.480 in.) and fin thickness of 0.076 cm (0.030 in.) are required. The total pipe length is divided into four serpentine tube tanks, with 61.6 m (202 ft) of finned pipe per serpentine having 28 legs of 2.19 m (7.2 ft) each. The design parameters are listed in Table 3-3 and detailed calculations are given in Appendix E.

The piping design is compatible with the A.S.M.E. and ANSI codes.

The pipe wall thickness is calculated from the empirical formulas and the table of pressure-temperature rating to meet the code requirements. The pipe material selected was A106B carbon steel. Corrosion tests with the ternary eutectic showed a corrosion rate of about (0.8 mil)/year for carbon steel. Using a corrosion allowance of 0.05 cm (0.020 in.) (20 years life) and a design pressure of 11032 kPa (1600 psi), the pipe wall was determined to be 0.22 cm (0.085 in.).

For the condenser the extended surfaces proposed were cylindrical fins. However, performance characteristics of other fins will be considered during detail design. The possible alternates are longitudinal fins, spined tubes and spiral fins. Bare tube exchangers will also be considered from an economic point of view. Their performance will be based on heat transfer characteristics and economics.

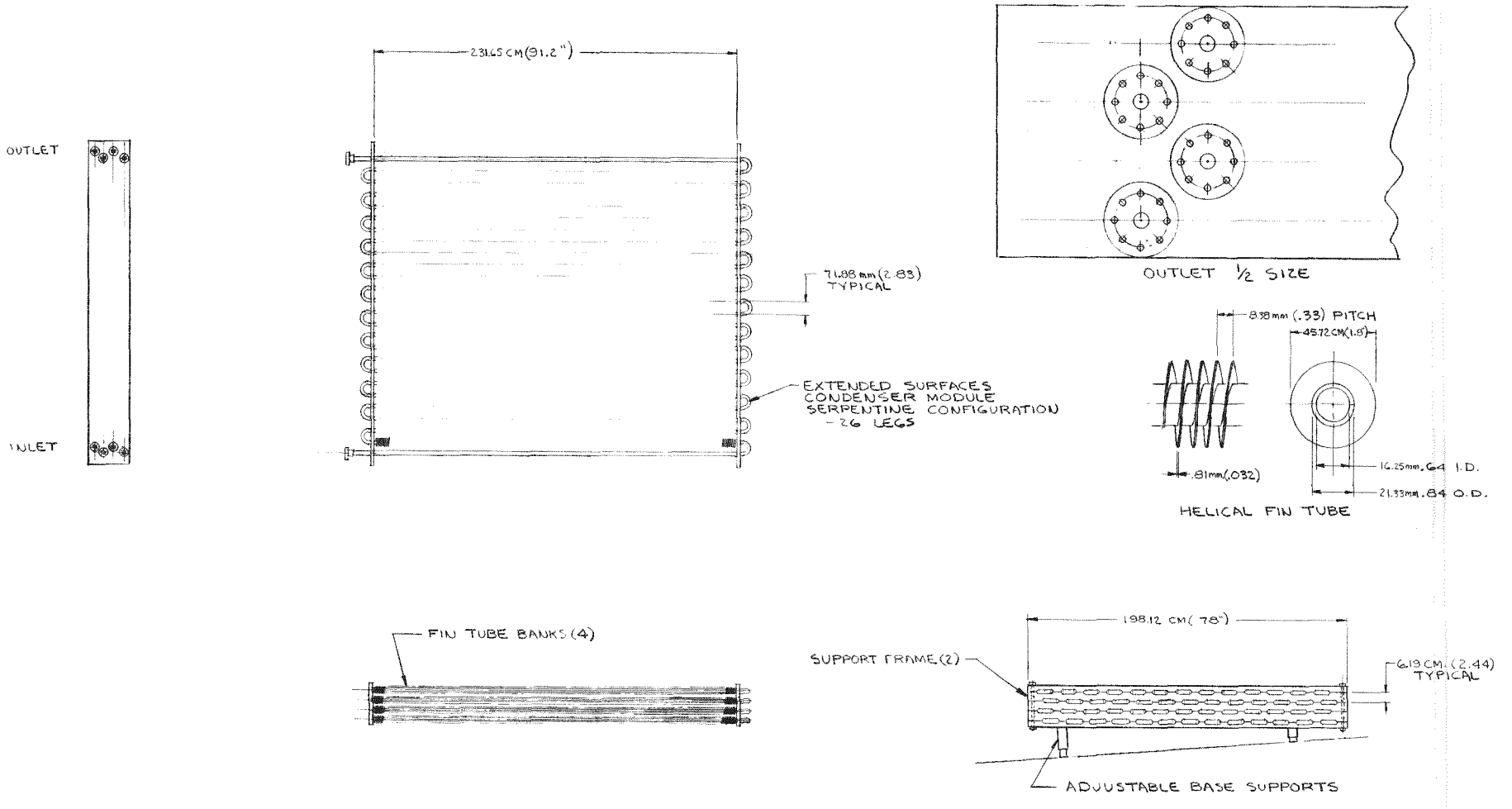

Figure 2-8. Thermal Tank Storage Condenser Module

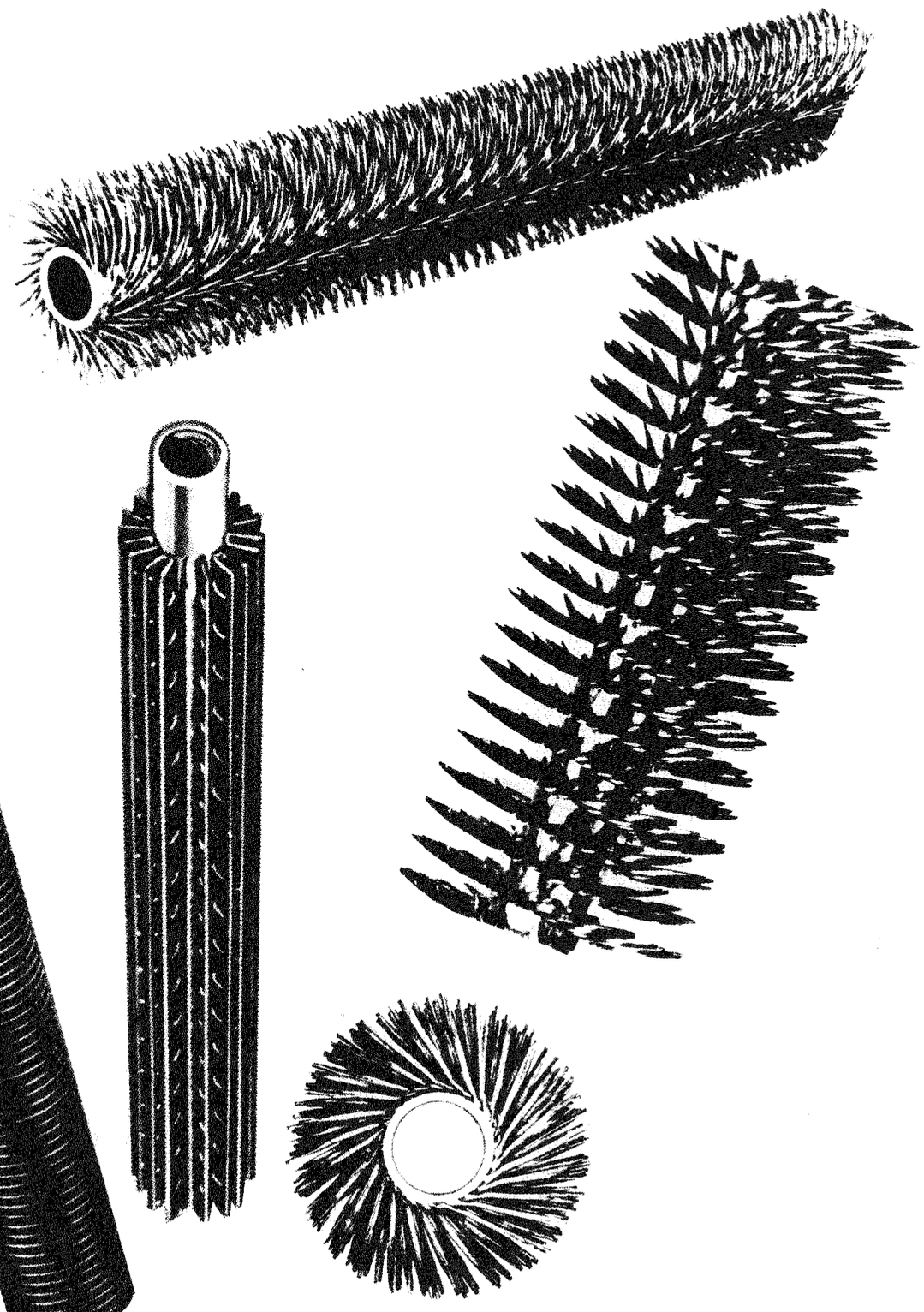

Figure 2-9. Condenser Tube Configurations

This page intentionally left blank.

Experiment Conceptual Design

Thermal Storage Unit

PHASE CHANGE MATERIAL

$NaNO_2$ has an effect on the thermal stability of the ternary eutectic NaCl-$NaNO_3$-Na_2SO_4.

Previous studies indicated that both $NaNO_3$-NaOH and NaCl-$NaNO_3$-Na_2SO_4 seem to undergo thermal degradation when stored at 475°C and 500°C respectively, and their melting temperatures and heats of fusion determined. The degradation can be attributed to the decomposition of $NaNO_3 \rightleftharpoons NaNO_2 + 1/2\ O_2$. Thermal decomposition experiments were conducted for the ternary eutectic in the presence of known amounts of $NaNO_2$ added with a view to slowing down the decomposition process. When 0.5 percent by weight of $NaNO_2$ was added to the ternary eutectic salt, and thermograms obtained, (see Figure 2-10) there was a very slight decrease in the fusion temperature, whereas there was considerable decrease in the heat of fusion. This trend became more pronounced with 1 percent and 5 percent by weight of $NaNO_2$ added to the sample.

The addition of a small quantity of $NaNO_2$ to the ternary eutectic does not seem to prevent the decomposition of $NaNO_3$, a major component of the ternary eutectic, at 500°C and above. Initial findings on long-term life studies on pure eutectics $NaNO_3$-NaOH and NaCl-$NaNO_3$-Na_2SO_4 indicate no significant changes in the thermal stability of these eutectics.

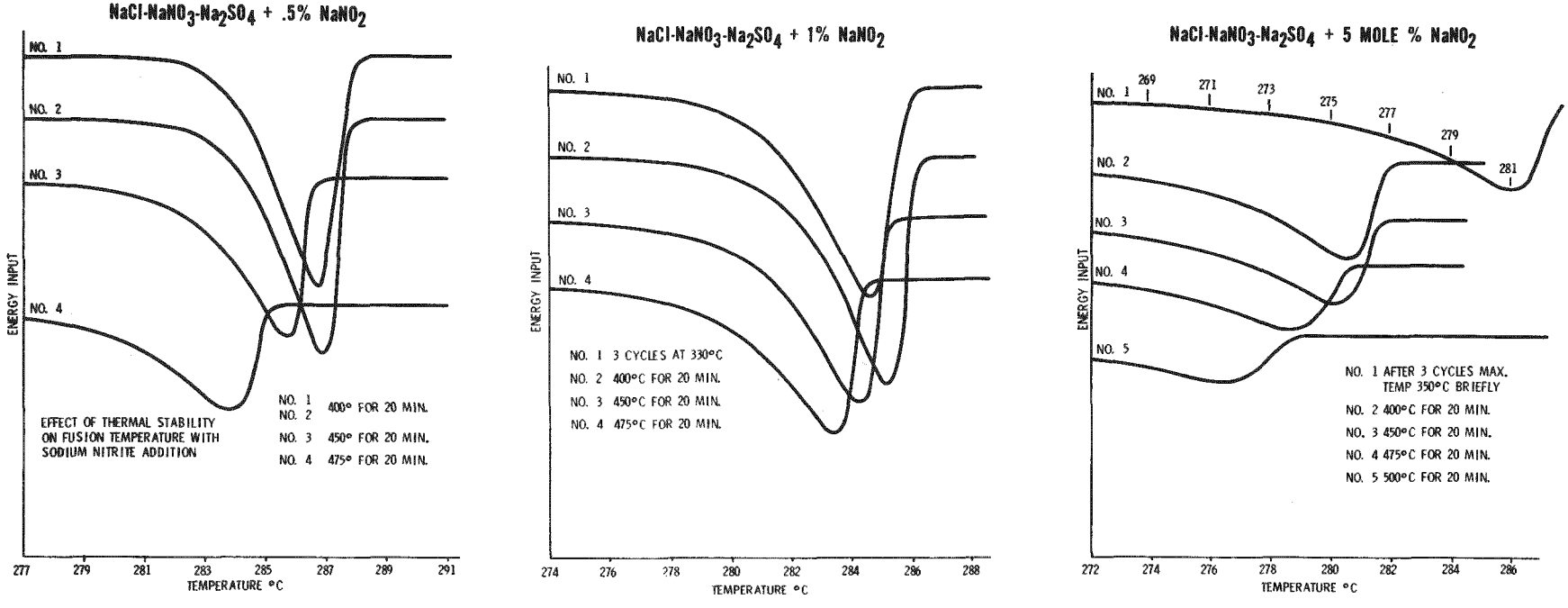

Figure 2-10. Effect of $NaNO_2$ Addition on Salt Stability

Experiment Conceptual Design

Thermal Storage Unit

PHASE CHANGE MATERIAL: THERMAL CYCLING

Thermal Cycling affects long-term life studies

The eutectics - $NaNO_3$-NaOH and NaCl-$NaNO_3$-Na_2SO_4 were placed in mild steel (AISI 1020) tubes and closed and thermally cycled between 50°C and 450°C through 140 cycles. After cooling, the material inside each tube was examined in the differential scanning calorimeter. The preliminary studies showed that the melting points of both the eutectics remained almost unchanged. There was no significant change in the heats of fusion when compared to fresh samples as shown in the thermograms (see Figure 2-11). The small depression in the thermogram of NaCl-$NaNO_3$-Na_2SO_4 appearing around 270°C can be attributed to the reversible phase transformation of Na_2SO_4 from orthorhombic to hexagonal.

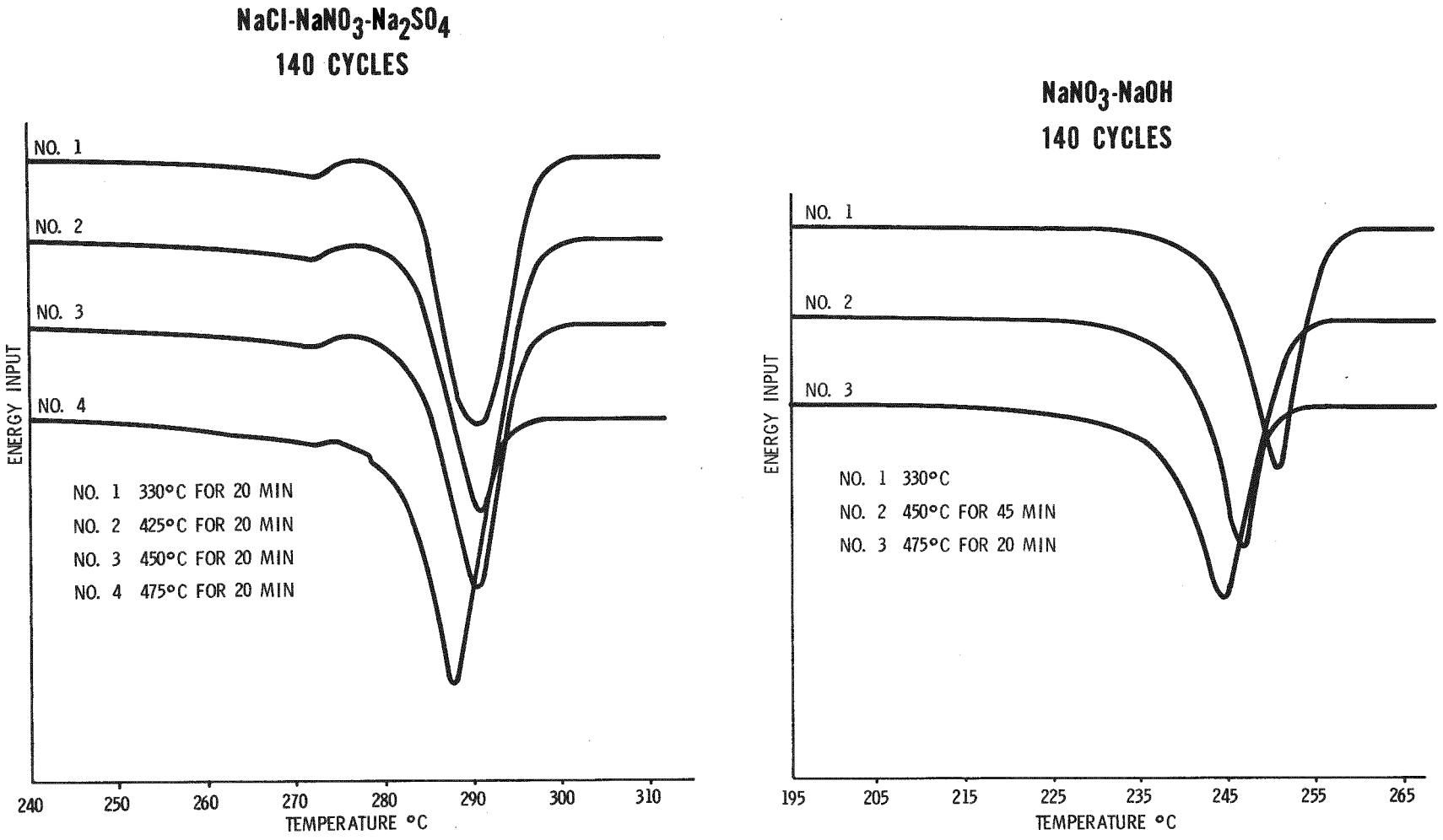

Figure 2-11. Effects of Cycling on Thermal Stability

Experiment Conceptual Design

Thermal Storage Unit

PHASE CHANGE MATERIAL: NUCLEATION AND CRYSTALLIZATION

Nucleation and crystallization of the molten eutectic is important for maximum recovery of thermal energy stored.

$Ca(NO_3)_2$ is a promising nucleating agent for the ternary eutectic. Both mild steel and stainless steel exhibit good corrosion resistance to the eutectic.

Preliminary studies using calcium nitrate as a nucleating agent for the ternary eutectic show that it increases the rate of nucleation and crystal growth. $Ca(NO_3)_2$ and $NaNO_3$ of the eutectic have similar crystal structure and their unit cell dimension spacings and ionic radii are comparable.

There are two steps involved in crystallization from a solution. The crystals must first form and then grow. The formation of a new solid phase either on an inert particle in the solution or in the solution itself is called nucleation. The increase in size of this nucleus with a layer-by-layer addition of solute is called growth.

Geometrically, a crystal is a solid bounded by planes. The shape and size of such a solid are functions of the interfacial angles, each face of a growing or dissolving crystal, as it moves away from or toward the center of the crystal, is always parallel to its original position. This concept is known as the "principle of the parallel displacement of faces. The rate at which a face moves in a direction perpendicular to its original position is called the translation velocity of that face or the rate of growth of that face.

Very small amounts of foreign substances will often completely change the crystal growth. The selective adsorption of dyes by different faces of a crystal or the change from an alkaline to an acidic environment will often produce pronounced changes in the crystal growth. The presence of other soluble anions and cations often has a similar influence. In the crystallization of ammonium sulfate the reduction in soluble iron to below 50 ppm of ferric ion is sufficient to cause a significant change in the habit of an ammonium sulfate crystal from a long narrow form to a relatively chunky and compact form. Information is available in the patent literature, and Table 2-2 lists some of the better-known agents and their effects.

Table 2-2. Agents Known to Modify Crystal Growth

Material Crystallized	Additive(s)	Effect	Concentration	References
$Ba(NO_2)^2$	Mg, Te^{+4}	Help growth		1
$LiCl-H_2O$	Cr, Mn^{+2}, Sn^{+2}, Co, Ni, Fe^{+3}	Help growth	Small	1
NaCl	Pb, Mn^{+2}, Bi, Sn^{+2}, Ti, Fe, Hg	Help growth	Small	1
	Urea	Forms octahedra	Small	2
	Tetraalkyl ammonium salts	Help growth and hardness	1-100 ppm	U.S. Patent 3,095,281
	Polyethylene-oxy compounds	Help growth and hardness	--	U.S. Patent 3,000,708
$NaClO_3$	Na_2SO_4, $NaClO_4$	Tetrahedrons	--	3
$Na_2CO_3-H_2O$	$SO_4^{=}$	Reduces L/D ratio	0.1-1.0%	Canadian Patent 812,685
	Ca^{++} and Mg^{++}	Increase bulk density	400 ppm	U.S. Patent 3,459,497
$Na_2B_4O_7$	Casein, gelatin	Flat crystals	--	2
Na_2SO_4	Alkyl aryl sulfonates	Aid growth	--	2
NH_4Cl	Mn, Fe, Cu, Co, Ni, Cr	Aid growth	Small	1
$(NH_4)_2HPO_4$	H_2SO_4	Reduces L/D ratio	7%	
$(NH_4)_2SO_4$	Cr^{+3}, Fe^{+3}, Al^{+3}	Needles	50 ppm	
	H_2SO_4	Needles	2-6%	
	Oxalic acid, citric acid	Chunky crystals	1000 ppm	U.S. Patents 2,092,073
	H_3PO_4, SO_2	Chunky crystals	1000 ppm	U.S. Patents 2,228,742
$MgSO_4-7H_2O$	$Na_2B_4O_7$	Aids growth	5%	1
$NaCO_3$, $NaHCO_3-2H_2O$	D-40 detergent	Aids growth	20 ppm	U.S. Patent 3,233,983
KH_2PO_4	$Na_2B_4O_7$	Aids Growth	--	1
$NH_4H_2PO_4$	Fe^{+3}, Cr, Al, Sn	Help growth	Traces	1
NH_4F	Ca	Helps growth	Small	
$ZnSO_4-7H_2O$	Borax	Aids growth	--	1
KCl	Pb, Bi, Sn^{+2}, Ti, Zr, Th, Cd, Fe, Hg, Mg	Help growth	Small	1
KNO_3	Pb, Th, Bi	Help growth	Small	1
KNO_2	Fe	Helps growth	Small	1
K_2SO_4	Cl, Mm, Fe, Ce, Cu, Al, Mg, Bi	Help growth	Small	1

Experiment Conceptual Design

Steam Generation System

STEAM DRUM SEPARATOR

The steam drum design is based on the proper separation of the entrained water in the two-phase flow, the liquid holdup requirements (capacity), and the fluid flow and state parameters.

The Steam Drum Separator consists of a liquid receiver tank and an internal entrainment separator (see Figure 2-12 and 2-13). The entrainment unit will be designed to separate up to 2965 Kg/hr (6500 lb/hr) a two-phase steam-water mixture with 99 percent removal of all liquid and solid particles where the particle size exceeds 10 microns.

The liquid receiver is sized to hold up to a maximum of 189 liters (50 gallons) of water and has 610 liters (21.5 ft^3) internal volume. The design of the receiver will be based on the latest revision of the ASME Code Section I for Power Boilers. This section of the code is required because the unit may be equipped with an immersion heater to preheat the feedwater for conducting special experimental tests. The design and manufacturing conditions are as follows:

Design pressure	6360 KPa (908 psig)
Design temperature	316°C (600°F)
Hydrostatic test pressure	9492 KPa (1362 psig)
Radiograph	full x-ray
National Board and ASME Stamps	required
Post heat treatment	per ASME Section I para. PN-39

Receiver Design Calculations (Ref. ASME Section I Pg 27.2.2.)

Steel Thickness

Material - carbon steel, SA106 Gr B

S = 15,000 psi 103,425 KPa (Table pg. -2.3.2, pg. 135), allowable stress

t = min. steel thickness, inches

P = 908 psig, 6360 KPa, maximum internal service pressure

R = 12 inches, 30.48 cm, internal radius

E = 1, weld joint efficiency

Y = 0.4, crelp coefficient

C = 1/8", 0.318 cm (corrosion allowance)

$$t = \frac{PR}{SE - (1-Y)P} + C$$

t = 7/8 inch, 2.22 cm

Head Thickness

Material - carbon steel, SA515 Gr 70

Heads of a semi-ellipsoidal form shall be made at least as thick as the required thickness of a seamless shell of the same diameter as provided in pg. 27.2.2, Reference ASME Code Section I, para. pg. 297.

Steam Drum Weights

Receiver	1200 lb	544 Kg
Separator	200 lb	91 Kg
Skirt	100 lb	45 Kg
Dry weight	1500 lb	680 Kg
Water hold up	350 lb	159 Kg
Wet weight	1850 lb	839 Kg

The design of the entrainment separator is based on off-the-shelf elements. The separator element is an efficient, two-stage, large-volume unit. The separator can be utilized with extreme flexibility and where experimental and finely-engineered systems are involved. The unique features of the entrainment separator include:

- Element size based on vapor flow - ΔP 0.03 psi, 0.21 KPa
- Large droplets removed by first-stage impingement plate before vapor passes through element
- Capable of handling large slugs of liquid
- Element constructed of carbon steel with 304L stainless steel blades
- Low pressure drop
- No moving parts - no replacement costs
- Self-cleaning - no maintenance costs
- Easily removed for alternate experimentation

1.- DESIGN TO BE IN ACCORDANCE WITH THE LATEST REV. OF ASME CODE SECTION I
DESIGN PRESS 908 PSI
" TEMP 600° F
HYDROSTATIC TEST AT 1362 PSI

2.- RADIOGRAPH : FULL X-RAY
POST WELD HEAT TREAT PER ASME SECT. I, PARA. PW-39

3.- CALCULATIONS: SHELL THICKNESS (MAT'L: C.S., SA 106 GR. B)
S = 15,000 PSI (TABLE PG-23.1 PG.135)
t = MIN. SHELL THICKNESS
P = 908 PSI
R = 12"
E = 1
Y = .4
C = 1/8 (CORROSION ALLOWANCE

$$t = \frac{PR}{SE-(1-y)P} + C \qquad t = \frac{(908)(12)}{15000-(1-.4)(908)} + .125$$

$$t = \frac{10896}{14455} + .125 \qquad t = 0.875 \text{ MIN.}$$

REF. ASME SECT. I PARA. PG 27.2.2

HEAD THICKNESS (MAT'L: C.S. SA 515 GR 70)
HEADS OF A SEMI-ELLIPSOIDAL FORM SHALL BE MADE AT LEAST AS THICK AS THE REQUIRED THICKNESS OF A SEAMLESS SHELL OF THE SAME DIAMETER AS PROVIDED IN PG-27.2.2
REF. ASME SECT. I PARA. PG 29.7

4.- NATIONAL BOARD & ASME STAMPS REQ'D

5.- WEIGHT (APPROX) 2000 LB.

6.- DESIGN & CALCULATIONS BASED ON NO. D75298 MOORHEAD MACHINERY & BOILER CO. DWG.

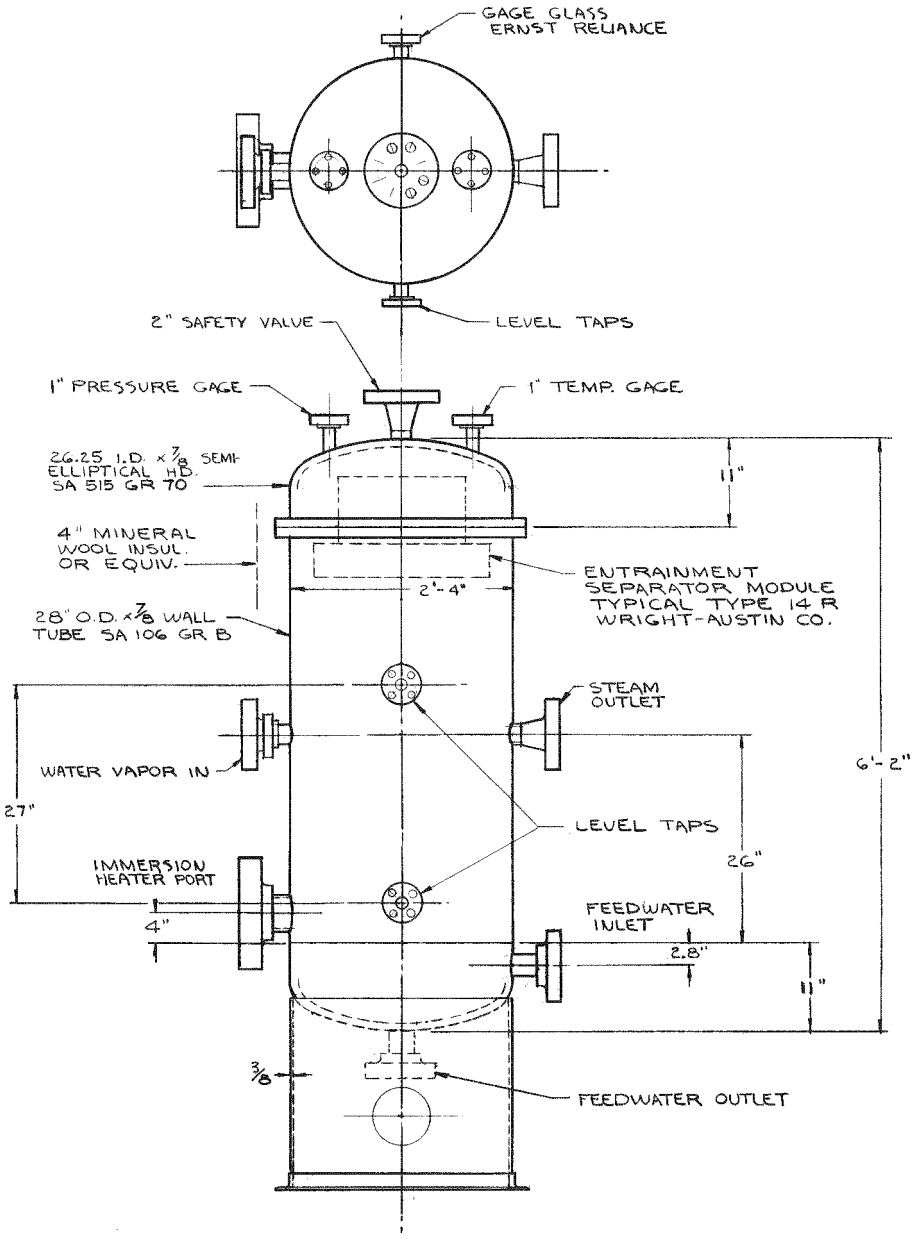

Figure 2-12. Steam Drum Unit

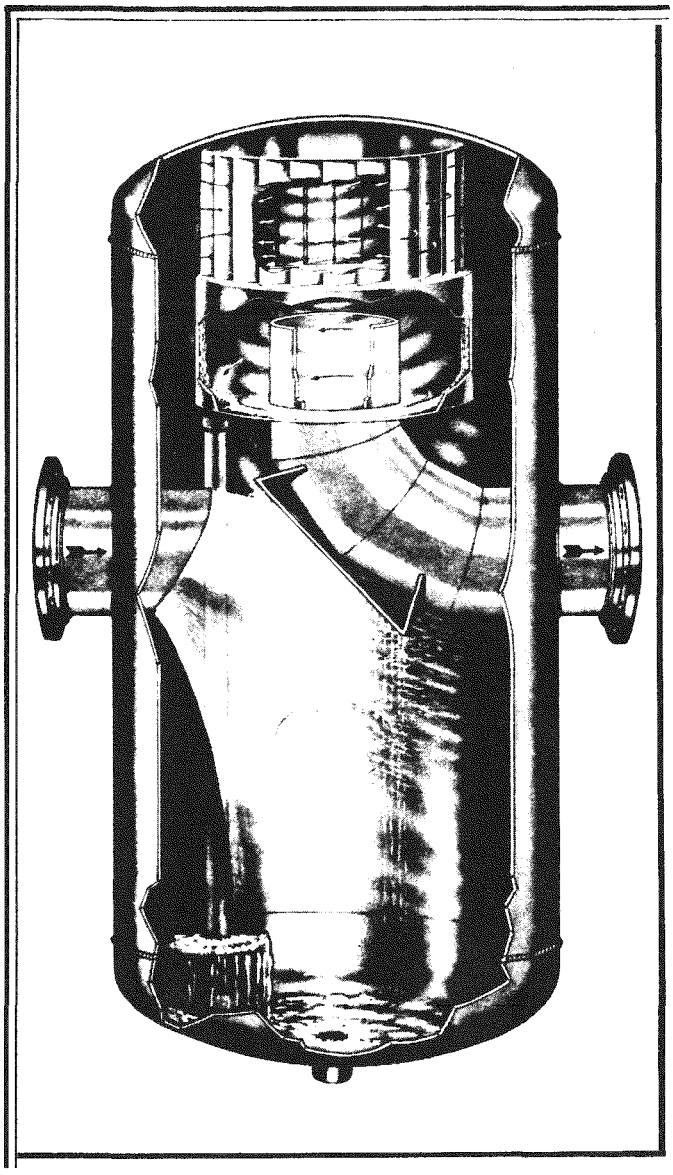

Figure 2-13. Entrainment Separator Receiver Type

RECIRCULATION CONTROL

The steam drum pressure control uses recirculation flow as a control variable. The recirculation flow control valve will be dynamically controlled by steam drum pressure.

The recirculation rate and steam quality will go to equilibrium values determined by the output steam rate and the overall heat transfer coefficient. The vaporizer output quality is related to the steam flow through the energy equations:

$$q = \dot{m} x_e h_{fg} = U_i A_i \Delta T = \rho_s Q_s h_{fg} + \rho Q_{fw} c_p (t_s - t_{fw})$$

where

$\dot{m}$ = Boiler feedwater rate, Kg/hr; (lb/hr)

x_e = Steam quality

h_{fg} = Evaporation enthalpy K Joules/Kg (B/lb)

U_i = Overall heat transfer coefficient, W/m^2-°C, (B/hr-ft^2-°F)

A_i = $\pi D_i L$ = Inside tube area; m^2, (ft^2)

ΔT = $T_{sat} - T_{salt}$ = Overall temperature difference, C°, (°F)

ρ_s = Density of steam, Kg/m^3, (lb/ft^3)

Q_s = Volume rate of steam, m^3/hr, (ft^3/hr)

ρ = Density of feedwater Kg/m^3, (lb/ft^3)

Q_{fw} = Volume rate of feedwater m^3/hr, (ft^3/hr)

c_p = Heat capacity of water, Joules/Kg-°C, (B/lb-°F)

t_s = Saturation temperature, °C, (°F)

t_{fw} = Feedwater temperature °C, (°F)

Until steam quality gets very close to one, the overall heat transfer coefficient is nearly independent of internal mass flow. This can be shown by an approximation of the heat transfer coefficient.

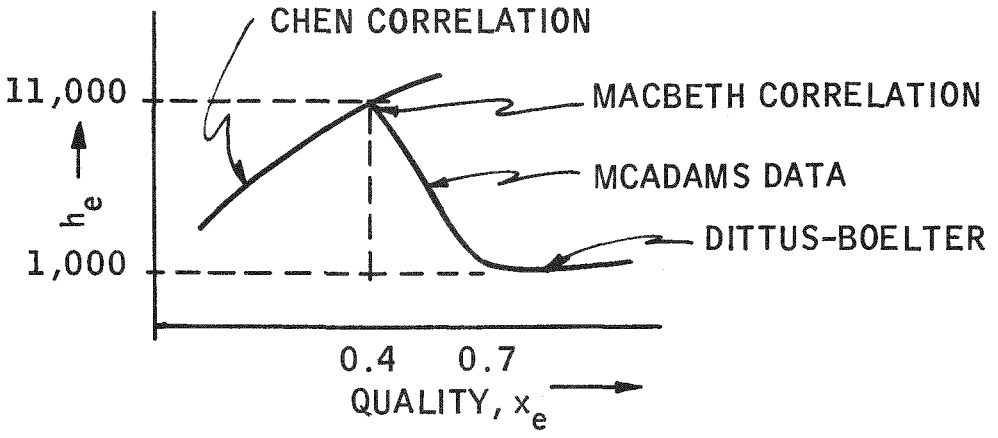

Given the dryout point from MacBeth correlation and using the slope of the dryout coefficient from McAdams, the coefficient has the following relationship to quality.

$$h_i = 24,000 - 33,000\, x_e, \quad 0.4 \le x_e \le 0.7$$

therefore, the overall coefficient becomes

$$U_i = \frac{1}{\frac{1}{24K - 33Kx_e} + \frac{1}{5000} + \frac{1}{600}}, \left(\frac{B}{hr - ft^2 - °F}\right)$$

$$= 600\left[\frac{0.72 - x_e}{0.74 - x_e}\right]$$

Note that the overall coefficient is nearly constant over this range. Therefore, from the energy equation, whenever the output steam rate goes below the design value, the steam quality will go to unity to reduce the area used in the tubes.

$$U_i A_i \Delta T = \dot{m}\, x_e\, h_{fg}$$

The only way the term on the left can be reduced is by reducing A_i. This can only be done by having x_e to to 1 before it gets to the end of the pipe.

At smaller values of output rate, the heat transfer coefficient h_i will become smaller at x_e near 1 according to the Dittus-Boelter equation.

$$h_i = 0.023 \frac{k}{D_i} (R_e^{0.8}) (P_r^{0.4})$$

$$V_e = \frac{\dot{m}}{(\rho_w - \rho_s x_e) A_f}$$

D_i = Inside pipe diameter

R_e = Reynolds number

P_r = Prandtl number

V_e = Exit velocity

ρ_w = Water density

ρ_s = Steam density

A_f = Flow area

Substituting V_e into h_i and putting h_i into U_i one can solve for x_e at values of output rate near zero.

STEAM DRUM LEVEL CONTROL

The feedwater rate to the drum should be a function of the steam generation rate and the liquid level.

The liquid level in the steam drum is controlled by the feedwater flow rate. The feedwater flow response is reduced by including liquid level rate feedback to the flow control valve. Liquid level rate feedback is accomplished by adding a signal from the output steam flow rate to the liquid level signal. The output steam rate is proportional to liquid rate. This is seen from the conservation of mass equation:

$$\frac{dm}{dt} = \rho_w A_d \frac{dx}{dt} = \rho_w Q_{fw} - \rho_s Q_s$$

$$\frac{dx_e}{dt} = \frac{Q_{fw}}{A_d} - \frac{s}{w A_d} \quad Q_s$$

where

x_e = drum liquid level

Q_{fw} = feedwater flow rate

Q_s = steam flow rate

A_d = drum crossection area

ρ_w = density of feedwater

ρ_s = density of steam

The control law for feedwater flow is

$$Q_{fw} = k_1 x_e + k_2 \frac{dx_e}{dt}$$

$$= k_1 x_e + k_2 \left[\frac{Q_{fw}}{A_d} - \frac{\rho_s}{\rho_w A_d} \quad Q_s \right]$$

$$Q_{fw} = \frac{k_1 x_e \frac{k_2 \rho_s}{\rho_w A_d} \quad Q_s}{1 - \frac{k_2}{A_d}}$$

where

k_1 and k_2 are constants

Experiment Conceptual Design

Steam Condensation System

STEAM TRAP

The steam trap is designed for condensate loads up to 770 kg/hr (1700 lb/hr) for a maximum pressure differential of 8515 KPa (1235 1si) and operating pressure differential of 6101 KPa (885 psi).

The steam trap is an inverted bucket-type mechanical trap which operates on the density difference between steam and water. The trap design is based on Armstrong 5133 configuration[1]. The trap is sized for a condensate capacity for continuous discharge of 2300 kg/hr (5000 lb/hr) using a safety factor of 3 to 1 and for pressure differentials from 885 psi to 1235 psi at this capacity. The back pressure in the condensate line was taken as 1482 KPa (215 psia). Thus for steam inlet pressures from 7584 KPa (1100 psia) to 10,000 KPa (1450 psia) and condensate loads up to 770 kg/hr (1700 lb/hr) a 1.58 cm (5/8 in.) orifice is recommended. Parts in contact with water will be made of stainless steel, with the body and cap made of carbon steel. The dimensions of the trap are given in Figure 2-14. The trap design is compatible for the high operating pressures and temperatures.

---

[1]Refer to Catalog L-4A, Armstrong Machine Works, Three Rivers, Michigan 49093.

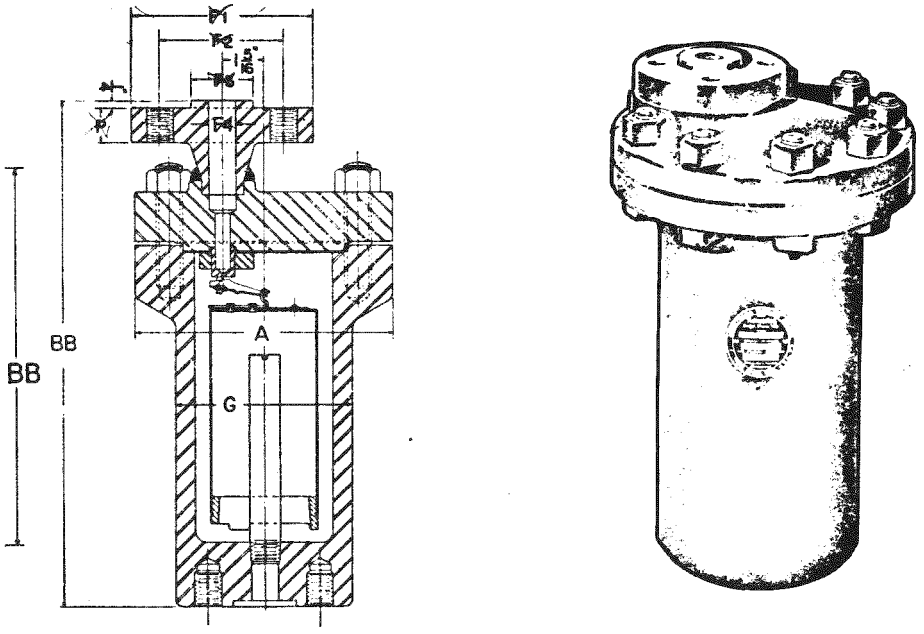

A.	FLANGE DIAMETER	=	8 1/2 IN.
B.	HEIGHT	=	14 3/8 IN.
BB.	FLANGED HEIGHT	=	16 1/4 IN.
G.	BODY O.D.	=	5 3/4 IN.

Figure 2-14. 5133F Flanged Inverted Bucket Type Steam Trap

Experimental Conceptual Design

Steam Condensation System

STEAM CHARGE CONTROL

Steam to the condenser is supplied at saturation conditions to maintain efficient heat transfer and good control.

In the charging mode, the thermal storage unit receives steam at pressures and temperatures above the design conditions. The steam is conditioned with a pressure regulator and a desuperheater. The steam is then condensed in the storage cell. The condensate flows into a trap which discharges the condensator without passing any steam. The condensate is still at fairly high pressure and hence partially vaporizes as it goes through the throttling to a low-pressure return line.

The input steam is from the No. 8 unit of the Riverside plant 2400 psig, 1000°F. The steam will first be expanded through a pressure regulator to 1450 psi, 950°F. An air failure-to-close isolation valve will protect the SRE test equipment. The steam will expand by the ratio of specific volume at instant mass flow and constant enthalpy.

$$\dot{m} = \left.\frac{A_f V_1}{v_1}\right|_{\substack{p = 2400 \\ h = 1462}} = \left.\frac{A_f V_2}{v_2}\right|_{\substack{p = 1450 \text{ psi} \\ g = 1462 \text{ Btu/lb}}}$$

$$\therefore \quad \frac{V_2}{V_1} = \frac{v_2}{v_1} = 1.66$$

where

$\dot{m}$ = mass flow (lb/hr)

A_f = flow area (ft^2)

V = steam velocity (ft/hr)

v = specific volume (ft^3/lb)

The steam will then go through a desuperheater to reduce the temperature to the saturation condition of 592°F. The feedwater flow rate will be governed by the energy balance.

$$\Delta Q_{ss} = \Delta Q_{fw}$$

$$\dot{m}_{ss} (h_{in} - h_{sat}) = \dot{m}_{fw} [h_{fg} + C_p (T_{sat} - T_{fw})]$$

$$\frac{\dot{m}_{fw}}{\dot{m}_{ss}} = \frac{h_{in} - h_{sat}}{h_{fg} + C_p \Delta T} = 0.37$$

where

m_{ss} = mass flow of superheater steam

m_{fw} = mass flow of feedwater

h_{in} = 1462 Btu/lb

h_{sat} = 1171 Btu/lb

h_{fg} = 566 Btu/lb

C_p = specific heat = 1.0 Btu/lb°F

T_{fw} = 370°F

T_{sat} = 592°F

Therefore, the steam input to the condenser will be 1.37 times the mass flow into the desuperheater.

When the steam goes through the condenser, it gives up its heat of vaporization, or 566 Btu/lb. However, at very low flow rates, the steam will transfer additional heat to the salt since the salt is at 550°F. During no flow conditions, the steam temperature will approach 550°F and 1050 psi. Therefore, the condensate output line must be below this pressure. Also, the trap should be designated to operate at that pressure.

TEMPERATURE MEASUREMENTS

Thermocouples will be installed to measure boiler temperatures, condenser tube and fin temperatures, tank wall temperatures, and the temperature of the salt within the tank.

The temperatures of greatest interest are those of the boiler and condenser tubes and the fluid in their immediate surroundings. A grid of thermocouples will be set up within the tank to obtain bulk fluid temperatures. These will provide information on the progression of melting zones and circulation of molten salt due to density currents during the heat extraction phase. It will be necessary to use sheathed thermocouples in the bath and provide flexible mechanical support to prevent their permanent dislocation due to movement of the solids during melt down.

Thermocouple Locations

Tank (Outside Surfaces)	
Sides of tank	15
Cover	2
Bottom	7
I-beam supports	4
	28
Condenser	
6 locations (tube wall, fin Salt 3 T.C. s)	18
Below condenser	8
	26
Boiler	
Unscraped tube walls	
One module	4
Three modules - 2 each	6
	10
Bulk Fluid	
Near top of condenser - 2 distances	8
Near boilers - 2 distances below	8
2 distances above	8
	24

Bulk Fluid

Four TC's spaced span wise in tank	24
at three levels at two longitudinal	10
locations in one quarter of volume	34

NOTE: Not all of the thermocouples need be monitored at all times such as when either the boiler or condenser is not being used.

THERMAL CAPACITY

Liquid surface level will be used as an indicator of the percentage of the storage capacity that is melted.

The eutectic salt mixture has approximately 12.5 percent volume change as it freezes, which changes the liquid level in the tank. To measure the level, a pipe will be placed into liquid, open end down, and a small flow of nitrogen gas will be injected into the top end. By measuring the pressure required to force bubbles out of the bottom end of the tube, the liquid level can be determined.

Figure 2-15 shows the basic scheme for measuring the level. A small dip tube is supplied by dry nitrogen through a regulator and orifice. A differential pressure gauge measures the pressure necessary to bubble nitrogen out of the dip tube. The pressure will be a direct function of the liquid level above the end of the tube and the fluid density. A variation of 24.4 cm (0.8 ft) will show a pressure difference of 0.5 kPa (0.7 psi). A pressure differential measurement between the dip tube and tank gas space is necessary since the gas pressure in the tank will be slightly above atmospheric. A resistance heater surrounding the dip tube would assure that the tube would not become blocked.

The temperature and capacity diagrams show the basic concept. Assuming a eutectic salt composition, melting or charging takes place at a fixed temperature until the entire charge is melted down. The liquid level and back pressure will rise until the salt is all melted. At this point a rise in salt temperature is now being added to the salt. The lower diagram indicates a simple chart which may be used to measure the energy charge status.

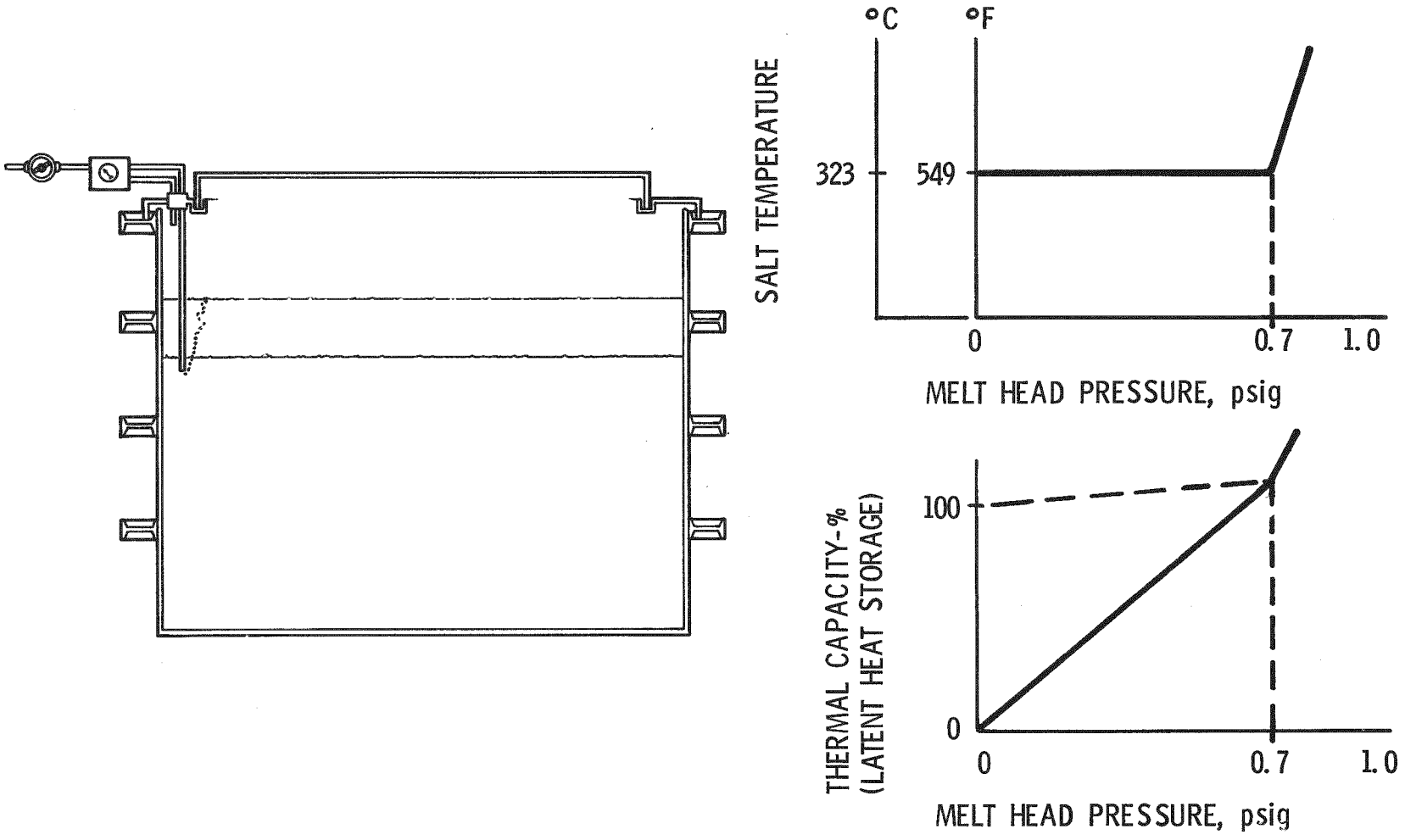

Figure 2-15. Thermal Capacity Measurement

Experiment Conceptual Design

Special Instrumentation

HEAT LOSS

The heat loss from the tank can be monitored with heat flux meters.

Heat flux meters will be attached to the sides, top and bottom of the insulation to determine the overall heat loss rate. An in-situ calibration can be made by heating the molten salt several degrees above the melting point and maintaining it at this temperature with the guard heaters.

It is necessary to calibrate at a temperature above the melting point to ensure that any change in heat content of the salt is sensible heat and thus can be measured with a thermocouple in the bath.

Measurement of tank surface temperatures, insulation outer jacket temperatures, and guard heater power input will give a good calibration of the heat flux meters. The heat flux meters can then be used to adjust guard heater power levels at other temperatures. A total of 15 heat flux gauges will be used to obtain the heat loss distribution necessary to balance the guard heaters.

Experiment Conceptual Design

Special Instrumentation

SALT BUILDUP ON TANK WALLS

Salt buildup on the tank walls will be measured to evaluate its effect on insulation requirements and storage cycle efficiency.

Salt will more readily freeze to those surfaces losing heat. The walls not being heated or scraped and having a constant heat loss can only be melted free by superheating the liquid during meltdown. Any salt remaining frozen to the walls will represent a decrease in capacity of the storage tank.

To measure the salt buildup, a rod will be inserted through a guide in the cover. The rod will have an arm in the salt bath and an indicator outside of the tank. To measure the salt thickness, the rod will be rotated until contact is made with the frozen salt, the zero point having previously been determined when the tank was sufficiently superheated to guarantee the walls were free of frozen salt. The device can be lowered and rotated 180 deg to measure two profiles from top to bottom of the tank.

SAFETY AND EQUIPMENT DESIGN

The experimental nature of this equipment requires a failure mode and affects analysis to ensure safety of life and property.

A number of safety-related factors are being considered for the SRE design. They include:

1. Electrical
2. Personnel protection
3. Fires
4. Condenser system leakage or failure
5. Steam generator leakage or failure
6. Seismic or mechanical shock effects
7. Gas blanketing failure
8. Tank leakage or failure

The SRE will be adequately grounded by electrical grounds to prevent personnel and equipment damage due to lightning or electrical failures in the motors and control circuits. The electrical control panel will be located in a separate control to permit safe operation in emergency conditions. Voltage levels of 240 and 110 are planned for motor drivers, valves, ect. Control circuits will be operated at 24 V to reduce electrical problems. All electrical lines and connections will be up to code standards.

Personnel Safety

Since the entire SRE steel tank will be in the vicinity of 315°C (600°F), personnel protection in the form of adequate external insulation and guards to prevent injury will be provided. Warning signs will also be displayed. Since the viscosity of the molten salt is low, on the order of water, splashing of the molten salt when agitated or objects are dropped into it can easily occur. Rotating shafts, scraper drives and other devices which cause salt agitation must be arranged to avoid spraying molten salt.

Use of protective clothing and full length face shields for close observation will be required. Overhead walkways with railings will be employed to improve safety and avoid damaging insulation. In addition to the static-type safety devices, a portable eye and face washer will be available. This device supplies a small shower head which can be used to wash down an injury quickly.

The salts to be used are dangerous in that the temperatures are high and also the latent heat of fusion of the freezing salt delivers considerable energy to the skin when it solidifies. Burns are usually deep and long lasting.

Fires

The salt is highly oxidizing and causes rapid burning of combustible materials which come into contact with it in the molten state. All tools, insulation and materials which contact the salt must be non-flammable. Special care must be taken to keep the area clear of combustible materials which could cause fires if inundated with molten salt.

Condenser Failure or Leakage

The failure of a steam line in the condenser or thermal charging system would release a mixture of steam and water under pressure of approximately 4825 kPa (700 psi) into the partially molten salt. The temperature difference between salt and steam would be on the order of 10° to 42 °C (50°to 100°F), with the salt being cooler. The reduction in pressure would cause large-volume expansion of the steam, possibly causing formation of large bubbles. This would be bollowed by the rapid movement of the bubbles to the tank surface, carrying salt with them. It has been estimated that the discharge of this steam (assuming a time lag of 4 sec between "sense pressure" and supply valve "closed") could bring the pressure above the liquid in the tank to a pressure of 14 kPa (2 psi). Since the tank cover is not bolted rigidly to the tank, the pressure buildup will be relieved by the lifting of the cover structure to release the excess pressure. In practice, at a pressure of 14 kPa (2 psi) a force of 5915 kg (13,900 pounds) is available to raise the cover. To control any possible discharges, the main cover will be restrained by hooks, chains, or hinges on one side. This will cause all discharge products to be released on the one side of the tank. This area will be barred to operating personnel and critical equipment. Quick-closing valves on the condenser sensing a pressure reduction, are being considered as a safety measure.

Vaporizer Leakage Failure

A vaporizer failure would be somewhat similar to a condenser failure. A major difference would be that a smaller volume of salt would be displaced before the steam reached the tank surface. Also, the pressures are considerably lower, so the problem should be less critical.

The tank, base and frame will be examined from a seismic failure mode and also from a mechanical damage standpoint. The tank will be equipped with thermally isolated restraints at the bottom to prevent accidental tipping due to seismic shocks or mechanical forces from loading equipment.

The foundation of the tank stands in a recessed ground area sufficiently large to contain the entire salt charge in the event of total rupture leakage for any reason.

Failure of the gas blanketing system will be a low-level problem. The gas blanket serves principally to maintain a clean, dry atmosphere above the salt and experience will indicate the actual need for this feature.

SECTION III
EXPERIMENTAL CONCEPTUAL DESIGN ANALYSIS

DESIGN SCALING - VAPORIZER

Pilot plant design and performance data can be obtained from the SRE if the SRE is a dynamically similar model of the pilot plant. A necessary condition for dynamic similarity is geometric similarity. Since the SRE was chosen to have one-fourth the capacity of one quarter of the unit cell, all dimensions in the SRE will have to be scaled by 63 percent. These scaled dimensions are summarized in Table 3-1.

It is not always possible to scale all the dynamic phenomena because there are not usually enough variables to meet all requirements. Certain parameters are difficult to vary, such as salt and water density, thermal conductivity or fabrication tolerances. The primary phenomena which should be preserved in scaling are those associated with the phase-change process on the exterior of the vaporizer tubes. The fluid properties on the interior of the tube are less important since the internal film coefficient is large compared to the external heat transfer coefficient[1]. However, the scaled system must preserve the large difference between outside and inside resistance.

There are at least four dynamic phenomena occurring in the vaporizer. They are: flow distribution, boiling water, solid salt formation and convective sedimentation of solid salt. Table 3-2 summarizes the dynamic phenomena and the equations which describe them. The nomenclature used and a brief explanation of each of the relations in Table 3-2 is given below.

Proper flow distribution requires that the pressure drop in the vaporizer tubes be large with respect to the pressure drop in the headers. This is not a critical constraint as a large range of pressure-drop levels work equally well. An industry standard is to choose the maximum liquid velocity in the system to be 3.05 m/s (10 ft/sec). At this condition the Reynolds number is far into the turbulent region, and hence, the friction factor is nearly independent of Reynolds number changes. The flow distribution phenomenon will not be tested in the SRE vaporizer since there is only one flow path. However, the pressure drop measured will be important for sizing pumps and header sizes in the pilot plant. In scaling, consideration will be given to obtain smooth pipes to maintain the relative roughness (e/D) in the smaller tubes. As listed in Table 3-2, the pressure drop will scale according to the relation

$$\Delta P = 4(L/d_i)\,(\rho V_i^2/2)\psi(R_e,\ e/$$

where

ΔP = pressure drop

d_i = inside diameter

[1] Refer to Appendix D for further discussion.

Table 3-1. Vaporizer Design Parameters

Parameters	SI Units		English Engineering	
	Pilot Plant	SRE	Pilot Plant	SRE
Geometric Similarity				
Tank size	4.6m x 3.7m x 3.7m	2.9m x 2.3m x 2.3m	15 ft x 12 ft x 12 ft	9.5 ft x 7.6 ft x 7.6 ft
Vaporiser module size	(4) 0.53m x 3.4m	(4) 0.34m x 2.13m	(4) 1.75 ft x 11 ft	(4) 1.1 ft x 7 ft
Total tube length	147m	94m	484 ft	308 ft
No. of tubes	1	1	1	1
No. of rows	2	2	2	2
No. of legs	44	44	44	44
Distance between centers	10.2 cm	6.4 cm	4 in.	2.5 in.
Tube I.D. /O.D.	2.21 cm/2.54 cm	1.4 cm/1.59 cm	0.87 in. /1.0 in.	0.55 in. /0.625 in.
Solid salt clearance/ thickness	0.015 cm	0.01 cm	0.006 in.	0.004 in.
Dynamic Similarity				
Steam output rate	1475 kg/hr	590 kg/hr	3250 lb/hr	1300 lb/hr
Water inlet velocity	3.4 in/sec	3.4 in/sec	11 ft/sec	11 ft/sec
Mass velocity	9.6×10^6 kg/hr-m^2	9.6×10^6 kg/hr-m^2	1.96×19^6 lb/hr-ft^2	1.96×10^6 lb/hr-ft^2
Exit steam quality	0.4	0.4	0.4	0.4
Overall ΔT	24.5°C	15°C	44°F	27°F
Overall coefficient, ν_i	3123 w/m^2-°C	4970 w/m^2-°C	550 B/hr-ft^2-°F	875 B/hr-ft^2-°F
Heat flux, q/A_i	76,300 w/m^2	76,300 w/m^2	2.4×10^4 B/hr-ft^2	2.4×10^4 B/hr-ft^2

Table 3-2. Dynamic Phenomena in Vaporizer Design

Dynamic Phenomenon	Governing Relation
Flow Distribution	$\Delta P = 4\left(\frac{L}{d_i}\right)\left(\frac{\rho V_i^2}{2}\right)\psi\left(Re, \frac{e}{D}\right)$
Internal Heat Transfer	$h_i = 0.023\ F\ (x, T, P)\ \frac{k}{d}\ Re^{0.8}\ Pr^{0.4}$
Boiling Water	$q/A_i = \rho V_i\ x_e\ h_{fg}$
Overall Heat Transfer	$q/A_i = U_i\ \Delta T$ $U_i = \frac{1}{\frac{1}{h_i} + \frac{r_i}{k_t}\ln\frac{r_o}{k_s} + \frac{r_i}{k_s}\ln\frac{r_o + t_s}{r_o}}$
Solid Salt Formation	$q/A_i = \rho_s\ h_\ell\ \frac{A_o}{A_i}\ \dot{t}_s$
Solid Salt Sediment	$V_s = C_o\ (\rho_s - \rho_\ell)\ g\ \frac{r^2}{\mu}$ $q/A_i = \rho_s\ \frac{A_T}{A_i}\ V_s\ h_\ell \cdot n$

e/D = relative roughness

L = tube length

Re = Reynolds number

ρ = fluid density

V_i = fluid velocity

ψ = friction factor

P = pressure

The boiling heat transfer coefficient is discussed in detail in Appendix E. In summary, the coefficient is primarily described by the forced convection part of Chen's correlation:

$$h_i = 0.023\ F\ (x, T, P)\left(k/d_i\right) Re^{0.8} Pr^{0.4}$$

where

$F(x, T, P)$ = empirical factor

h_i = boiling heat transfer coefficient

k = thermal conductivity of the fluid

Pr = Prandtl number

T = temperature

x = quality

This heat transfer coefficient is very large compared to the resistance of the salt film. Therefore, its importance in scaling is small. However, it is important to maintain the steam quality level at which wall dryout occurs. The MacBeth correlation predicts this value:

$$(q/A_{crit.} \cdot 10^{-6}) = A - 1/4\ C\ d_i\ [G(10)^{-6}]\ h_{fg}\ x_e$$

where

$A = y_o\ d_i^{y_1}\ [G\ (10)^{-6}]^{y_2}$

$C = y_3\ d_i^{y_4}\ [G\ (10)^{-6}]^{y_5}$

y's = empirical coefficient as functions of P, T

G = mass velocity ρV_i

dryout occurs when

$$(q/A_{crit} \cdot 10^{-6}) = 0$$

During off-design operation of the vaporizer, the automatically adjusted recirculation flow will be affected by the critical steam quality. This is because the internal heat transfer coefficient will become much smaller when steam quality is higher than the critical value.

The total heat transfer from the fluid to the salt, q, can be expressed in terms of the inside area of the tube, A_i, and the temperature difference between the fluid and salt, ΔT, by the relation

$$q = A_i U_i \Delta T$$

The term U_i is the overall heat transfer coefficient and is directly proportional to geometry changes as noted in the relation

$$U_i = \frac{1}{\frac{1}{h_i} + \frac{r_i}{k_t} \ln\frac{r_o}{r_i} + \frac{r_i}{k_s} \ln\frac{r_o + t_s}{r_o}}$$

where

k_s = thermal conductivity of the solid salt

k_t = thermal conductivity of the tube wall

r_i = inside radius of the tube

r_o = outside radius of the tube

t_s = thickness of solid salt on the outside of the tube

The overall heat transfer coefficient is seen to be the inverse of the sum of the three series resistances to heat flow. The resistance from the fluid to the tube wall is represented by $1/h_i$. The thermal resistances of the tube wall and the layer of solid salt on the exterior of the tube are represented by $\left(\frac{r_i}{k_t} \ln \frac{r_o}{r_i}\right)$ and $\left(\frac{r_i}{k_s} \ln \frac{r_o + t_s}{r_o}\right)$ respectively.

In general, the internal heat transfer coefficient, h_i, is large, and consequently the thermal resistance at the inside tube surface is small compared to the conductive resistances. Therefore, the heat transfer from the fluid to the salt is dominated by the tube wall and solid salt layer around the tube. Similarity for this process can then be obtained by the careful geometric scaling of the tube and salt layer. The scaling requirement for the inside heat transfer coefficient is simply that it be large.

It is also observed that, for large h_i, the value for U_i is inversely proportional to r_i. Therefore, the value of the overall heat transfer coefficient of the model will be larger than that of the pilot plant. If one recalls that the heat transfer is given by

$$q/A_i = U_i \Delta T$$

it is seen that both the heat flux and the temperature difference cannot be the same in the model as in the pilot plant. At this point in time it is recommended that two sets of tests be conducted, one in which the heat flux is the same as in the pilot plant and the other in which the temperature difference is the same.

The solid salt formation is directly proportional to heat flux:

$$q/A_i = \rho_s h_\ell \frac{A_o}{A_i} \dot{t}_s$$

where

A_o = outside area of the solid salt

ρ_s = density of solid salt, lb/ft^3

h_ℓ = heat of fusion of salt, BTU/lb

$\dot{t}_s$ = rate of growth of salt film, ft/hr

The sedimentation of the solid salt to the bottom of the tank is related to the particle size, density differences and viscosity of the fluid. It has been noted in experiments that scraped solid material results in very small crystals which cloud the liquid. For particles of this size, the Reynolds number is very low, and their velocity is described by Stokes equation for viscous motion:

$$V_s = C_o (\rho_s - \rho_{1s}) g \frac{r^2}{\mu}$$

where

V_s = velocity of solid particles

C_o = constant which is a function of particle shape

ρ_{1s} = density of liquid salt

g = gravity

r = radius of particle

μ = viscosity of liquid salt

The heat flux through the vaporizer tubes determines the slurry density of solid particles which are settling to the bottom of the tank:

$$q/A_i = n \rho_s \frac{A_t}{A_i} V_s h_\ell$$

where

n = slurry density (ft^3 solid/ft^3 slurry)

A_t = horizontal cross-sectional area of tank (ft^2)

Design for Dynamic Similarity

A basic relation which ties most of these dynamic phenomena together is the conservation of energy:

$$q/A_i = \rho V_i x_e h_{fg}$$

$$= U_i \Delta T$$

$$= \rho_s \frac{A_o}{A_i} h_\ell \dot{t}_s$$

$$= \rho_s \frac{A_T}{A_i} V_s h_\ell \cdot n$$

One can list many reasons for having the same heat flux in the model as in the pilot plant. Given geometric similarity, the fixed and variable parameters can be listed:

Fixed Parameters	Variable Parameters
ρ	x_e
ρ_s	U_i
h_{fg}	ΔT
h_f	t_s
A_o/A_i	V_s
A_T/A_i	V_i
	n

The steam exit quality should be the same as the pilot plant to maintain recirculation rate and maintain high heat transfer coefficients; V_i should be the same to maintain mass velocity and dryout quality levels. The rate of solid salt formation should be the same to evaluate scraper performance. V_s has to be constant because of the same salt material. The overall heat transfer coefficient is higher due to geometric scaling of tube by salt film thickness. Thus in order to maintain constant heat flux, the ΔT must be reduced. Reducing ΔT also makes the temperature gradients similar to the pilot plant.

Since V_i is held constant while scaling down, the Reynolds number will be 63% smaller. This, however, will have no effect on pressure drop since it is still turbulent. The internal heat transfer coefficient will remain essentially constant in the scaling. Even though the outside coefficient increases from 550 to 875 Btu/hr-ft^2-°F, the overall is based on outside controlling.

DESIGN SCALING - THERMAL STORAGE CONDENSER

The SRE condenser is a scale model of the pilot plant unit cell condenser module.

Geometric similarity is a necessary condition for the model to be similar to the prototype.

SRE is a 63% linear scale model of the pilot plant unit cell. Therefore, all the linear dimensions should be scaled down by this factor. The condenser pipe O.D. was scaled down by 63%, and the nearest available pipe size was chosen. The pipe wall thickness was calculated to meet the pressure code requirements (reference to Section IV). A 1.91 cm O.D. with 0.026 cm well thickness (3/4 in. O.D. and 14 gauge) tube is selected. Since fins are associated with the tube diameter, all fin dimensions were scaled down by the ratio of tube O.D.'s, and the nearest available dimensions were chosen (Table 3-3). Figure 3-1 shows the condenser tube for model and prototype.

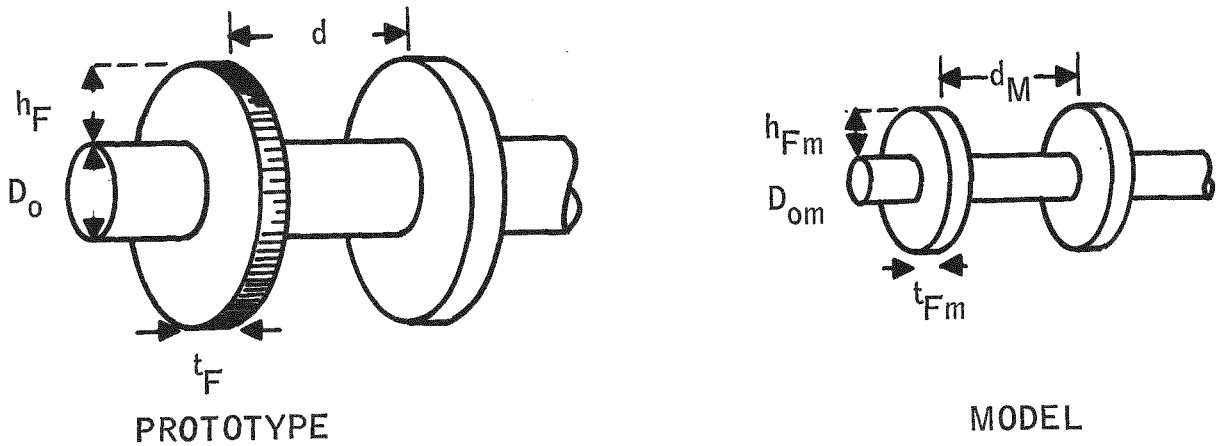

Figure 3-1. Condenser Tube

For complete similarity, dynamic similarity should be maintained when scaling. But, all of the dynamic phenomena cannot always be maintained.

Table 3-3. Condenser Design

Storage Capacity Parameter	Symbol	SI Units			English Engineering Units		
		Units	Pilot Plant	SRE	Units	Pilot Plant	SRE
Storage Capacity	L	MWH(t)	5	1.25	BTU	17.1×10^6 BTU	4.27×10^6
Tank Size							
Length	L	M	4.57	2.90	ft	15	9.5
Width	W	M	3.66	2.32	ft	12	7.6
Height	H	M	3.66	2.32	ft	12	7.6
Pipe Size							
Outside Diam.	D_o	M	0.0318	0.0191	in.	1.250	0.750
Inside Diam.	D_i	M	0.0264	0.0147	in.	1.040	0.580
Wall Thickness	t_w	M	0.0027	0.0022	in.	0.105	0.085
Exterior area/length	A_o/L	M^2/M	0.0997	0.0598	ft^2/ft	0.3271	0.1963
Interior area/length	A_i/L	M^2/M	0.0829	0.0463	ft^2/ft	0.272	0.152
Pipe Fins							
Fin Height	h_f	M	0.0191	0.0114	in.	0.750	0.450
Fin Thickness	t_f	M	1.27×10^{-3}	7.62×10^{-4}	in.	0.050	0.030
Fins/length		M^{-1}	0.051	0.076	$in.^{-1}$	2	3
Fin area	--	M^2	6.36×10^{-3}	2.29×10^{-3}	in^2	9.86	3.55
Fin area/length	A_F	M^2/M	0.501	0.271	ft^2/ft	1.643	0.888
Fin Effectiveness			0.45	0.5		0.45	0.5
Bare Tube Area	A_b	M^2/M	0.0896	0.0546	ft^2/ft	0.294	0.179
Effective Area	A_o	M^2/M	0.315	0.190	ft^2/ft	1.034	0.623
Outside/Inside Area			3.8	4.1		3.8	4.1
Condenser Module							
Total Pipe Length	--	M	4-9.7	245.7	ft	1344	806
No. of Serpentines	--	--	4	4	ft	4	4
Length/Serpentine	L	M	102.4	61.6	ft	336	202
No. of Legs	--	--	28	28		28	28
Length/Leg		M	3.66	2.19	ft	12	7.2
Spacing of Legs (center to center)	--	M	0.10	0.06	M	4	2.4
Module Size							
Length		M	3.96	2.38	ft	13	7.8
Width		M	2.90	1.74	ft	9.5	5.7
Height		M	0.37	0.23		1.23	0.74

Table 3-3. Condenser Design (Concluded)

Parameter	Symbol	SI Units			English Engineering Units		
		Units	Pilot Plant (Quarter Cell)	SRE	Units	Pilot Plant (Quarter Cell)	SRE
Input Parameters							
Steam Rate		Kg/hr	2304	755	lb/hr	5080	1664
Steam Rate/Serpentine	W	Kg/hr	576	189	lb/hr	1270	416
Steam Velocity (Entrance)		M/s	5.33	5.88	ft/s	17.5	19.3
Mass Velocity	G	$KgS^{-1}M^{-2}$	295.7	306.5	$lb\ hr^{-1}\ ft^{-2}$	218,000	226,000
Condensate Loading	Γ	$KgS^{-1}M^{-1}$	1.56×10^{-3}	8.52×10^{-4}	$lb\ hr^{-1}\ ft^{-1}$	3.78	2.06
Heat Rate		Watts	8.43×10^{5}	2.84×10^{5}	Btu/hr	2.88×10^{6}	0.97×10^{6}
Heat Rate/Serpentine	q	Watts	2.11×10^{5}	0.709	Btu/hr	7.2×10^{5}	2.42×10^{5}
Heat Rate/Unit Length	q/L	W/M	2056	1149	$Btu\ hr^{-1}\ ft^{-1}$	2140	1196
Heat Flux to							
Effective Outside Area	q/A_o'	W/M^2	6526	6053	$Btu\ hr^{-1}\ ft^{-2}$	2070	1920
Inside Tube Area	q/A_i	W/M^2	24,810	6053	$Btu\ hr^{-1}\ ft^{-2}$	7870	1920
Charge Time		hr	5.94	4.41	hr	5.94	4.41
Heat Transfer Coefficients							
Inside	h_i	W/M^2-C	11,215	13,856	$Btu/hr\text{-}ft^2\text{-}°F$	1975	2440
Tube Wall Conductance	hw	W/M^2-C	17,808	22,856	$Btu/hr\text{-}ft^2\text{-}°F$	3136	4025
Fooling Coeff (assumed)	h_d	W/M^2-C	5678	8518	$Btu/hr\text{-}ft^2\text{-}°F$	1000	1500
Outside - Bare Tube	h_{ob}	W/M^2-C	411	449	$Btu/hr\text{-}ft^2\text{-}°F$	72.4	79
Effective Outside Coeff Based on Inside Area	h_{ofi}	W/M^2-C	1562	1840	$Btu/hr\text{-}ft^2\text{-}°F$	275	324
Overall Ceoff Based on Inside Area	U_i	W/M^2-C	1039	1283	$Btu/hr\text{-}ft^2\text{-}°F$	183	226
Estimated Temperature Drops							
$t_{sat} - t_{wi}$	Δt_i	C	2.2	1.8	F	4	3.2
$t_{wi} - t_{wo}$	Δt_{wo}	C	5.8	13.5	°F	10.5	24.3
$t_{wo} - t_{salt}$	Δt_o	C	9.0	4.0	°F	28.5	7.2
Overall Temp Diff	Δt	C	23.9	19.3	°F	43.0	34.7
Salt Temp	T_{salt}	C	287.2	287.2	°F	549	549
Steam Temp	T_{sat}	C	311.1	306.7	°F	592	584
Steam Pressure	P	kPa	9998	9481	psi	1450	1375

The basic principle for dynamic similarity is that fluids with the same dimensionless numbers behave similarily. The dynamic phenomena outside of the condenser pipe is fluid circulation due to free-convection heat transfer, for which Grashof number is an important parameter. Since the outside coefficient controls heat transfer, the equality of Grashof number will assure dynamic similarity:

$$Gr = \frac{D_o^3 g\beta \Delta to}{\nu^2}$$

where

D_o = outside pipe diameter, ft; m

β = salt expansivity, $F^{\circ -1}$; $C^{\circ -1}$

ν = kinematic viscosity, ft^2/hr, m^2/hr

Δt_o = $t_{\omega_o} - t_{salt}$, °F; °C

g = acceleration due to gravity, ft/hr^2, m/hr^2

Given the same fluid, to obtain same Grashof number, Δt_o should be inversely proportional to the cube of the characteristic dimension. For a 0.63 scale model, we should have:

$$(\Delta t_o)\ \text{model} = 4\ (\Delta t_o)\ pp$$

However, increasing the Δt_o would increase the heat transfer coefficient, h_o, by a factor of (1/0.63) and hence heat flux by a factor of 6.35. To keep the same heat flux and also the same Grashof number, a fluid with following property should be used:

$$\left(\frac{\beta}{\nu^2}\right)\text{model} = 6.35\left(\frac{\beta}{\nu^2}\right)\ PP$$

However, with the constraint of working with the same salt, and at or near a steam pressure of 1450 psi, we must accept a lower Grashof number.

Looking at the macroscopic phenomena as the melt front moves away from the condenser, the heat exchange between the molten salt and the solid becomes a function of the condenser-to-solid-front separation distance, X. The rate of change of X is proportional to the heat flux, since

$$\frac{q}{A}_t = \rho_s \Delta h_\ell X$$

where A_t is the tank area, q is the heat rate, and Δh_ℓ is heat of fusion of salt.

Now, the circulation phenomena is represented as a function of Grashof number based on distance X which, for the same heat flux, will change at the same rate on the pilot plant and in the SRE. Since the SRE tank is geometrically similar to PP, a same $(q_t/A)_t$ would mean same q/A'_o or q/A_i, i.e., the same heat flux based on condenser surface, where A'_o is the effective outside surface area of the condenser and A_i is the inside tube surface area. Table 3-3 lists the dynamic parameters for pilot plant and SRE for the same (q/A_i) condition.

Table 3-4 lists the relationships for the heat transfer coefficients, heat flux and the flow distribution. Looking at the heat transfer coefficients, the main resistance is on the outside of the pipe. Therefore, when D_o decreases, h_o, and hence the overall coefficient, will increase. To maintain an identical heat flux in SRE and PP, ΔT should be lowered.

Design calculations have been done for identical q/A_i and identical q/A_o. The discrepancy between q/A_i and q/A_o is due to a difference in A_o/A_i, which is due to a difference in fin effectiveness.

Geometric similarity gives the same L/D ratio, and the identical heat flux condition gives the same velocity in tubes, which gives the same pressure drop, for the same tube roughness. The pressure drop measured will be important in the sizing of the steam trap for the pilot plant.

In Table 3-4, the equation for pressure drop is that for single-phase flow. For two-phase flow, the Lockhart-Martinelli pressure drop equation should be used.

Table 3-4. Heat Transfer Coefficients, Heat Flux and Flow Distribution Relationships

Phenomenon	Relation
Flow Distribution	Lockhart-Martinelli pressure-drop relation, or, for approximation: $\Delta P = 4\psi\left(\frac{e}{D}\right) \cdot \frac{L}{D} \cdot \frac{\rho V^2}{2g^2}$
Inside h.t. (steam side)	$h_i = 0.53 \left(\frac{D_i^3 \rho_\ell^2 g}{\mu \Gamma}\right)^{1/3} \frac{k}{D_i}$ $\Rightarrow h_i = 3067 (\Delta t_i)^{-0.25}$
Outside h.t. (salt side)	$h_o = 0.55 \frac{k}{D_o} \left(\frac{D_o^3 \rho^2 \beta g \Delta t_o}{\mu^2} \frac{C_p \mu}{k}\right)^{0.25}$ $h_o = 17.8 \left(\frac{\Delta t_o}{D_o}\right)^{0.25}$
Overall h.t.	$U_i = \frac{1}{\frac{1}{h_i} + \frac{k_i}{k_t} \ell n \frac{k_o}{k_i} + \frac{A_i}{A_o h_o}}$
Heat Flux	$\frac{q}{A_i} = U_i \Delta T = h_o' \Delta t_o = h_i \Delta t_i$
Melting Interface	$(q/A)_t = (\rho_s \Delta H_f) \dot{x}_s$ (tank heat flux)

Experiment Conceptual Design Analysis

TANK DESIGN TRADEOFF

A tradeoff exists between the number of external stiffeners and the plate wall thickness of minimum weight (see Table 3-5).

The design of the storage tank requires that external stiffness be located around the tank. Design parameters for a number of possible configurations are presented in Table 3-4. A preferred tank design is also presented in the table. This preferred design has 1/2 inch wall plate with four I beams 8 in. x 23 lb/ft located 22.3 inches apart running around the tank.

The assumptions and formulas employed to structurally analyze the tank configurations are given below.

Assumptions:

1) 2.32m x 2.32m x 2.90m (7.6 ft wide x 7.6 ft high x 9.5 ft long)

2) Test pressure 62 kPa (9 psi)

3) Horizontal stiffenings of standard I-beams
   a) Beams welded at corners and to tank
   b) No side wall reinforcement at bottom

4) Tensile stress allowed = 86,200 KPa (12,500 psi) for CS-SA-283B at 379°C (650°F)

5) Tank bottom structure is fixed 1.6 cm (5/8 in.) plate on five 8-in. x 23-lb/ft I beams, lying on top of three 8-in. x 23-lb/ft I beams.

Formulas:

Length of span (L_s) for a given plate loading and plate thickness (t)

$$L_s = \left(\frac{2\sigma t^2}{P}\right)^{1/2}$$

Beam loading - w

$$w = \frac{H}{n} P \quad \frac{\text{height x test pressure}}{\text{number of stiffenings}}$$

Bending moments - M

$$M_{max} = \frac{w\, l^2}{12}$$

Section modulus - (S)

$$S = \frac{M}{\sigma}$$

Table 3-5. Tank Design Tradeoffs

Item	Symbol	Unit	Number of Horizontal Stiffenings					Preferred Design 4.
			1	3	4	5	6	
Spacing	L_s	inches	91.2	29.73	22.30	17.84	14.87	22.30
Loading	W	lb/in	410.4	267.57	200.70	160.56	133.80	200.70
Bending moment	M	ft-lbf	37038	24148	18113	14491	13075	18,113
Section modulus	S	in^3	35.56	23.18	17.39	13.91	11.59	17.39
I beam		height x weight						
tank side			12x31.8	10x25.4	10x25.4	8x18.4	8x18.4	8x23.0[2]
tank end			10x25.4	8x23.0	7x20.0	6x17.25	6x17.25	8x23.0
Side-wall thickness	t	inches	1-3/4	5/8	7/16	3/8	5/16	1/2
Wall weight		lb	18194	6498	4549	3900	3249	5198
I-beam weight		lb	1215	2860	3813	3392	4070	3436[1]
Base plate weight		lb	1805	1805	1805	1805	1805	1805
Base I-beam weight		lb	1526	1526	1526	1526	1526	1526
Total weight		lb	22740	12689	11693	10623	10650	11965
Kilograms			10315	5756	5304	4819	4831	5427

[1]Tank has tie rods across long walls.

[2]8 x 23.0 means 8-inch (20.3 cm) web height x 23.0 lb/ft (343 kg/m) lineal weight.

SECTION IV
TEST CONCEPTUAL DESIGN

Test Conceptual Design

TEST OBJECTIVES

The SRE test objectives for the thermal storage subsystem require verification of the design, performance, and operational characteristics of the selected thermal storage concept.

Design and performance data will be obtained for the following alternative modes of operation:

- Charge
- Storage
- Discharge
- Charge/Discharge

Test conditions will be established to simulate scaled operation based on the various duty cycle conditions anticipated for the pilot plant. Design condition tests will be performed to verify that the design objectives for storage system capability will be met. These design objectives include:

- Store 1.25 MWH(t) heat energy at input rate of 0.28 MW(t)
- Discharge at a 0.27 MW(t) rate
- Maintain heat loss while storing of 1.5 KWH(t)/hr

Key test areas for obtaining component design and performance data are given in Table 4-1.

Operational tests will be conducted to verify satisfactory performance and control under the following conditions:

- Safety
  - Over temperature
  - Over pressure
  - Ruptured components
- Cycling
- Start up/shut down
- Repair and replacement of parts

Table 4-1. Key Design/Performance Test Areas

Component	Areas of Investigation
	Primary
Condenser	• Heat transfer coefficients • Temperature distributions • Pressure drop • Environmental effects
Vaporizer	• Heat transfer coefficients • Scraper efficiency - Salt removable - Mechanical performance • Temperature distribution • Pressure drop effects • Environmental • Interface tolerances
Tank	• Usable volume • Salt thickness
Salt	• Effect of "high" temperatures • Melt rate and pattern • Convection flow condition • Cycle effect
	Secondary
Steam Drum	• Liquid-level variation • Efficiency
Steam Trap	• Liquid-level variation • Efficiency

TEST PARAMETERS

Design and performance data for the thermal storage unit are determined by monitoring and recording the thermodynamic parameters (properties) of the various fluid flows of the system.

The hardware of the storage system is included in two main control loops: the charge loop and the discharge loop. Each of these loops includes several flow paths, which are shown schematically in Figure 4-1.

The thermodynamic properties and physical parameters that will be used to establish the performance of the various components are given in Table 4-2; parameter accuracies are indicated in the TES/SRE test specification. In general, the parameters include temperature, pressure and volumetric flow rate. Also, the quality of two-phase flows and liquid and solid levels are determined in several places.

The baseline piping and instrument diagram for the Storage SRE which illustrates the layout of test instruments for the various flow paths of the system is shown in Figure 4-1.

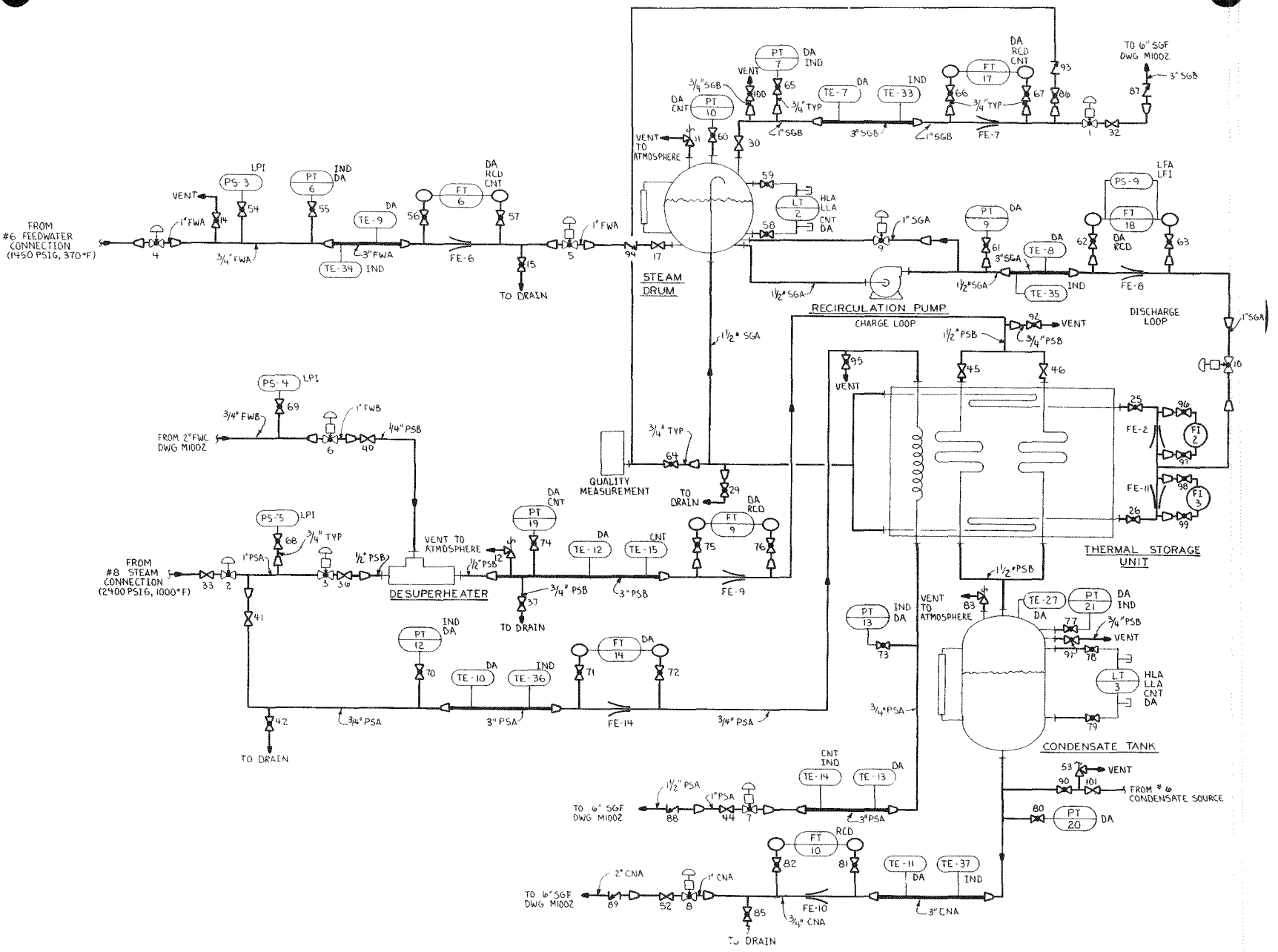

Figure 4-1. Piping and Instrument Diagram

Table 4-2. Test Parameters

Flow	Test Parameter				
	Temperature	Pressure	Flow Rate	Quality	Liquid Level
Charge Loop					
Feedwater Supply	X	X			
Steam Supply	X	X			
Condenser Inlet	X	X	X		
Condenser Outlet	X				
Steam Trap	X	X			X
Condensate Supply	X	X	X		
Deicer Inlet	X	X	X		
Deicer Outlet	X	X			
Discharge Loop					
Feedwater Supply	X	X	X		
Vaporizer Inlet	X	X	X		
Vaporizer Outlet	X			X	
Steam Drum	X	X			X
Steam Exhaust	X	X	X	X	

This page left blank intentionally.

Test Conceptual Design

Test Facility

SCHEDULE OF SOURCES/SINKS

Experiment-produced steam and water will be wasted to minimize risk of upset to normal power generating operation at Riverside and to reduce test costs; i.e., demineralized water is cheaper than conditioning equipment needed for closed cycling.

The selection of sources and sinks for water and steam for testing the steam generator and thermal storage unit has been made to minimize test expense and hazard to the power generating function of the NSP Riverside Station.

The cost of demineralized water at the station -- less than $2.00 per 1000 gallons -- is low enough to permit wasting (discharge to the river). Consideration was given to water recycling (e.g., by insertion either to the No. 6 unit condenser or deaerator). However, equipment costs for insertion and for pressure-temperature conditioning are significantly greater than the cost of water treatment. Moreover, risk of upset to the normal power generating operation of Riverside is minimized if the experiment-generated steam and water effluent is wasted. Demineralized water cost for the steam generator test program will be less than $600, assuming 30, 8-hour periods of testing at conditions averaging 2/3 load. Water cost for thermal storage unit testing will be appreciably less. The schedule of sources/sinks is given in Figure 4-2.

The No. 8 unit of Riverside will provide feedwater for the steam generator and a supply of high-pressure water for interstage desuperheating for controlling the temperature of the steam leaving the generator. It will also be a high-pressure water source for desuperheating the steam supply for the thermal storage unit in the charge mode. The No. 6 unit of the station will provide feedwater for the thermal storage unit in the discharge mode. The No. 8 unit of the station will also supply the steam for the thermal storage unit in the charge mode.

All experiment-generated steam and water will be discharged to the cooling water leaving the No. 6 unit condenser. These discharges will have an immeasurable effect in raising the river temperature even at its minimum flow stage.

Cooling water for the solar simulator will be taken from the low-service water line of the station and will be discharged to the No. 7 unit condenser circulating water.

SRE test program continuity is not expected to be interrupted by economic shutdown of the No. 6 or No. 8 units, but could be interrupted by equipment breakdown in those units. Such an interruption might occur four or five times a year and are expected to last the four or five days.

REQUIREMENT	SOURCE					SINK	
	NO. 8 UNIT FEEDWATER 3000 PSI 440°	NO. 6 UNIT FEEDWATER	NO. 8 UNIT MAIN STEAM 2400 PSI 1000°	LOW-SERVICE WATER 80 PSI 55°	NO. 6 UNIT CONDENSATE WATER 100 PSI 100°	NO. 6 UNIT CONDENSER DISCHARGE	NO. 7 UNIT CONDENSER DISCHARGE
STEAM GENERATOR TEST							
FEEDWATER SUPPLY	X						
ATTEMPERATOR WATER SUPPLY	X						
STEAM DISPOSAL						X	
BLOW-DOWN DISPOSAL						X	
COOLING WATER SUPPLY				X			
COOLING WATER DISPOSAL							X
THERMAL STORAGE TEST							
CHARGE MODE:							
STEAM SUPPLY			X				
ATTEMPERATOR WATER SUPPLY (INLET STEAM CONDITIONING)	X						
WATER DISPOSAL						X	
"THAW" STEAM DISPOSAL						X	
TRAP FILL (START-UP)					X		
DISCHARGE MODE:							
FEEDWATER SUPPLY		X					
STEAM DISPOSAL						X	

Figure 4-2. Schedule of Sources/Sinks (NSP Test Site)

Test Conceptual Design

Test Facility

RELATIVE LOCATIONS: TEST AREAS, SOURCES, SINKS

The SRE testing at Riverside will be in the vacant No. 7 Unit area with steam and water services from the adjacent No. 6 and No. 8 Unit locations. A schematic of the area is given as Figure 4-3.

The steam generator test will be located in the vacant No. 7 Unit area. The steam generator will be installed through the 22 by 42 foot opening in the turbine room floor (elevation 38 feet) and will be mounted on the basement floor (elevation 4 feet).

The thermal storage test will be located in the vacant No. 7 Unit transformer vault, which is adjacent to the station west wall. It will be mounted on the transformer pad at elevation 13 feet. The exterior vault can be enclosed by erection of a single wall and roof. Provisions will be made for space heating/illumination and for drainage of condensate and molten salt.

Steam and feedwater sources and steam/water sink will be provided from the adjacent No. 6 and No. 8 Units. The selection of steam and water services for SRE tests has been made to minimize the length of piping runs and need for temperature conditioning. Conditioning is required only for the charging steam to the thermal storage unit. The No. 8 Unit has a sufficiently high operating pressure to derive the steam and feedwater conditions selected for the Solar Pilot Plant. The longest pipeline distances are required for steam and water from this unit. Approximate distances from services to test areas and pipeline sizes are given in Table 4-3.

Table 4-3. Relative Distances of Service

	Distance (ft)	Pipe Size (in.)
Steam Generator		
Feedwater	155	2
Steam disposal	10	2-1/2
Cooling water, in	45	4
Cooling water, out	50	4
Thermal Storage (Charge)		
Steam input	117	1-1/4
Attemperator water	235	1/2
Water disposal	40	3/4
Thermal Storage (Discharge)		
Feedwater	78	3/4
Steam disposal	40	1

Pipe friction and temperature losses from source locations to the test areas are not critical as pressure and temperature reductions are deliberately made, or can be tolerated, in all cases before steam and water use. Discharge of test-generated steam and water to the No. 6 Unit condenser circulating water instead of recycling via NSP power production equipment avoids the expense of conditioning equipment and the possibility of upset to NSP operations.

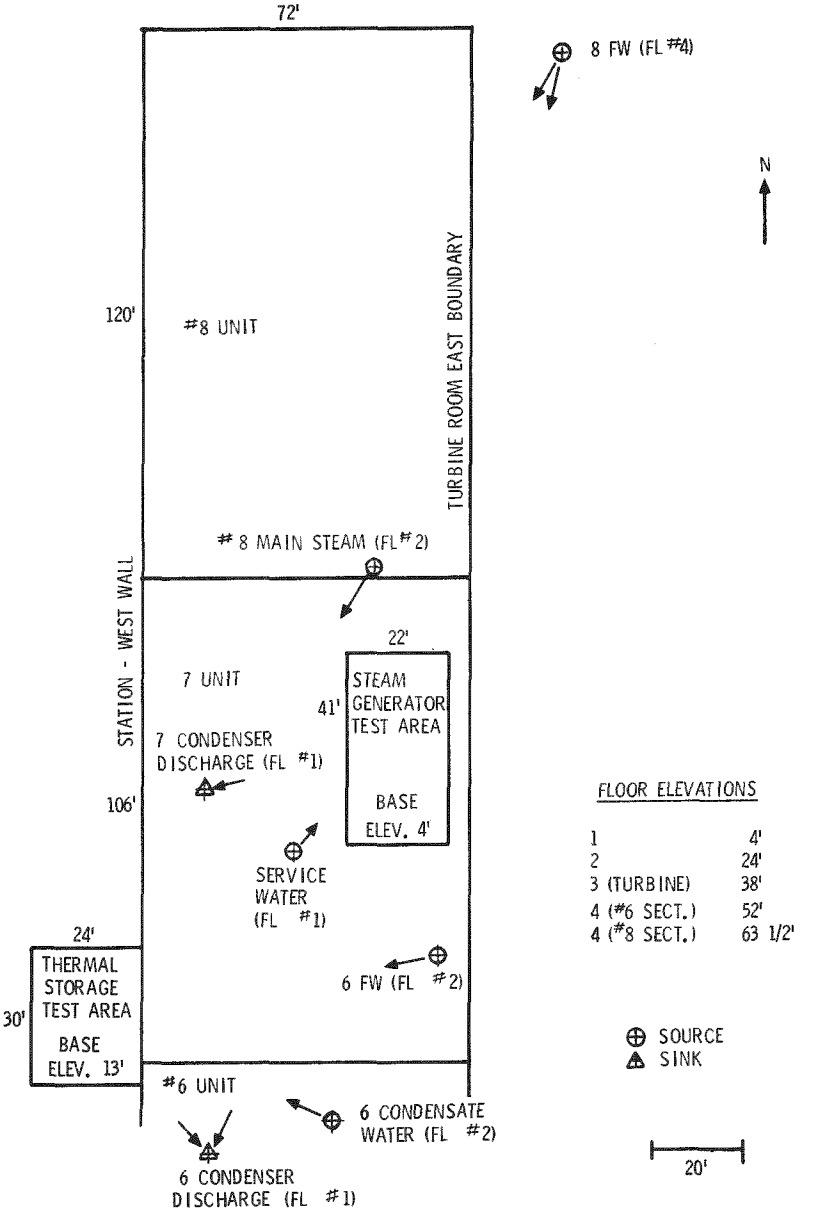

Figure 4-3. Relative Locations: Test Areas, Sources, Sink

Test Conceptual Design

Test Facility

PLAN OF TEST INSTALLATION: THERMAL STORAGE

The thermal storage test arrangement provides for molten salt handling remote from power production operations at NSP, and yet provides for an indoor environment proximate to steam and water services.

The thermal storage unit will be installed in the vacant No. 7 Unit transformer vault, which is exterior and adjacent to the Riverside Station's west wall. The plan of the test installation thermal storage is shown in Figure 4-4. Temporary construction will be used to enclose the test space. Because fire walls are already in place, only one wall and a roof have to be constructed. Provision will be made in the construction to permit installation and removal of tank and boiler tube assemblies as well as drainage of molten salts to transportable containers.

The thermal storage tank is almost the size of the existing transformer foundation upon which it will rest. The insulated construction of the tank bottom will limit the temperature of the transformer foundation upper surface to about 150°F maximum. The ceiling height of the test space is about 23 feet such that adequate gravity head between the steam drum and recirculation pump suction can be made available. The condensate trap will be mounted in the station basement opposite the vault area so it is low enough for gravity drainage from the thermal storage tank.

Operation of the thermal storage test will be from the control console in the mobile trailer located on the turbine floor in the No. 7 Unit location.

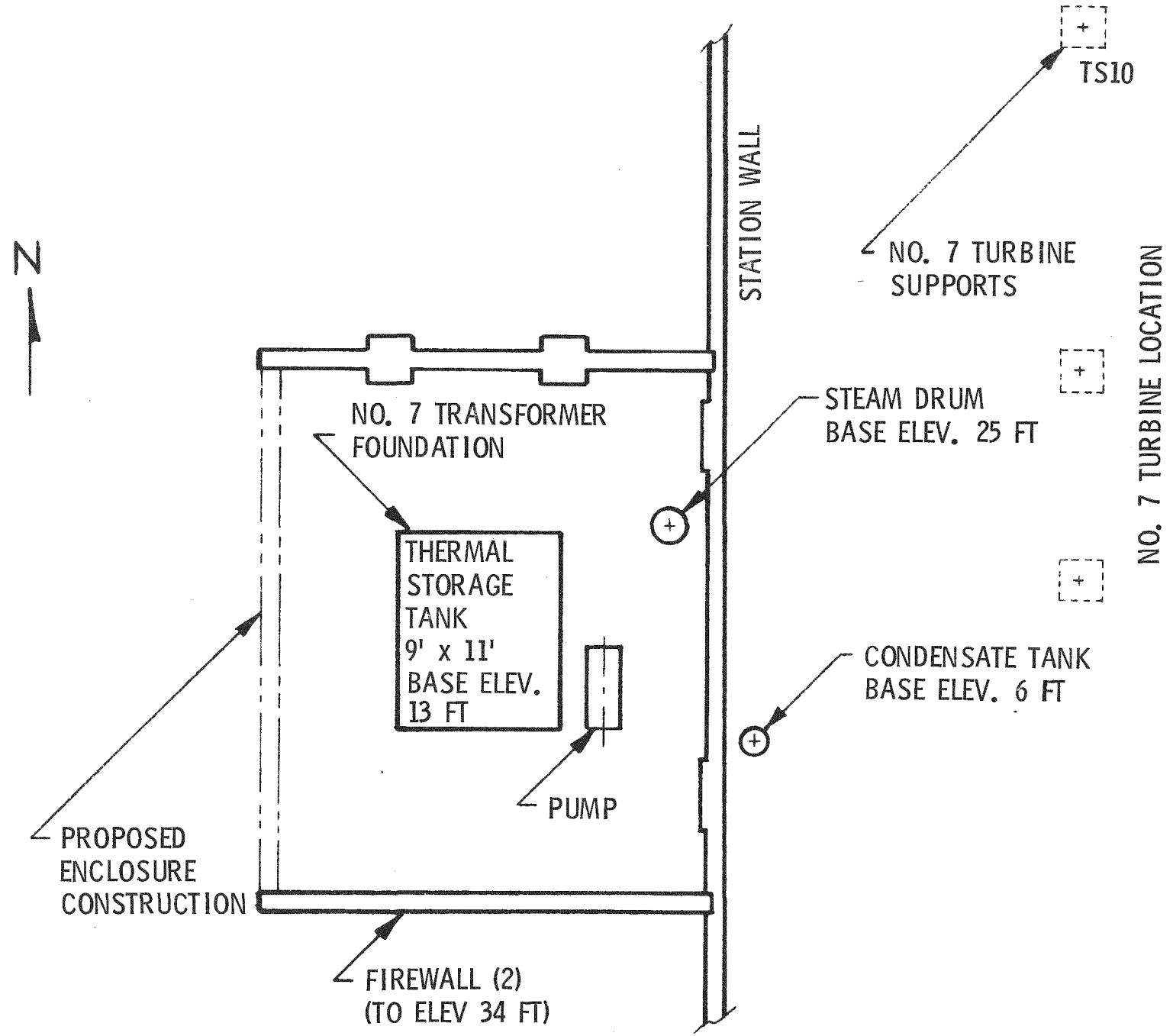

Figure 4-4. Plan of Test Installation Thermal Storage

CONCEPTUAL CONFIGURATION

The SRE test control center will contain the display and control elements required to conduct the SRE test sequences.

The test control center will contain the SRE control panel and the simulator control panel. The SRE control panel will have the operational controls for the receiver and storage SRE tests.

The Data Acquisition System (DAC) will also be located in the instrumentation trailer. The DAC consists of the system 700, magnetic tape unit, plotter/printer, typer, CRT and quick disconnect assembly. An air conditioner will be required (Figure 4-5) to protect the system 700 from the high ambient temperatures of the NSP plant.

All the test control center instrumentation will be movable for installation and servicing, but will be secured during transport.

All signal lines to and from the control center will be routed through an access port located behind the quick disconnect assembly.

The power required to operate the instruments in the control center will be 230 VRMS center tapped (115 VRMS) 60 Hz. One-hundred ampere service should be adequate to operate all the instruments and controls.

The test control center will include the necessary control and display equipment such that the test personnel can start, conduct and conclude a SRE test sequence without leaving the trailer.

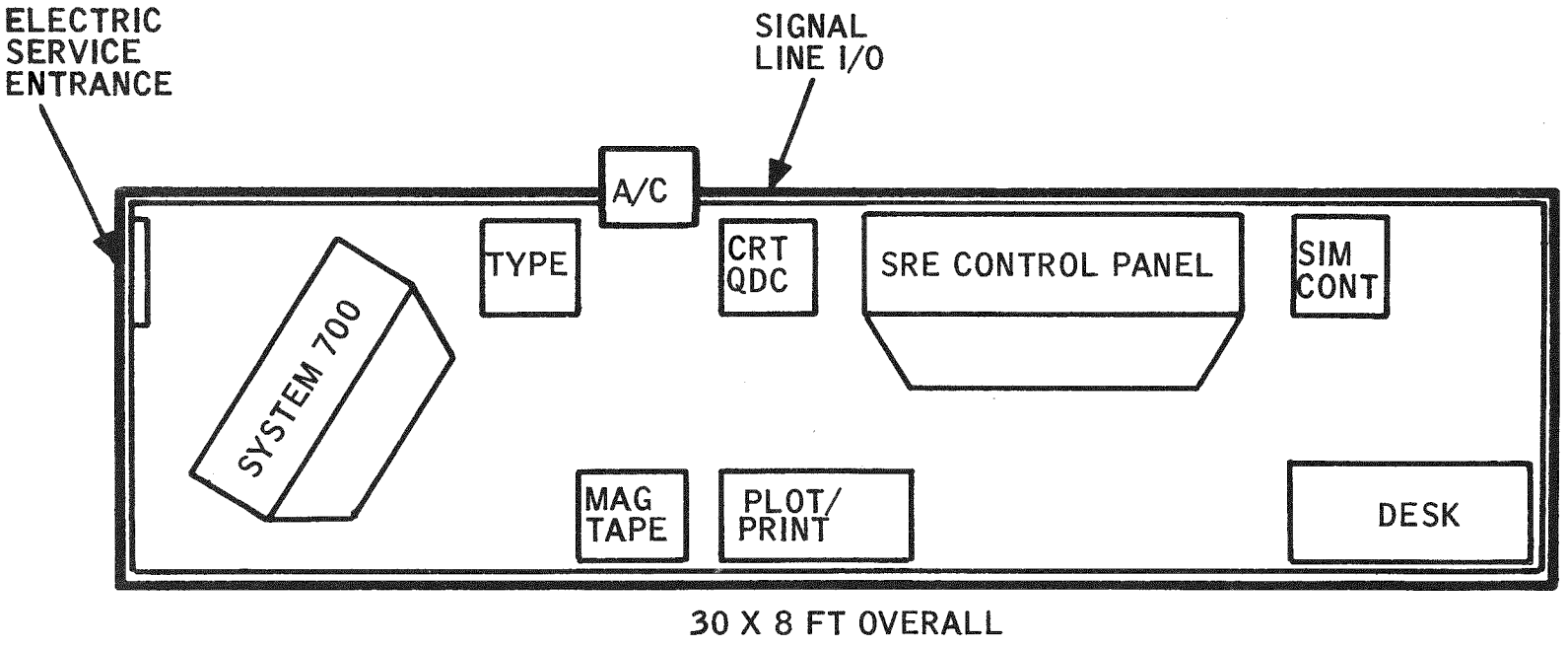

Figure 4-5. SRE Test Control Center

Test Control Design

Test Facility

SRE CONTROL PANEL CONFIGURATION

The SRE Control Panel will have the required controls and indicators to operate the SRE test items.

The receiver controls (Figure 4-6) will be on the left end of the panel. The thermal storage controls (Figure 4-7) will be the right half of the SRE control panel.

The SRE Control Panel is made up of set point controllers and indicators. The circles shown on the lower part of some items identify the set point controllers. Moving dial indicators and indicating recorders are also shown. The three larger squares are the indicating recorders.

The SRE Control Panel will resemble a conventional power plant control panel. The set point controllers and indicators will be functionally grouped.

The set point controllers are manual/automatic electrical controllers. The control signals are generated electrically and used to control pneumatic actuators on the SRE test items.

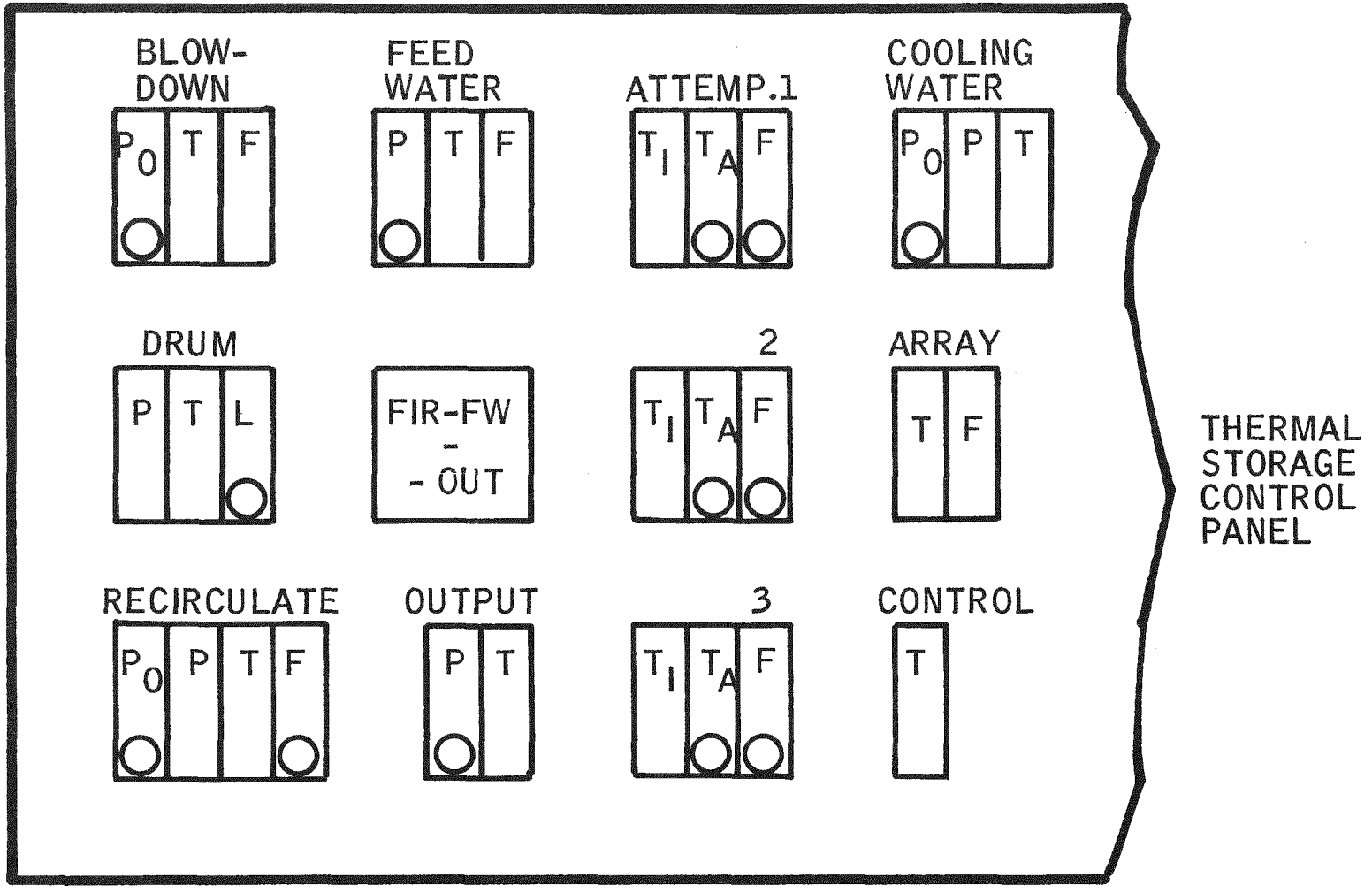

Figure 4-6. Receiver Control Panel

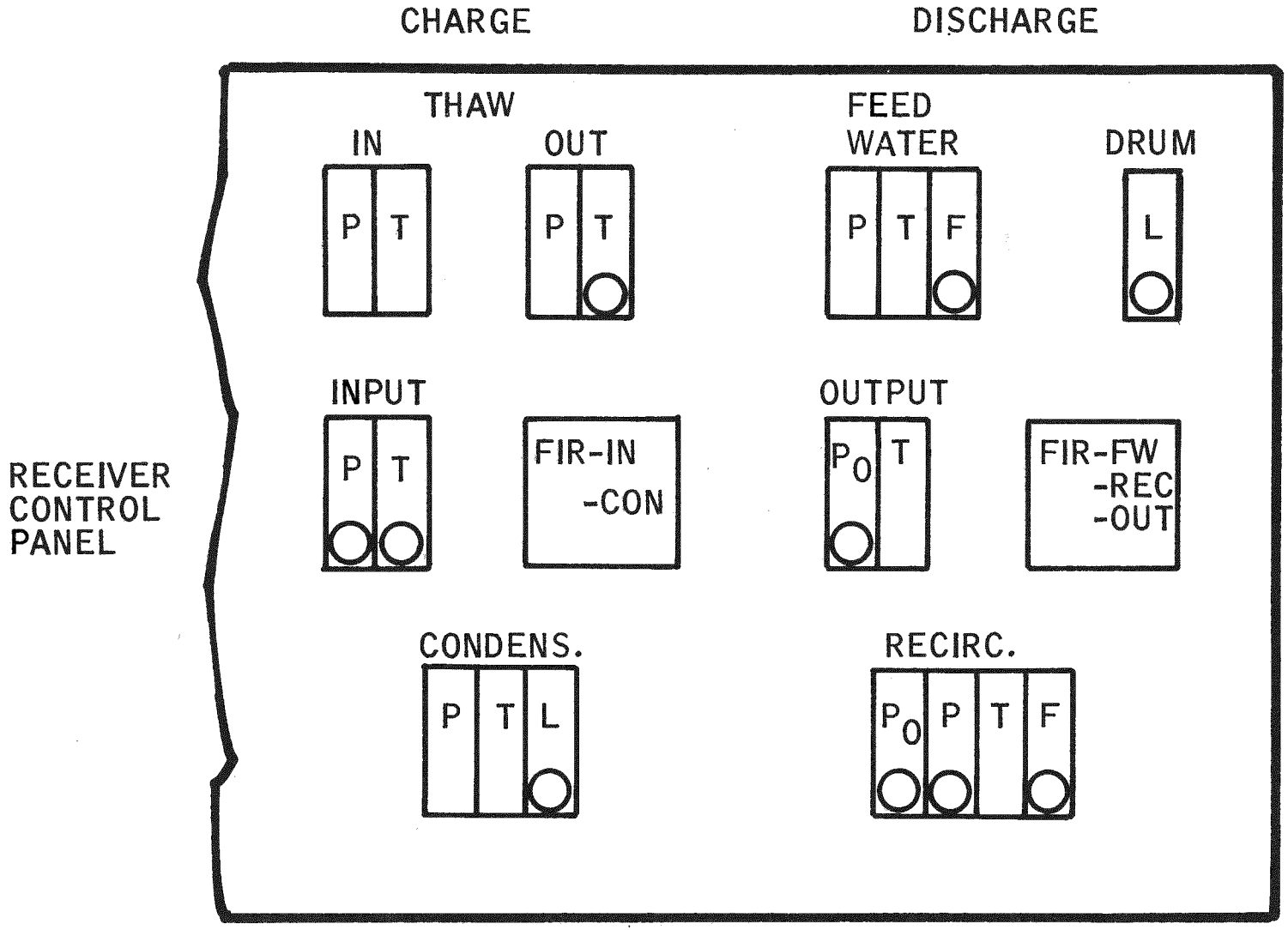

Figure 4-7. Thermal Storage Control Panel

This page left blank intentionally.

SET POINT/INDICATING CONTROLLER DESCRIPTION

VUTRONIK set point/indicating analog controllers will provide positive versatile control and display of the SRE test item operational parameters.

The VUTRONIK set point controller is a deviation from set point indicating device (Figure 4-8). The thumb wheel to the right of the indicating scale moves the scale such that the set point is always under the stationary (green) pointer. A deviation from set point is indicated by a red indicator emerging from behind the stationary green indicator. VUTRONIK indicators are essentially the same except the scale is moved to position the nominal reading in the center. The red pointer indicates a deviation from nominal operating point.

VUTRONIK set point controllers are manual/automatic control loop devices. Change over from auto to manual is by a switch located under a protective bar on the front of the controller. The control constants (gain, time constants, offsets) are adjustable on the side of each controller. The controllers can be rolled out as shown and the control constants adjusted without turning off the controller power.

In the event a controller fails, the unit may be replaced with a manual controller without shutting down the control panel. The faulty controller is extended to the rail limit (about 4 inches more than shown) and a smaller manual controller is plugged in. Plugging in the manual controller disconnects the primary unit so it can be unplugged and serviced. The test sequence may now be completed with the manual controller.

A high- and low-level alarm is provided on the set point controller or indicator. The levels are adjusted on the side of the device. When an alarm level is exceeded a light behind the mylar process name label is illuminated. Relay contacts are also provided to activate a remote audio alarm.

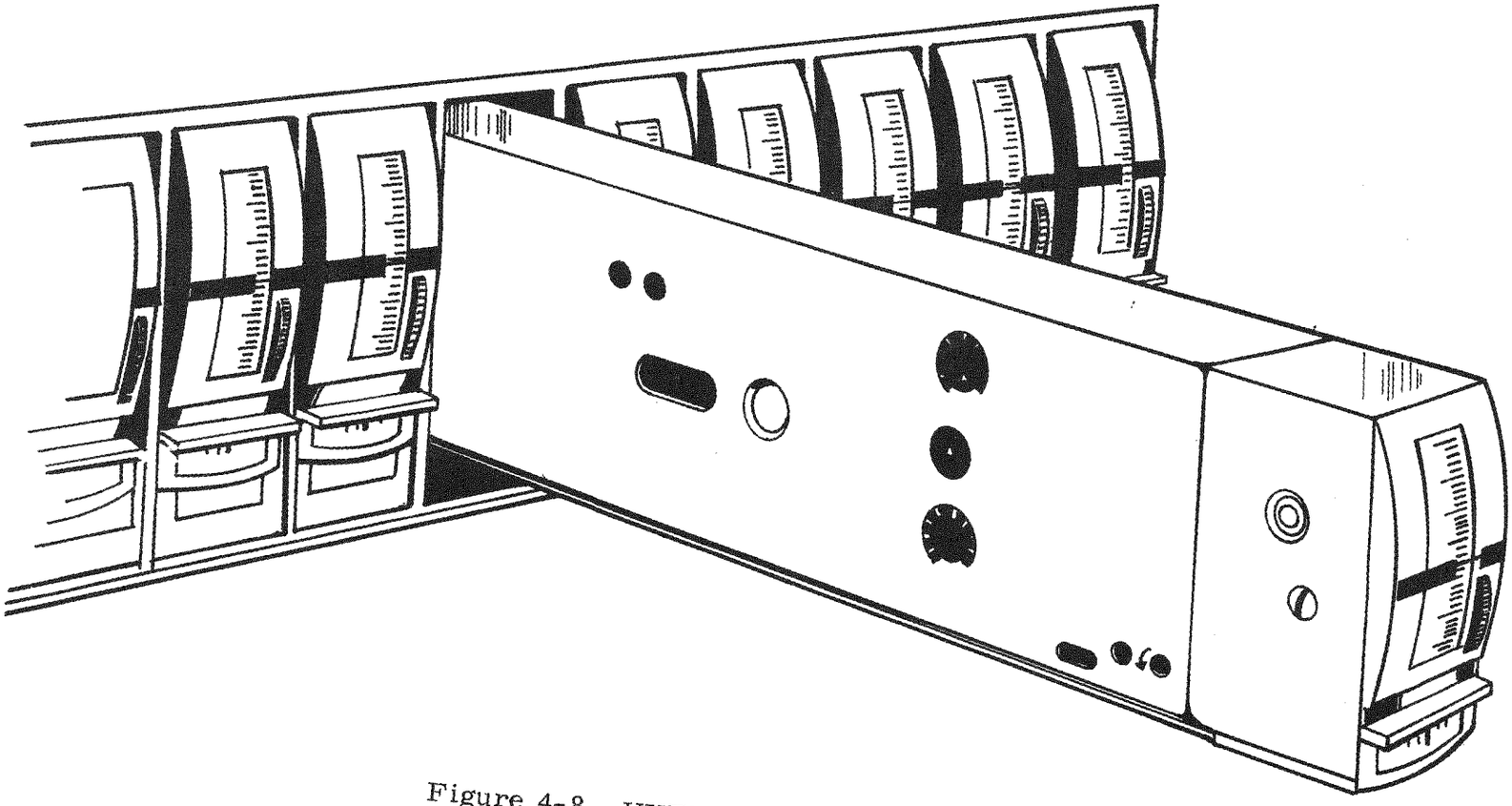

40284

Figure 4-8. VUTRONIC Controllers

SRE Data Acquisition System

REQUIREMENTS - OPERATIONAL

The DAC system must provide engineering data in real time to facilitate efficient - safe SRE testing and permanent records to document the test results.

The DAC system must measure all pertinent SRE operating parameters. Each measurement must be converted to process dimensions and stored. Data reduction and analysis calculations must also be performed (e.g., enthalpy and heat balance). All measured and calculated data must be available in real time and in a format easily used by test personnel. The data processing required is shown in Figure 4-9.

The DAC system measurement cycle must be short so SRE transient conditions can be defined.

The DAC system must perform limit tests on operating parameters. These limit tests must alert operating personnel when a parameter reaches its design maximum or alarm condition. Emergency shutdown independent of operator action should be considered and mechanized if feasible. Mechanization of a warning signal should also be considered. This warning would occur when a parameter deviates a significant distance from its normal operating level toward its design maximum level.

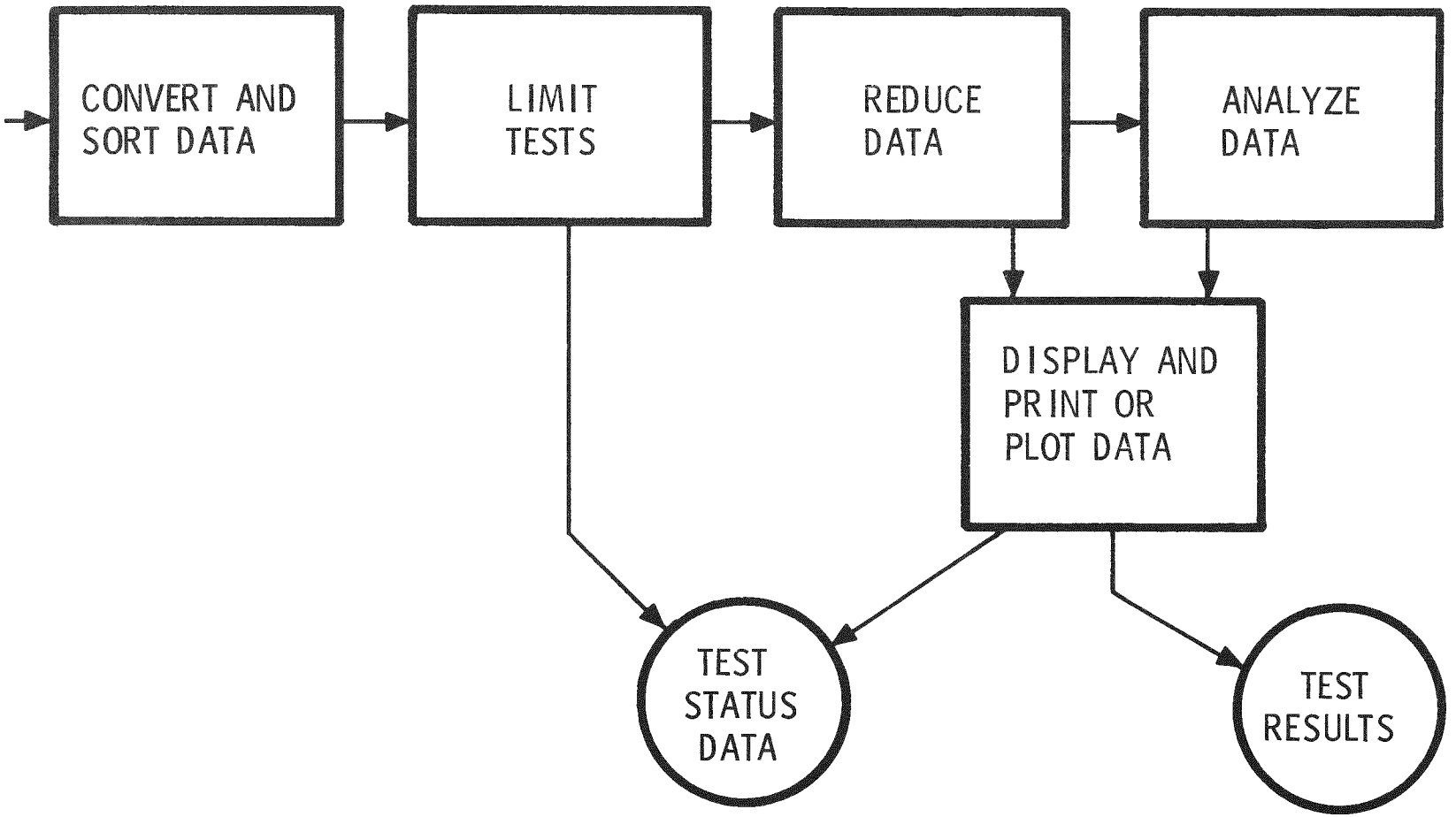

Figure 4-9. SRE Data Acquisition System Data Processing

Test Conceptual Design

SRE Data Acquisition System

REQUIREMENTS - SIZE

The DAC system must be sized to process all measured data of the receiver and thermal storage SRE tests.

Receiver and thermal storage SRE testing should use the same DAC system. Receiver and storage tests will not be performed simultaneously.

Table 4-2 lists the estimated number and duration of the receiver and storage SRE tests along with the number and type of measurement points. The receiver test measurement requirements will determine the size of the DAC.

Table 6-3. SRE Measurement Estimate

RECEIVER SRE TESTS (30-8 HOUR SEQUENCES)

400 TEMPERATURE POINTS

200 ANALOG POINTS (P, Δ P ETC.)

STORAGE SRE TESTS (30-1 TO 6 HOUR SEQUENCES)

57 TEMPERATURE POINTS
16 ANALOG POINTS

SRE Data Acquisition System

CONCEPT CONFIGURATION

The system 700 Process Analyzer will meet the DAC requirements.

The greatest advantage of the System 700 Process Analyzer (Figure 4-10) is its flexibility. Input flexibility will be exploited by using some of the receiver test inputs to measure all the storage test points. Data handling flexibility will be used to get optimum reduction, analysis and display records for both the receiver and storage tests.

Test measurements are made through the real time interface-multiplexer (RT1-MUX) of the System 700. The RT1 is expandable by eight input blocks. Temperature measurements on the SRE receiver test will require 50 (T.C.) input blocks. Temperature measurements on the storage SRE tests will use eight of these same input blocks. Twenty-five input blocks will be required by the analog (flow, pressure, etc.) measurements of the receiver SRE tests. Two of these analog input blocks will be also used for the storage SRE test instrumentation.

The System 700 sample rate is 125 points/sec. In the receiver SRE test, the measurement cycle time can be less than five seconds and the storage SRE measurement cycle can be less than one second. A five-second measurement cycle will be used for the shorter SRE test sequences. If the SRE response time constants are long enough, a "wait time" will be inserted between measurement cycles. The flexibility of the System 700 timing will also allow zero wait time during transient testing (power on, shutdown, load transients, etc.) and a nonzero wait time during steady-state tests.

Limit tests will be performed on all data taken. Rates of change as well as operating levels will be checked as part of each measurement cycle. Warning and alarm messages can be shown on the teleprinter, plotter-line printer and/or CRT display. The plotter-line printer will have a usage priority of: first-alarm messages, second-warning messages, and third-real time data display. Appropriate emergency action independent of operator action may be mechanized through relay contacts.

All measured data will be converted to process dimensions and stored. During each measurement cycle data reduction and analysis will be performed. All the measured and calculated data will be available for display. The display output format can be plots on the CRT or plotter (subject to the warning/alarm priority limitation) or tabulated on either of the three output media.

Permanent test history records will be made after each test sequence by the plotter-line printer. All data outputs will be in process dimensions. It will be desirable to have a complete tabular listing of some data. Other data will be more conveniently used in a reduced/analyzed and plotted format.

The DAC system will be controlled by a minicomputer. The computer software specification (SK133245) is included as Appendix H.

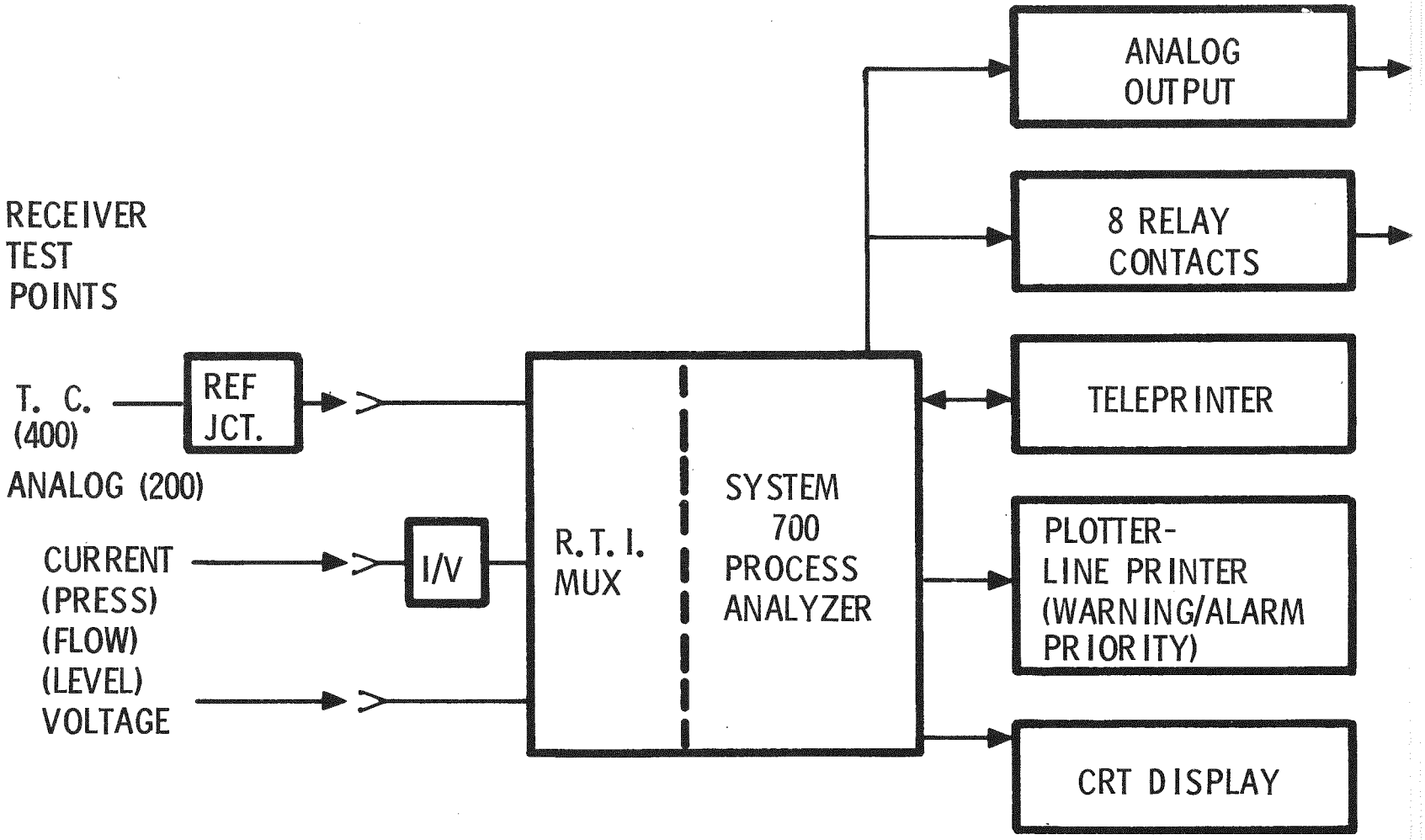

Figure 4-10. SRE Data Acquisition System Configuration

Test Conceptual Design

Test Operation

TEST CONTROL RATIONALE

SRE testing at Riverside will be controlled from a central monitoring location in a mobile trailer, which is adjacent to the steam generator test site.

The steam generator and thermal storage unit testing will be controlled from a central location in a mobile trailer, which is located on the turbine floor in the vacant No. 7 Unit location. Test instrumentation will be electronic with electrical-to-pneumatic conversion for operating the control valves. This instrumentation will be selected from the standard product lines of instrument control manufacturers. Instrumentation of this type provides fast and versatile control mode selection and range adjustment such that stable operation of the tests can be achieved. In addition, electrical transmission eliminates instrument piping between the mobile trailer and the remote test equipment.

In addition to the control system, a data acquisition system will be located in the mobile trailer. This system will accept 1 to 5 vdc signals from the control system which is indicative of the magnitude of the controlled parameters. The data acquisition will process these signals such that real-time information on test performance and outcome is available to the test operator. Moreover, the data acquisition system will provide a test supervision function to assist the test operator in the indication and control of "alarm" conditions.

While the control system will provide for maintenance of set-point accuracies typical of modern power station installations, the objective will be to provide accuracy in the "reading" of parameter values by the data acquisition system rather than maintaining absolute values by the control system. In this connection, temperature measurements for computation of steam and water flows and enthalpies will be made independently by the control and data acquisition systems using adjacent sensors in the flow steam. For the data acquisition system, these sensors will be thermocouples with direct millivolt outputs to the flow computation process.

For pressure and differential pressure measurements, the control system will first convert the measured value to a proportional 1 to 5 vdc signal for transmission to the data acquisition system. These pressure measurements will be made by converting pressure to electrical resistance using piezoresistive sensing elements. The transmitted electrical signal will reflect pressure magnitude with an accuracy typically 0.1 percent of instrument span.

The steam generator and thermal storage tests can be isolated from NSP services in an emergency by actuation of an air-failure-to-close isolation valve. Typically, emergency situations caused by equipment failure or operator error, will be presaged by audio/visual alarms to the operator followed up by automatic control action. The objective in the design of emergency controls will be to protect equipment and personnel in the event of any single component or source failure.

SUMMARY OF TEST CONTROL RATIONALE

- Electronic Control:
  - Fast response
  - Versatility as to control mode selection/adjustment
  - Minimizes instrument piping
- Data Acquisition System:
  - Accepts proportional 1 to 5 vdc signals
  - Can provide real-time test performance information
  - Provides a test supervisory function in the indication and control of "alarm" situations
- Set-Point Accuracy Secondary to Readout Accuracy:
  - Separate temperature measurement for control and data acquisition
  - Pressure measurement by piezoresistive sensing elements (no mechanical linkages)
- Emergency Control:
  - Isolation of test sites from NSP operations
  - Automatic interlock controls

Test Conceptual Design

Test Operation

THERMAL STORAGE CONTROL (DISCHARGE MODE)

Steam delivery at a selected pressure is controlled by the rate of recirculation through the boiler with drum-level control, incorporating a balance of feedwater and steam delivery rates.

The thermal storage unit receives feedwater in the discharge mode from the No. 6 Unit at Riverside. Feedwater at the station line condition (1450 psig, 370°F) is delivered into the unit through an air-fail-to-close isolation valve. Flow is then measured* with readouts to the control console, data acquisition system, and drum-level control subsystem. A schematic of the thermal storage control in the discharge mode is given in Figure 4-11.

The drum-level control subsystem is a three-element control using a feedforward signal from the existing steam flow to promote stable control. The level indicator-controller (LIC) maintains a selected drum level; but during transient conditions, its control function is biased by the action of the flow indicator-controller (FIC) which maintains a set relationship between feedwater and steam flows. The drum-level control subsystem is operated manually during start-up and shut-down.

Pressure in the drum is maintained by controlling the recirculation of water through the boiler. A pressure-indicator controller (PIC), which is responsive to drum pressure, controls throttling in the recirculation loop causing more or less evaporation to take place in the boiler to achieve the desired drum pressure. Steam delivery from the drum is controlled at operator discretion using the manual control station (P_oIC), which simulates the turbine throttle valve or load upon the system. Steam delivery is measured in the flow-measuring section before exhausting to the No. 6 condenser circulating water discharge. Another manual control station (P_oIC) is provided as a fixed trim control on the recirculation loop.

A three-channel recorder (FIR) located in the control panel gives visual indication and recording, as well as output to the data acquisition system, of feedwater delivery, recirculation rate, and steam delivery.

---

*Flow measurement involves inlet pressure and temperature at the primary element and differential pressure across the element.

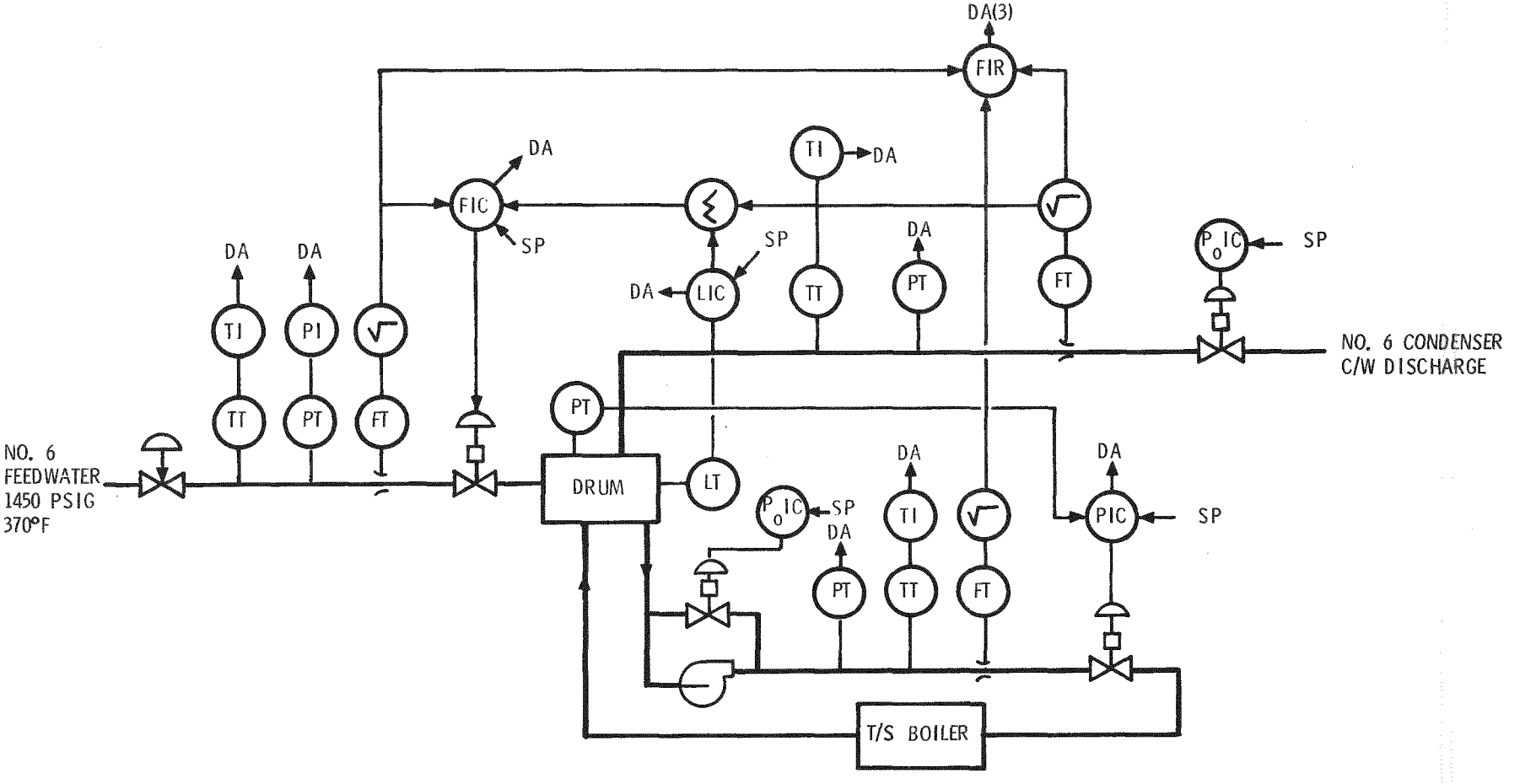

Figure 4-11. Thermal Storage (Discharge Mode) Control Schematic

THERMAL STORAGE CONTROL (CHARGE MODE)

Basic control of the thermal storage unit in the charge mode is by liquid-level maintenance in the condensate trap with selected pressure and temperature of charging steam.

In the charge mode, the thermal storage unit receives charging steam from the No. 8 Unit of Riverside at 2400 psig, 1000°F through an air-failure-to-close isolation valve. Throttling and desuperheating is done to bring the steam to test pressure and temperature. The pressure indicator-controller (PIC) operates the steam throttling valve to achieve pressure reduction; the temperature indicator-controller (TIC) controls the feedwater injection valve to obtain the desired temperature at the attemperator discharge. The flow of desuperheated steam is then measured, with indication and data acquisition readouts, before entry to the thermal storage condenser section. A schematic of the thermal storage control in the charge mode is given in Figure 4-12.

Condensate goes to the trap whose liquid level is maintained by the level controller (LIC) and the actuation of the condensate discharge valve. In effect, this controller regulates the condensation rate and system throughput. This throughput is measured in the flow-metering section of the condensate line before discharge to the No. 6 condenser circulating water discharge.

A "thaw" line, using steam from the No. 8 Unit, operates in the charge mode to initiate a liquid channel in the frozen salt, thereby preventing stress build-up due to the difference in densities of the molten and frozen salt. The "thaw" line may also be operated in a standby mode to maintain the liquid state in the salt tank.

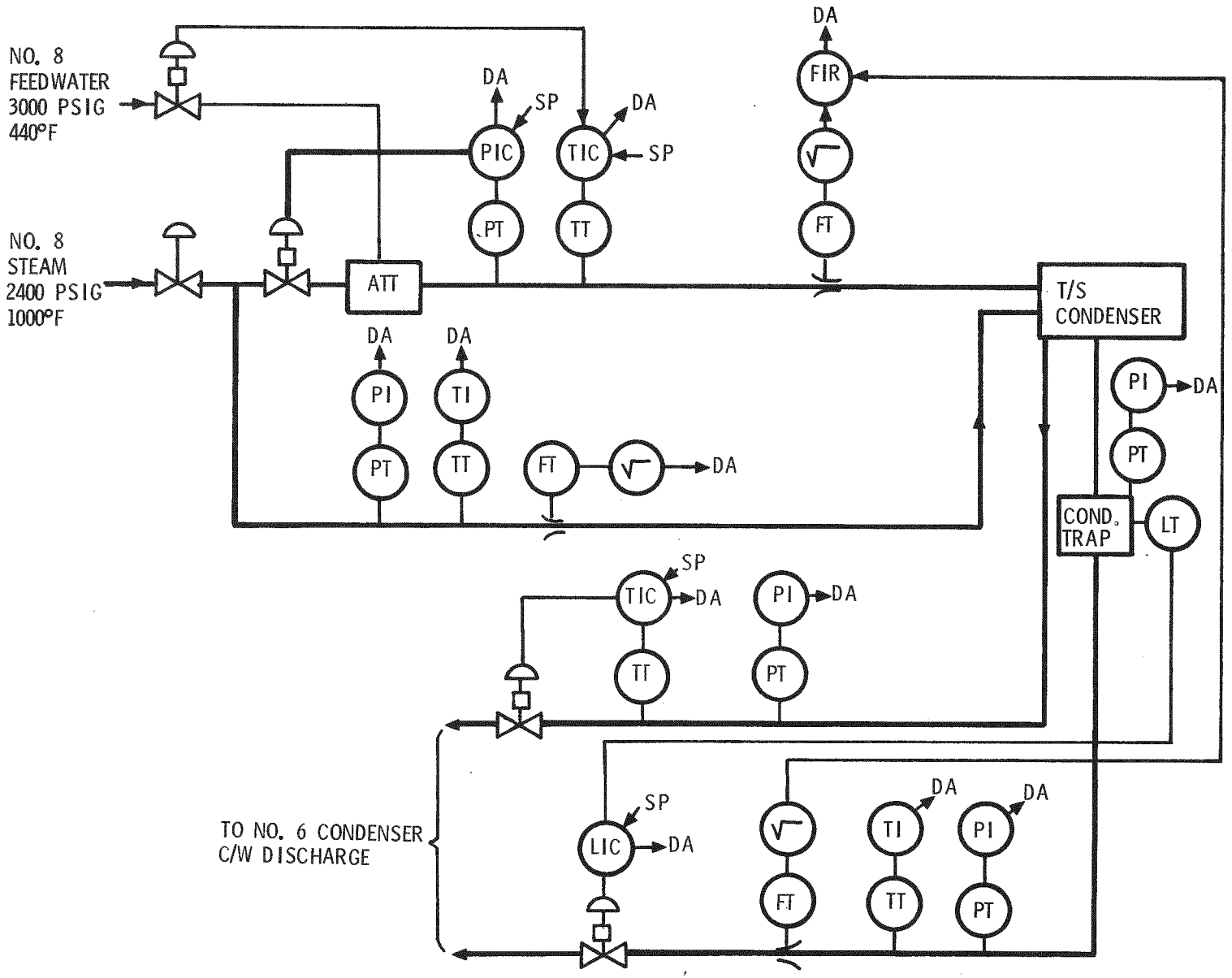

Figure 4-12. Thermal Storage (Charge Mode) Control Schematic

Test Conceptual Design

Test Operation

PROCEDURES

Operating procedures for the test will provide the necessary control of test equipment and test data.

SRE tests will be conducted in accordance with the predetermined test plan. The detail plan, established jointly between design and test personnel, will allocate approximately 30 days of test time in a 3-month test period. Test periods will alternate on approximately a daily basis with the receiver SRE tests. The tests will be allocated to include evaluation in the charge, storage, and discharge modes and combinations of these modes.

Test procedures will be standardized prior to testing to ensure that the test data is reliable, repeatable, and accurate. These procedures will be established based on the decreasing order of precedence: performance, safety, and cost.

Tests will be conducted in accordance with, and will be subject to, the conditions of the Thermal Energy Storage (TES) Subsystems Research Experiment (SRE) Design Specification.

This page left blank intentionally.

Test Conceptual Design

Test Operation

SUPPORT EQUIPMENT

Equipment is required to ensure that the experiment can be adequately serviced.

Nitrogen Supply

Dry nitrogen will be used to keep the molten salts clean and dry. Nitrogen will be supplied for SRE from a bank of six standard cylinders. A pressure regulator will be used on the system to maintain a pressure of approximately 1.38 kPa (0.2 psi) above the salt to exclude oxygen. A flow meter in the connecting system will be used to assure a steady supply of nitrogen gas. Seepage characteristics of the seals will govern the minimum necessary flow rates.

Lifting Equipment

The vaporizer sections and other major components will require mechanized lifting gear. Either a crane or small gantry-type lift will be stationed to permit removing the vaporizer sections. This equipment will enable the vaporizer and its scraping equipment to be readily serviced. This equipment shall be so situated as to not be damaged in the event of main tank leakage.

Observation Platform and Ports

Observation of the salt bath scrapers and mechanisms will be facilitated by covered ports. A suitable observation platform shall be installed either on or beside the SRE to permit observation and servicing of the system. A series of heavy duty, high temperature glass viewing ports shall be built into the SRE cover. Adequate interior lighting shall also be installed to permit visual observation of the system.

Ports which will permit insertion and removal of probes for temperature and specimen withdrawal shall be installed near the observation ports.

OPERATIONAL EQUIPMENT AND TOOLS

1. Overhead crane and necessary lifting attachments
2. Test frame for vaporizer sections for repair and listing
3. Washing equipment to remove salts from probes, and vaporizer section
4. Portable potentiometers
5. Probe type thermocouples
6. Power measuring equipment:
   a) Wattmeter
   b) Tachometer
   c) Torque meter
7. Test sampling probes
8. Pressure gauges
9. Electrical control panels/local control
   a) Switch gear for drives
   b) Lighting panels
   c) Auxiliary heaters
10. Ladders
11. Storage cabinets
12. Miscellaneous tools
13. Salt mixer
14. Weighing scales for mixing
15. Transfer containers for supplying salt to SRE

Test Conceptual Design

Test Operation

TEST SCHEDULE

The schedule for accomplishing the test program on time implies attention to the procurement of equipment and definition of events in chronological order.

The steam generator tests (Figure 4-13) will be accomplished at the NSP Riverside Plant. Preparation of the test site includes installing the required plumbing; steam lines, feedwater lines, water drain lines, vent lines, conditioning equipment, instrumentation, solar simulator and simulator power substation.

The test items will be installed following installation of the piping modifications performed in the plant. The substation will be installed prior to installing the steam generator because of installation space requirement interference. The solar simulator installation will take place after the steam generator is erected.

The control center will be assembled at the Honeywell Ridgway facility and transported to the NSP plant after construction of the pipes are modified, the simulator installed, and the steam generator erected.

The test area for the storage experiment will be prepared prior to the installation of the piping modifications required for storage test operation.

The storage tests will commence before the steam generator tests. Completion of the steam generator will be a pacing item because of the presently envisioned long-lead time for the recirculating pump delivery. Erection of the steam generator can proceed, however, with the pump installation being the last equipment to be installed.

Critical tests will be performed to meet the test requirements. It is planned to alternate test operation of the storage and steam generator on approximately a one to two day basis. Unexpected complications on one experiment should not delay operation of alternate testing.

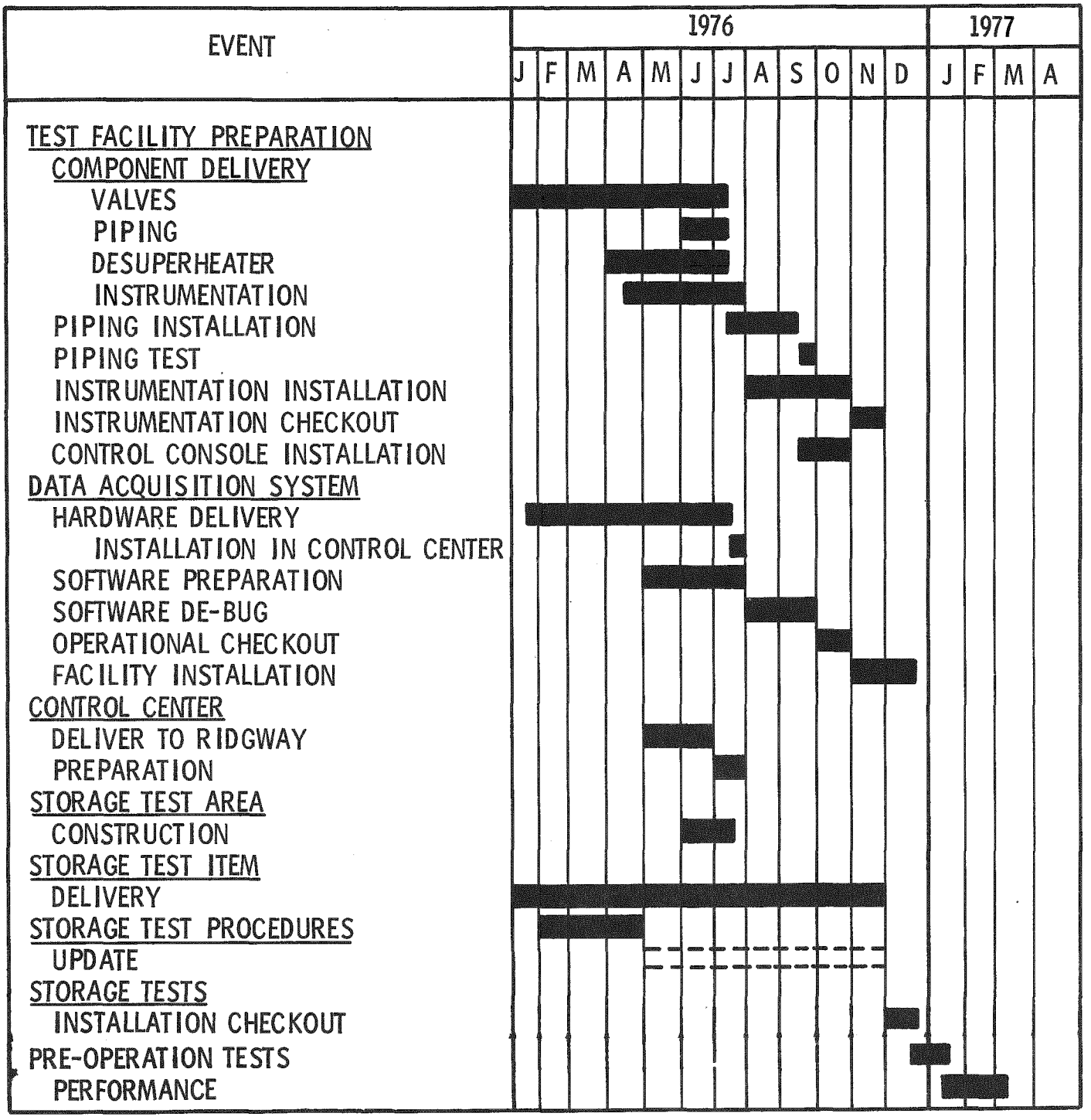

Figure 4-13. Storage SRE Test Schedule

SECTION V
PLANS AND SCHEDULES

LONG-LEAD-TIME ITEMS: THERMAL STORAGE (SRE) AND TEST ITEM INSTALLATION

The long-lead-time schedule assumes a July 15 piping installation start at Riverside and a November 30 completion of the test installation.

The long-lead-time items (Table 5-1) are those required for the installation and service of the SRE test item. These items are functionally shown on the piping and instrument diagram[1] and are based on vendor price and delivery responses. To date there have been several iterations of the piping and instrument drawing to effect design improvements and lower cost. Further refinements will be made during detail design, and these may result in costs somewhat different than those shown. The total cost indicated for long-lead-time items is about 90 percent of the total cost for test installation material.

The longest lead times are for check valves of larger size and higher-pressure-rated control valves.

[1] See Section IV: "Piping and Instrument Diagram No. M1004 - Storage Unit, SRE."

Table 5-1. Long Lead Time* Items - Thermal Storage (SRE) Test Installation

ITEM	ORDER DATE	DELIVERY DATE	COST
VALVES, CONTROL	1-15-76	7-15-76	$16,630
VALVES, MANUAL	1-15-76	7-15-76	6,190
VALVES, CHECK/RELIEF	1-15-76	7-15-76	1,790
DESUPERHEATER	3-31-76	7-15-76	4,340
INSTRUMENTATION	4-15-76	7-31-76	39,030
INSTRUMENT MANIFOLDS	3-15-76	7-15-76	4,600
			$72,580

* PRE-DDR

SCHEDULE

A schedule detailing the work plan is required to ensure that work proceeds in an orderly and timely manner.

The significant highlight of this schedule (Figure 5-1) is the continuation of engineering model tests during detail design (516 to 530). To date, the engineering model tests have been directed toward determining the heat transfer and scraper configuration for design of the SRE vaporizer. Condenser models have been designed but will not be tested prior to CDR (512). It is planned to construct various condenser tube bundle configurations to evaluate the overall effectiveness of tube arrangements.

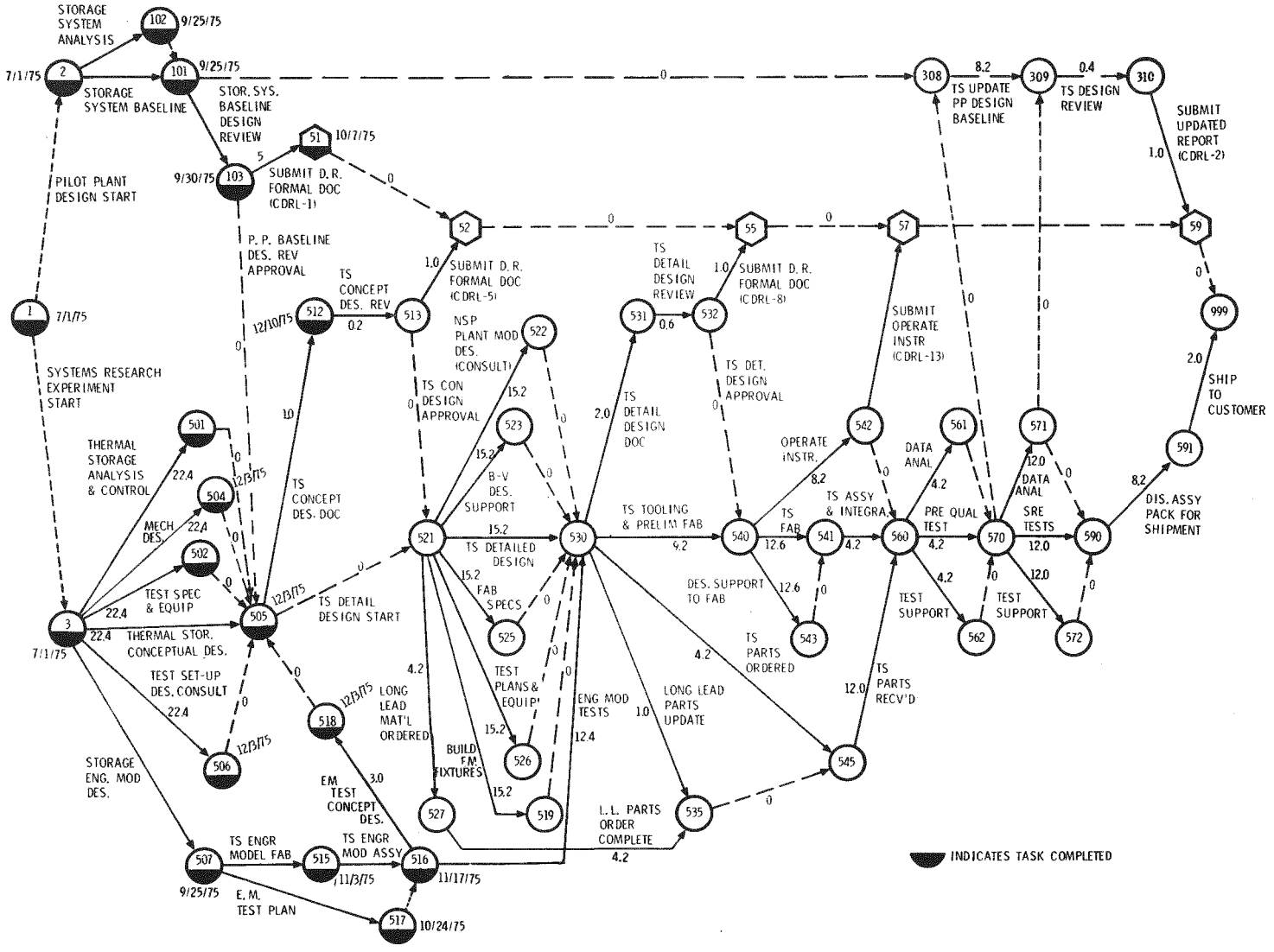

Figure 5-1. Solar Power Plant Program Thermal Storage

Plans and Schedule

SUPPLIER INFORMATION

Technical information from potential suppliers of equipment and components required for the Thermal Storage SRE is required to synthesize a realistic design concept.

Technical interchange of information was made with the following companies:

- Moorhead Machinery provided data and designs for the storage tank and steam drum.
- Brown Tank Co. provided data and designs for the storage tank and steam drum.
- Heatron supplied a sample of the spined finned tubing.
- Brown Fintube supplied, free of charge, 12-foot sections of helical and longitudinal finned tubes.

A more complete list of supplier information sources is provided in Table 5-2.

Table 5-2. Supplier Information Sources

Source	Data
Penn Separator Corporation, Brookville, PA	Fluid separators
Wright-Austin Co; Detroit, Michigan	Fluid separators and steam drums
Moorhead Machinery, Minneapolis, Minn.	Tanks and pressure vessels
Brown Tank & Fabricating Co.; Minneapolis, Minn.	Tanks and pressure vessels
Votator Div. of Chemetron Corp.; Louisville, Kentucky	Crystallizers with mechanical scrapers
Armstrong Co.; Westchester, PA	Crystallizers
Swenson Div. of Whiting Corp.; Harvey, Illinois	Crystallizers
Heatron Inc.; York, PA	Heat exchangers
Voss Finned Tube Products Inc.; Cleveland, Ohio	Heat exchangers
Brown Fintube Company; Tulsa, Oklahoma	Heat exchangers
Ecodyne; Massillon, Ohio	Heat exchangers
American Standard; Buffalo, N.Y.	Heat exchangers
Chicago Tube & Iron Co.; Chicago, Illinois	Pressure piping
Louis Larson Co.; Minneapolis, Minn.	Insulation
Kenny Boiler, Minneapolis, Minn.	Tanks and vaporizer tubes
Thompson-Hayward Co.; Minneapolis, Minn.	Phase-change materials
Betelle & Renwick, Inc.; Clark, N.J.	Phase-change materials
Armstrong Machine Works, Three Rivers, Michigan	Steam traps

APPENDIX A

THERMAL ENERGY STORAGE (TES) SUBSYSTEMS RESEARCH EXPERIMENT (SRE) DESIGN SPECIFICATION

Honeywell

SYSTEMS & RESEARCH CENTER Code Ident No. 27327

SPECIFICATION NO. SK 133242

TYPE: ☐ SYSTEM ☒ DEVELOPMENT ☐ PRODUCT ☐ OTHER

TITLE: THERMAL ENERGY STORAGE (TES) SUBSYSTEMS RESEARCH EXPERIMENT (SRE) DESIGN SPECIFICATION

SIGNATURES		DATE
PREPARED BY		
APPROVED BY PROJECT ENGR.	R. T. LeFrois R.T. LeFrois	12/12/75

REVISIONS

LTR	DESCRIPTION	DATE	APPROVAL	LTR	DESCRIPTION	DATE	APPROVAL

PAGE																																
REVISION																																
PAGE																															PAGE	OF
REVISION																															A-1	

HS-256

1.0 SCOPE

This specification establishes the design, performance, and test requirements for a Thermal Energy Storage (TES) Subsystem Research Experiment (SRE).

2.0 APPLICABLE DOCUMENTS

The following documents, of the latest issue, form a part of this specification to the extent specified herein. In the event of a conflict between the documents referenced herein and the contents of this specification, then the contents of this specification shall be considered a superseding requirement.

a. Preliminary Design Baseline Report, CDRL No 1., 30 Sept. 1975

b. American Society of Mechanical Engineers, Boiler and Pressure Vessel Code:

SECTION I	Rules for construction of Power Boilers
SECTION II	Material Specifications
SECTION V	Nondestructive Examination
SECTION VIII	Unfired Pressure Vessels
SECTION IX	Welding and Brazing Qualifications

c. American National Standards Institute

B31.1	Power Piping

d. Standards of the American Institute of Steel Construction and American Concrete Institute

e. Interstate Commerce Commission Shipping Standards Regulations

f. Uniform Building Codes

g. Standards for Tubular Exchanger Manufacturers Association, Class R

h. American Petroleum Institute Code 620,650

3.0 REQUIREMENTS

3.1 Thermal Energy Storage Subsystem Research Experiment TES/SRE Definition

The aim of the TES/SRE is to provide the necessary experimental test data

3.1 (Continued)

and operating experience to specify the design of an efficient, economical thermal storage subsystem for the Pilot Plant.

The Thermal Storage Subsystem Research Experiment shall provide a means of transferring thermal energy from a working fluid to a thermal energy storage medium and, subsequently, transferring stored thermal energy to a working fluid in a form suitable for generating electrical power with a conventional turbine/generator. The working fluids in the subsystem research experiment shall be the same as that in Solar Thermal Power System (Pilot Plant). The TES/SRE may consist of:

a) the inlet heat exchanger containing tubing, valves, and fittings required to transfer the thermal energy from the heat transfer fluid into the storage material.

b) the thermal storage tank, including the structure, insulation piping, foundation required for the containment of the phase change material and heat exchange surfaces.

c) the outlet heat exchanger, tanks, drums, pumps, valves, fittings, and tubing required to transfer the stored thermal energy to the working fluid.

d) the pumps, controls, required to safely regulate and direct the fluid flows and instrumentation to measure state and other parameters as necessary to quantify the required test parameters and variables.

The Thermal Storage Subsystem Reasearch Experiment test hardware shall have a thermal storage capacity of not less than 1 MW hours thermal and be capable of scaling to a capacity to provide thermal energy for a least 7 MW(e) net for 6 hours for the Central Receiver Pilot Plant and larger for the commercial power generating system if possible.

3.1.1 Thermal Storage Subsystem Research Experiment Diagram

Figure 1 shows a schematic of the Thermal Storage Subsystem Research Experiment and its interfaces.

3.1.2 Interface Definition

The physical and functional interface between the Thermal Storage Subsystem Research Experiment and facility or elements thereof are as follows:

3.1.2.1 Fluid

Piping, connections and mounting fixtures shall be provided at the facility at the following fluid interfaces:

STORAGE SRE INTERFACES

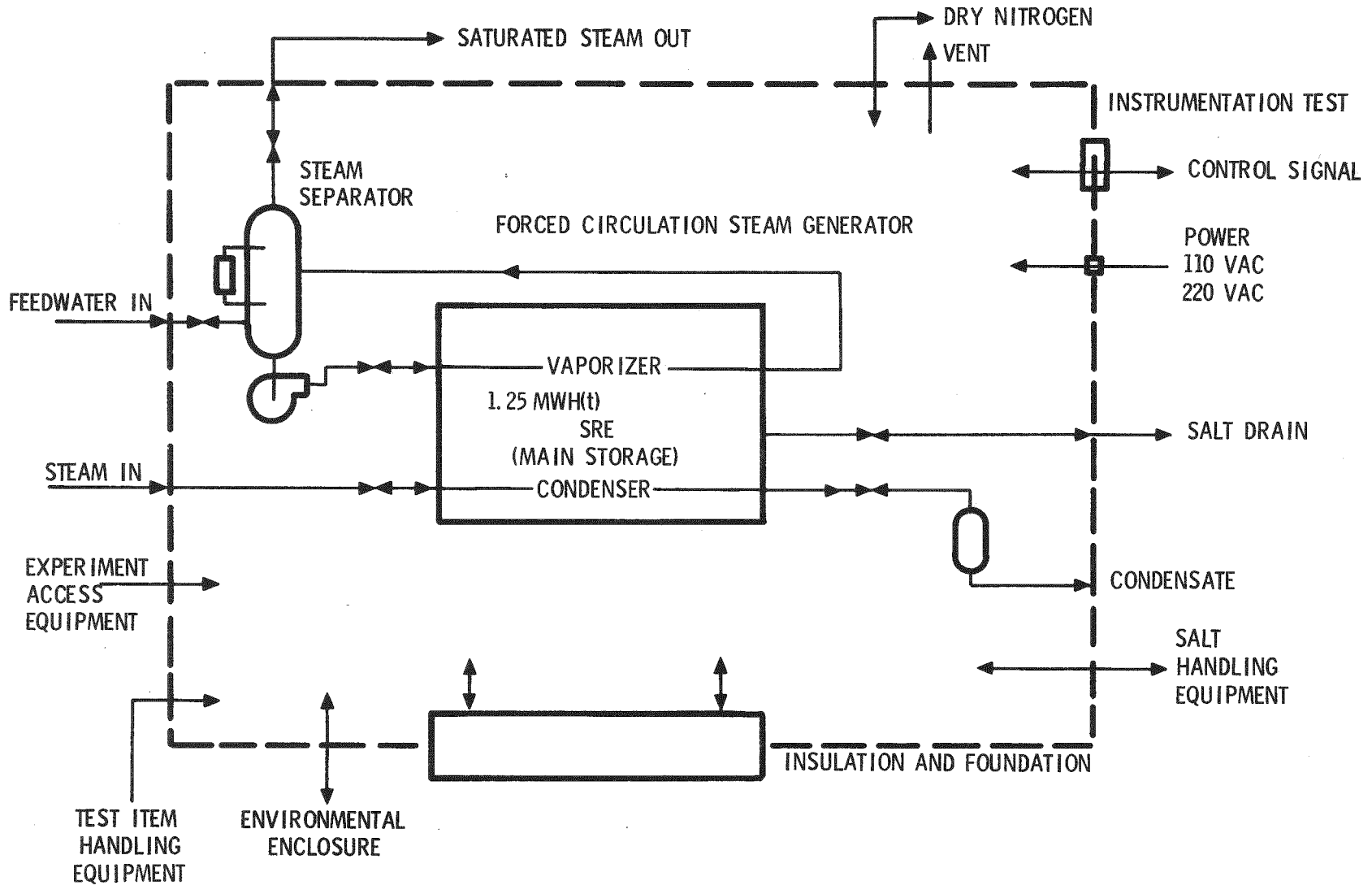

3.1.2.1 Fluids (Continued)

a) Entrance and exit of the charging working fluid

b) Entrance and exit of the discharging working fluid

c) Salt drainage

d) Gases used in the operation, including instrument air and gaseous nitrogen.

3.1.2.2 Electrical Power

Electrical power to the test item shall be provided at a junction box within the test enclosure. It shall contain 120 VAC and 240 VAC at TBD and TBD KVA, respectively. This power shall be used to drive test item motors and auxiliary equipments. The auxiliary equipment includes heaters used to melt the phase change materials which require 55 KW power.

3.1.2.3 Instrumentation - Test Data

All test data instrumentation output shall terminate at a patch panel located within the test item enclosure. The instrumentation shall make it possible to measure and record temperatures, pressures, mass flows, heat loss, thermal capacity and other special parameters taken during the test. The instrument accuracies shall permit an overall heat balance to be determined to within ±3%.

3.1.2.4 Instrumentation - Process Data

All process data instrumentation shall terminate at a patch panel located within the test item enclosure. This instrumentation shall insure that the process is properly functioning and shall provide appropriate signals for automatic shutdown of the operation when necessary. This shall include monitoring the inlet and outlet fluid conditions, the ullage pressure, tank drain status, feedwater recirculation rate, and fluid levels.

3.1.2.5 Facility Foundation

A raised pad shall be provided to support a rectangular storage tank with a dead weight load not to exceed 45500 kg and a cold face temperature not to exceed 316°C for its operating life. The tank/foundation interface shall withstand seismic loads corresponding to zone 2 intensity.

3.1.2.6 Environmental Enclosure

An enclosure shall be provided to insure protection from the elements, i.e., snow, wind and rain and provide space conditioning to the storage unit to 18°C ± 8C° during winter operations. The enclosure shall allow for installation and removal of the test unit as well as draining and filling the tank with the phase change material.

3.1.2.7 Support Equipment

Equipment to install, remove or repair the test unit or its components, shall be provided. Equipment shall be provided to insure the safe handling and preparation of the phase change material at the test site. Electric heaters shall be provided to permit the melting of the phase change material in the event of a malfunction. Containers or receivers shall be supplied to permit the tank to be drained in an efficient manner. Special tools and test equipment shall be provided to install, maintain, repair or replace critical storage components and to provide access where required.

3.1.2.8 Thermal Storage Subsystem Experiment Controls/Master Controls

The Thermal Storage Subsystem Research Experiment controls shall be responsive to standard control signals from the master control center or may be remotely manual or manual if adequate safety requirements are met.

3.2 Characteristics

3.2.1 Performance

The Thermal Subsystem Research Experiment test hardware shall have a thermal storage capacity of not less than one Megawatt hour operating and be capable of scaling to a capacity to provide thermal energy for at least 7 MW(e) for 6 hours for the Central Receiver Pilot Plant and larger for the commercial generating system. The working fluid conditions shall be (100 bars) saturated steam for charge cycle and the output steam from subsystem experiment shall be staurated steam at (47.6 bars). Adjustment of stable conditions for proper scaling will be allowed.

Specific design characteristics of the Thermal Storage Subsystem Research Experiment shall be provided as follows:

a. The design shall be based on scaling a quarter size of the Pilot Plant Unit Cell described in Preliminary Design Baseline, CDRL NO. 1. The output from the thermal shorage unit shall be equivalent to 23 boiler horsepower and will represent 1/16 of the power generated by the unit cell.

b. The design shall maximize the recovery of useful thermal energy from storage consistent with cost and performance considerations.

3.2.1 Performance (Continued)

c. The deisgn shall provide for the control of the conductive, convective and radiative thermal losses. The allowable losses are 10% of the total storage capacity over a period of 4 days.

d. Instrumentation and controls shall respond to transient conditions rapidly enough to prevent any adverse effects with regard to the safety and operation of the research experiment and the facility interfaces thereof.

e. The design shall provide for the removal of crystallized salt from the outside of the vaporizer tubes. Primary consideration should be given to mechanical techniques. In addition, it may be necessary to "de-ice" the vaporizer tubes during the course of an experiment in an attempt to evaluate various salt removal techiques. Consequently, the design should be capable of supplying facility steam to the vaporizer tubes at a temperature above the eutectic salt temperature.

f. The design shall provide for the salt input of plant steam heat to melt the salt in the storage tank. The salt may be in a granular or crystallized state. When in either of these states a liquid vent, protuding through the solid bulk must be insured prior to transferring steam heat at rated conditions.

3.2.2 Physical Characteristics

The Thermal Storage Tank shall be rectangular in shape. The dimensions shall be based on geometric scaling to the greatest extent possible. The weight of the tank with salt heat exchangers, insulation, cover and attached base support shall not exceed 46,000 kg (101,200 lb.). The outside envelope dimensions, of the insulated tank shall not exceed (4.6 meter) in height, (3.28 meter) in width and (4.6 meter) in length. The base of the tank shall be located sufficiently above local grade to allow gravity drain of the salt. The tank shall be filled with salt from the top. The tank closure must allow for accessability for salt loading, handling, equipment installation's removal.

3.2.3 Reliability

Consideration shall be given in the data gathering system and operating procedure in the Thermal Storage Subsystem Research Experiment to permit extrapolation of useful reliability data for Pilot Plant Design.

3.2.4 Maintainability

Consideration shall be given in the data gathering system and operating procedures on Thermal Storage Subsystem Research Experiment design to permit extrapolation of useful maintainability for Pilot Plant Design.

3.2.5 Environmental Conditions

The Thermal Storage Subsystem Research Experiment shall be designed to withstand natural environmental conditions expected to be encountered during installation within an environmental enclosure and operation at NSP Riverside plantsite in seismic zone 2. Electrical components shall be protected from electrical distrubances and currents.

3.2.6 Transportability

Transportation of all elements of the Thermal Storage Subsystem Research Experiment to the test site shall be subject to all pertinent federal and state transportation regulations. The storage subsystem may be shipped disassembled as required.

3.3 Design and Construction

The Thermal Storage Subsystem Research Experiment shall be designed and constructed in accordance with the applicable ASME and API Codes. Piping shall meet cable ANSI codes. Structures, facilities and enclosures shall be designed and constructed in accordance with the best engineering practices and the Standards of the American Institute of Steel Construction, American Concrete Institute, Uniform Building Code, and special state codes where applicable.

3.3.1 Materials

The Thermal Storage Subsystem Research Experiment components shall be fabricated from materials as specified in the applicable specifications or codes.

3.3.2 Phase Change Materials

The thermal energy storage medium shall be a phase change material, single salt or a mixture of inorganic salts of a particular composition. The material of fabrication shall be compatible to the storage medium with regard corrosion to containment.

3.3.3 Electrical Transients & Grounding

The electrical components of the Thermal Storage Subsystem Research Experiment shall be protected against normal power line and sudden power outages transients and all required elements grounded.

3.3.4 Nameplates

All components, instruments, and controls shall have identifying markings on nameplates which shall be permanently attached to the respective items.

3.3.5 Workmanship

The Thermal Storage Subsystem Research Experiment and all associated items shall be constructed, fabricated and assembled in accordance with the best modern engineering, shop, and field practices, consistent with cost and performance requirements.

3.3.6 Interchangeability

Components, with standard tolerances where available, shall be used to permit interchangeability for servicing. Consideration shall be given to components to permit extrapolation of useful part selection function data to the Pilot Plant Design.

3.3.7 Safety

The Thermal Storage Subsystem Research Experiment shall be designed to minimize safety hazards to operating and service personnel and the public. Electrical components shall be grounded. All parts or components with elevated temperatures shall be insulated against contact with or exposure to personnel. Any moving elements shall be shielded to avoid entanglements and safety override controls shall be provided for servicing. Safe salt handling and mixing equipment shall be used to prevent any direct contact to personnel. All pertinent OSHA rules and regulations shall be observed. Design of the storage tank shall accomodate a rupture causing spillage of the maximum tank salt contents of 20,500 kg (45,000 lb.). The spillage must be contained with a designate area. Design of the storage tank shall also consider rupture of the high pressure wate and/or steam tubing causing ullage pressure increase with possible tank failure.

3.3.8 Public Display

It is anticipated that the thermal storage SPE will stimulate considerable public interest and the test facility will be inspeced from time to time by the public, public officials and other dignitaries. The test item, facility and immediate area should be designed to meet this scrutiny.

3.4 Documentation

3.4.1 Instructions

Instructions shall cover assembly, installation, alignment, adjustment, checking, lubrication, salt handling and mixing, and maintenance. Operating instructions shall be included for startup, routine and normal operation, regulation and control, shutdown, salt draining, and emergency conditions.

3.4.2 Characteristics and Performance

Equipment functions, normal operating characteristics, limiting conditions, test data, and performance curves, where applicable, shall be provided.

3.4.3 Construction

Engineering and assembly drawings shall be provided to show the equipment construction, including assembly and disassembly procedures. Engineering data, wiring diagrams, and parts list shall be provided.

4.0 QUALITY ASSURANCE PROVISIONS

Verification of conformance to designs and drawings as approved by ERDA at the DDR is required prior to initiation of the subsystem tests.

4.1 Test Program

All tests will be directed by Honeywell Incorporated. These tests may be witnessed by ERDA or its representatives or the witnessing may be waived. In either case, substantive evidence of hardware compliance with all test requirments is required. All tests will be conducted per a formalized test plan and procedure.

4.1.1 Engineering Test and Evaluation

The performance of the instrumentation and control system shall be measured to verify compliance with power level control requirements, cooling requirments, emergency responses, and ability to maintain total system control under variable test conditions.

4.1.1.1 Thermal storage performance shall be tested to demonstrate the effective transfer of heat energy to the storage medium using the working fluid same as that available from the Receiver Subsystem in the Central Receiver Solar Thermal Power System Pilot Plant, to verify the storage of heat energy, and also to demonstrate the generation of steam vapor comparable as in Pilot Plant, Unit Cell.*

4.1.1.2 Mechanical integrity shall be verified by subjecting the Thermal Storage Subsystem Research Experiment to simulated operating conditions for various environmental situations.

4.1.1.3 Thermal storage controls will be tested to verify that they respond to standard control signals and function over the full range of operating conditions.

4.1.1.4 Thermal Storage Cycling and Off Design

Capability will be tested to determine the useful life of the phase change material and to insure that the system is capable of responding to the full range of conditions anticipated in the pilot plant operations.

* Tests shall be conducted to demonstrate that the Thermal Storage unit can be simultaneously discharged while charging.

4.1.1.5 Thermal Storage Phase Change Material Safety

It shall be verified that the use of inorganic salts as storage medium is not hazardous.

4.1.2 Preliminary Qualification Tests

Hydrastate tests of the vessels and tanks shall be accomplished per the applicable code at the manufactures facility or prior delivery to the NSP test facility. Pressure piping tests can be conducted on site. Subsequent to assembly on the test pad pre-operational, tests shall conducted prior to starting the operational testing.

4.1.3 Life tests and Analysis

Results from the tests will be reviewed and conponents requiring life test data and analysis be recommended to ERDA for a specific test program.

4.1.4 Engineering Critical Component Qualification

Components for which reliability data are not available nor estimatible from the test program shall be identified to ERDA for consideration of additional testing.

APPENDIX B

TEST SPECIFICATION, THERMAL ENERGY STORAGE (TES), SUBSYSTEMS RESEARCH EXPERIMENT (SRE)

Honeywell

SYSTEMS & RESEARCH CENTER Code Ident No. 27327

SPECIFICATION NO. SK 133248

TYPE: ☐ SYSTEM ☒ DEVELOPMENT ☐ PRODUCT ☐ OTHER

TITLE: TEST SPECIFICATION,
THERMAL ENERGY STORAGE (TES)
SUBSYSTEMS RESEARCH EXPERIMENT (SRE)

SIGNATURES	DATE
PREPARED BY	
APPROVED BY PROJECT ENGR. R. T. LeFrois R. T. LeFrois	12-12-75

REVISIONS

LTR	DESCRIPTION	DATE	APPROVAL	LTR	DESCRIPTION	DATE	APPROVAL

PAGE																															
REVISION																															
PAGE																														PAGE	OF
REVISION																															

HS-256

TABLE OF CONTENTS

Page

SECTION 1. PURPOSE

SECTION 2. SCOPE

SECTION 3. REFERENCE DOCUMENTS AND DEFINITIONS

SECTION 4. CLASSIFICATIONS

SECTION 5. REQUIREMENTS

SECTION 6. INSTRUMENTATION

SECTION 7. TEST PROGRAM OF TESTING

SECTION 8. TEST PROCEDURE AND CALCULATIONS

SECTION 9. DATA TO BE RECORDED AND TEST REPORT

SECTION 10. NOMENCLATURE

SECTION 11. REFERENCES

TABLES

FIGURES

1.0 PURPOSE

The purpose of this specification is to provide standard test and evaluation procedures for determining the design and performance characteristics of a Thermal Energy Storage (TES) Subsystem Research Experiment (SRE).

2.0 SCOPE

This specification applies in general to thermal energy subsystems and in particular to the latent-heat type storage system described in the reference documents.

This specification is subordinate to the DESIGN SPECIFICATION for the TES/SRE in case of conflicts.

The constraints on this specification are subject to the interface requirements at the test site.

3.0 REFERENCE DOCUMENTS & DEFINITIONS

1. Preliminary Design Baseline Report, CDRL No. 1, 30 September 1975.
2. Thermal Energy Storage (TES) Subsystem Research Experiment (SRE) Design Specification.
3. Method of Testing for Rating Thermal Storage Devices Based on Thermal Performance, NBSIR-74-634, May 1975.
4. ASHRAE Standard 41-66.
5. ANSI Standard C96.1-1964.
6. ASME Performance Test Codes:

Pressure Measurement	PTC 19.2	1964
Temperature Measurement	PTC 19.3	1974
Water & Steam in Power Cycle	PTC 19.11	1970

7. ASME Power Test Codes:

Steam Generating Units	PTC 4.1	1964
	(ANSI PTC 4.1	1974)

3.1 Ambient Air

Ambient air is the air in the space surrounding the thermal energy storage system.

3.2 Cycling

Cycling of a latent-heat type storage device is a process in which the temperature of the system is raised and lowered in a cyclic manner and the phase of the storage medium is changed twice in each temperature cycle.

3.3 Effective Capacity for Heat Removal

The effective capacity for heat removal is the amount of heat that can be removed from the storage system during a period of time.

3.4 Effective Capacity for Heat Storage

The effective capacity for heat storage is the amount of heat that can be stored in the storage system during a period of time.

3.5 Fill Time

The fill time is the duration of a single transient test in which energy is either added or extracted from the storage system.

3.6 Rate of Heat Loss

The heat loss rate is the rate that heat is lost from the storage system per degree temperature difference between the storage medium temperature and the average ambient air temperature.

3.7 Total Storage Capacity

The storage capacity of a thermal energy storage system is defined as the heat that can be stored in a system including the sensible and latent portions.

3.8 Performance Coefficient for Heat Removal

The performance coefficient for heat removal is the ratio of the effective capacity for heat removal to the amount of heat that could be removed from an equal volume of water in an ideal water tank under the same conditions.

3.9 Performance Coefficient for Heat Storage

The performance coefficient for heat storage is the ratio of the effective capacity for heat storage to the amount of heat that could be stored in an equal volume of water in an ideal water tank under the same conditions.

3.10 Standard Air

Standard air is weighing 1.2 kg/m^3 (0.075 lb/ft^3), and is equivalent in density to dry air at a temperature of 21.1°C (70°F) and a barometric pressure of 1.01×10^5 N/m^2 (29.92 in. of Hg.).

3.11 Standard Barometric Pressure

1.01×10^5 N/m^2 (29.92 in. of Hg.).

3.12 Storage Medium

The storage medium is the material in the storage system in which the major portion of the energy is stored.

3.13 Storage System

The storage system is defined as the container(s) plus all contents of the container(s) used for storing thermal energy in a system. The transfer fluid and other accessories such as heat exchangers within the thermal storage container(s) are considered as part of the storage system.

3.14 Specific Heat

The specific heat of a substance is the quantity of energy necessary to produce a unit change in temperature of a unit mass.

3.15 Transfer Fluid

The transfer fluid is the fluid that carries energy in and out of the storage system.

4.0 CLASSIFICATION

In this specification storage systems are classified according to the method they use to store energy and the transfer fluid employed.

Latent-heat storage system are those involving a change of phase of the storage medium. In this type of system, most of the heat added to or removed from the system goes into changing the enthalpy of the storage medium during a change of phase process. Some heat is also stored as sensible heat, since charging and discharging of the storage device usually involves a finite change in the temperature of the system.

Sensible heat storage systems are those in which the heat absorbed by or removed from the system results in an increase or decrease in the temperature of the storage medium and there is no change of phase of any portion of the storage medium. Typical systems employ pressurized water, unpressurized water, rock, brick or concrete as the storage medium.

A storage system will use either a liquid or a gas as the transfer fluid. The most common liquids are water or a water-ethylene glycol solution. The most common gas is air.

The TES/SRE baseline subsystem is a latent-heat system which employs steam as the transfer fluid and an eutectic salt as the storage medium.

5.0 REQUIREMENTS

5.1 Latent-heat type storage systems evaluated under this specification shall have been cycled (see definition of cycling) through their change of phase at least 30 times prior to being tested.

5.2 The transfer fluid used in evaluating the performance of a thermal energy storage system shall have a known property over the temperature range encountered during a test.

5.3 The area where the testing of the storage system is performed shall have its temperature controlled to the extent to be specified.

5.4 Manually recorded data shall be logged in "controlled" data books (Honeywell or equivalent). Control of these records shall be by name and book number.

5.5 Tests shall be logged as to date, run time, objective etc. and shall be in accordance with a predetermined, detail test plan.

5.6 Data accuracies are subject to the overall accuracy of the TES/SRE DESIGN SPECIFICATION. Accuracy budgets can be adjusted accordingly.

6.0 INSTRUMENTATION

6.1 Temperature Measurements

6.1.1 Temperature measurements shall be made in accordance with ASHRAE Standard 41-66, Part 1 (1) and ASME PTC 19.3 1974.

6.1.2 The temperature difference of the transfer fluid across the thermal storage system shall be measured with:

a. Thermopile (air or liquid as the transfer fluid)

b. Calibrated resistance thermometers connected in two arms of a bridge circuit (only when a liquid is the transfer fluid)

6.1.3 The accuracy and precision of the instruments and their associated readout devices shall be within the limits TBD.

6.1.4 The instruments shall be configured and used in accordance with Section 7.

6.1.5 When thermopiles are used, they shall be constructed in accordance with ANSI Standard C96.1-1964 (R 1969) 2 .

6.2 Liquid Flow Measurements

6.2.1 The accuracy of the meter including a calibration, if furnished, shall be equal to or better than ±1.0% of the measured value.

6.3 Recorders and Integrators

6.3.1 Strip chart recorders used shall have an accuracy equal to or better than ±0.5% of the temperature difference and/or voltage measured for each test with the exception of the heat loss rate test. In the test to determine the heat loss rate, the accuracy of the strip chart recorder shall be equal to or better than ±2.0%.

6.3.2 Electronic integrators used shall have an accuracy equal to or better than ±1.0% of the measured value for each test with the exception of the heat loss rate test. In the test to determine the heat loss rate, the accuracy of the electronic integrator shall be equal to or better than ±4.0%.

6.4 Pressure Measurements

6.4.1 The pressure measurement shall be made with instruments that shall permit measurements of pressure to within ±2.0% absolute and whose smallest scale division shall not exceed 2 1/2 times the specified accuracy.

6.4.2 The static pressure drop across the thermal storage system shall be measured with an accuracy of 2.49 N/m^2 (0.01 in. of water).

6.5 Time and Mass Measurements

Time measurements and mass measurements shall be made to an accuracy of ±0.20%.

7.0 TEST PROGRAM

All tests will be directed by Honeywell Incorporated. These tests may be witnessed by ERDA or its representatives or the witnessing may be waived. In either case, substantive evidence of hardware compliance with all test requirements is required. All tests will be conducted per a formalized test plan and procedure to be established under a separate cover.

Thermal storage performance shall be tested to demonstrate the effective transfer of heat energy to the storage medium using a working fluid the same as that available from the Receiver Subsystem in the Central Receiver Solar Thermal Power System Pilot Plant, to verify the storage of heat energy, and also to demonstrate the generation of steam vapor comparable as in Pilot Plant, Unit Cell. For this purpose the test program shall include the tests indicated below.

7.1 Performance Tests

7.1.1 Charge Mode

The storage subsystem shall be configured so that no discharge steam flow occurs. In this configurations, by design, only heat is transferred into storage. Transmit response data will be obtained for this mode of operation.

7.1.2 Discharge Mode

The storage subsystem shall be configured so that no charge flow occurs. In this configuration, by design, only heat is transferred out of storage. Transient response data will be obtained for this mode of operation.

7.1.3 Storage Mode

The storage subsystem shall be configured so that neither charge or discharge flows occur. In this configuration only heat is lost through the walls of the subsystem.

7.1.4 Charge/Discharge Mode

The storage subsystem shall be configured so that charge and discharge flows occur simultaneously. In this configuration heat flows into and out of storage. The net heat flux is a controlled test variable and independent upon pilot plant duty cycle simulations.

7.2 Critical Function Tests

The subsystem shall be subjected to test conditions which simulate a malfunctioning subsystem. These tests shall include, but not be limited to the following:

7.2.1 Over Temperature

7.2.2 Over Pressure

7.2.3 Ruptured Components

7.2.4 Adverse Liquid/Solid Levels

7.2.5 Component Hazards

- o Chemical
- o Mechanical
- o Pneumatic

7.3 Preliminary Qualification Tests

It is desirable that preliminary tests be conducted as soon as practical to confirm, or better define, any characteristics of the thermal storage subsystem experiment which involve unusual materials or unconventional applications.

8.0 TEST PROCEDURE AND CALCULATIONS

8.1 Procedures

Alternate procedures are available for evaluating thermal storage devices. The following are listed as alternatives to be considered in establishing a detail test plan for the TES/SRE. Subsequent tests shall be in accordance with the Detail Test Plan to be established under a separate cover.

The method that has been commonly employed in testing of water storage tanks is to cause the transfer fluid entering the storage device to undergo a step change in temperature and to measure the temperature of the transfer fluid leaving the storage unit. By integrating the difference in temperature between the inlet and outlet over the testing period and multiplying the result by the transfer fluids' mass flow rate and specific heat, one can determine the amount of heat added or removed during this time period. The area under the curve represents the energy absorbed during the time period shown. If the time period chosen for the test were some characteristic time depending upon the size of the storage device chosen, the heat storage capability of different devices could be compared.

A second method that could be employed would be to subject the transfer fluid entering the storage unit to a constant influx of heat, Q. This would result in raising the temperature of the entering transfer fluid (assuming the specific heat of the transfer fluid is constant) by a fixed number of degrees above the outlet temperature. By measuring the time dependent outlet temperature one could obtain information that would be useful in designing collector-storage systems. While this method simulates more closely the real interaction between a collector and a storage device, it has the disadvantage that one cannot measure the energy storage and removal capability of the unit. This is due to the fact that if one measured the heat absorbed by the storage unit over a period of time, it would just be equal to $\dot{Q}$ x the test period of the amount of energy added to the system. Thus the only way of comparing different storage devices would be to compare plots of outlet temperature versus time for different values of Q chosen so as to take into account the different sizes of the storage units being compared. The storage device with the lowest average outlet temperature would probably be considered best because this would tend to maximize the efficiency of a collector.

A third method would be to use a time varying Q and to measure the outlet temperature as a function of time during the testing period. This would allow one to simulate the output of a collector over one or more days and to determine the response of the storage device. If the time dependence of Q resulted in an oscillating inlet temperature, one would also be able to look at the degree of stratification attained in the storage unit. This method has the same disadvantage as the second method in that it would be very difficult to compare the performance of different storage

8.1 Procedures (Continued)

devices. In addition, one has the problem of deciding on what is the typical cycle for $\dot{Q}$; not an easy task when one considers that the output of the collector depends not only on the weather but on the particular storage unit employed. The major advantage of this method would be that by inserting an array of thermocouples in the storage medium, the experimenter could measure the temperature stratification in the unit.

Of the three types the first method is the most advantageous because:

a) it permits the determination of effective storage capacity and thus allows an easy comparison of different types of storage units,

b) it appears to be the most fundamental approach since linear theory shows that the outlet temperature response to a constant or variable heat flux $\dot{Q}$ can be predicted if one knows how the outlet temperature changes with a step change in inlet temperature.

The procedure selected for this application shall be based upon the heat and mass balance equations established for the test subsystem, and shall be tailored to the final subsystem mechanizations.

Detailed procedures for conducting the various tests described in SECTION 7 shall be established in conjunction with the Detail Test Plan.

8.2 Calculations

The calculations will include those necessary to establish the static and dynamic performance characteristic of the storage subsystem. These are determined by the heat and mass balance equations of the system. The desired performance characteristics include but are not limited to storage capacity, effective capacities for heat storage and heat removal, charge and discharge time constants.

The data reduction techniques will be established with the appropriate design personnel to minimize test turn around time. The approach of Reference 3 will be considered as a baseline.

9.0 DATA & TEST REPORT

Test data to be obtained shall be in accordance with a predetermined data list. The data shall include test date, relative ambient air conditions, observer names, temperatures, pressures, flow rates, etc., as required for determining the performance characteristics of the test item, as well as the identification necessary to identify test components such as manufacturer's name, serial number, and model number.

10.0 NOMENCLATURE - TBD

11.1 REFERENCES - TBD

APPENDIX C
ENGINEERING MODEL PROGRAM

APPENDIX C
ENGINEERING MODEL PROGRAM

PART I - DESCRIPTION AND TESTS

In order to specify the design of the SRE and assure a measure of confidence in the overall feasibility there must be a technical basis from which to formulate the design. The Engineering Model (EM) Program was created to serve this purpose.

At least two model configurations are planned: 1) Condenser Model and 2) Vaporizer Model.

The Vaporizer Model (VM) is used to investigate various salt removal techniques and the attendant heat transfer coefficient. In addition, various vaporizer tube configurations and mechanisms will be evaluated. The nucleation process can be studied on a bulk scale and the effects of impurities evaluated.

The Condenser Model (CM) will be used to investigate the capability of various pipe configurations, with and without extended surfaces, to transfer heat from condensing steam inside tubes to the salt mixture outside. The primary objective to be met with this model is an assessment of the heat transfer coefficient of a single tube and an estimate of the effects of multiple tube arrangements. It is also expected that the heat transfer mechanisms currently being hypothesized will be substantiated or modified in light of the experiments. This data will make it possible to specify the EM condenser heat exchanger with high confidence or to specify an alternate or augmented scheme. EM testing will demonstrate the design specified by the CM and the SRE testing will evaluate the performance capability when used in several modules or banks.

Both models will provide valuable information on salt handling and properties, test methods and techniques, materials compatibility, and operating and safety procedures.

Based on the scope of the experimental effort a set of priorities were established as follows:

1) Investigate various salt scraping techniques and heat transfer.

2) Investigate various condenser tube configurations and tube bank arrangements and the attendant heat transfer

3) Investigate the thermal convection of the bulk salt in the bank.

The following discussions are a summary of accomplishing the first priority.

A series of preliminary tests were made to study the scraping problem and heat transfer on a small tank approximately 38 cm (15 in.) long, 23 cm (9 in.) deep and 27 cm (10 3/4 in.) wide. The tank was equipped with five 1.3 cm (one half inch) diameter stainless steel tubes on 5.1 cm (2 in.) centers near the upper surface of the tank. The tubes were connected in series. Three immersion heaters supplied heat for melting down the charge.

An air supply regulator, Rotometer and an air preheater were connected to the tank heat exchangers, which permitted a low flow of heated air to be used for cooling. The tank was filled with an 83 percent $NaNO_3$ and 17 percent NaOH (by weight) salt mixture and melted down. Temperatures were measured with the use of in-line thermocouples.

Figure C-1 shows a schematic of the system. An additional element was added to the system, a stirring device consisting of a 7.6 cm (3 in.) diameter impeller. This allowed vigorous flow of molten salt over the heat transfer tubes. Figure C-2 is a photograph of the test set while Figure C-3 is a close up of the tank, stirring rod and heaters. A leak in the tank sealed itself by freezing during a test.

The small size of the preliminary tank and practical problems with the heat exchanger and heaters led to the design and construction of a considerably larger and more flexible system. Figure C-4 is a schematic view of the larger system. The steel salt storage tank 61 cm x 45.7 cm x 45.7 cm (24 in. x 18 in. x 18 in.) was set into a large steel pan mounted on a movable base. A close-fitting cover was designed and built to carry the necessary heat exchangers, and electric bayonet-type immersion heaters were used to supply heat. A separate pump, oil lines, and Rotometer allowed the circulation of controlled quantities of oil at various temperatures for cooling the bath heat exchangers. A serpentine cooling system of five 45.7 cm 1.3 cm (18 in. by 1/2 in.) pipe lines was fitted on a vertically adjustable frame. Mechanical rotary scrapers were fitted to these tubes and driven from an overhead sprocket through a 0.95 cm (3/8 in.) roller chain with sprockets on each scraper. The initial scrapers were two simple straight blades mounted on bearings on each end and also on the sprocket at the center. A different design consisted of a zig-zag scraper consisting of small plates of steel machined with elliptical holes to closely fit the tube and driven by a central sprocket. Figure C-5 shows both designs mounted on the heat transfer tubing and driven together.

Instrumentation was acquired consisting of two precision millivoltmeters, a recording millivoltmeter and several digital thermocouple readouts. A differential thermopile arrangement for measuring temperature changes in the oil was connected to the input and output locations of the coolers.

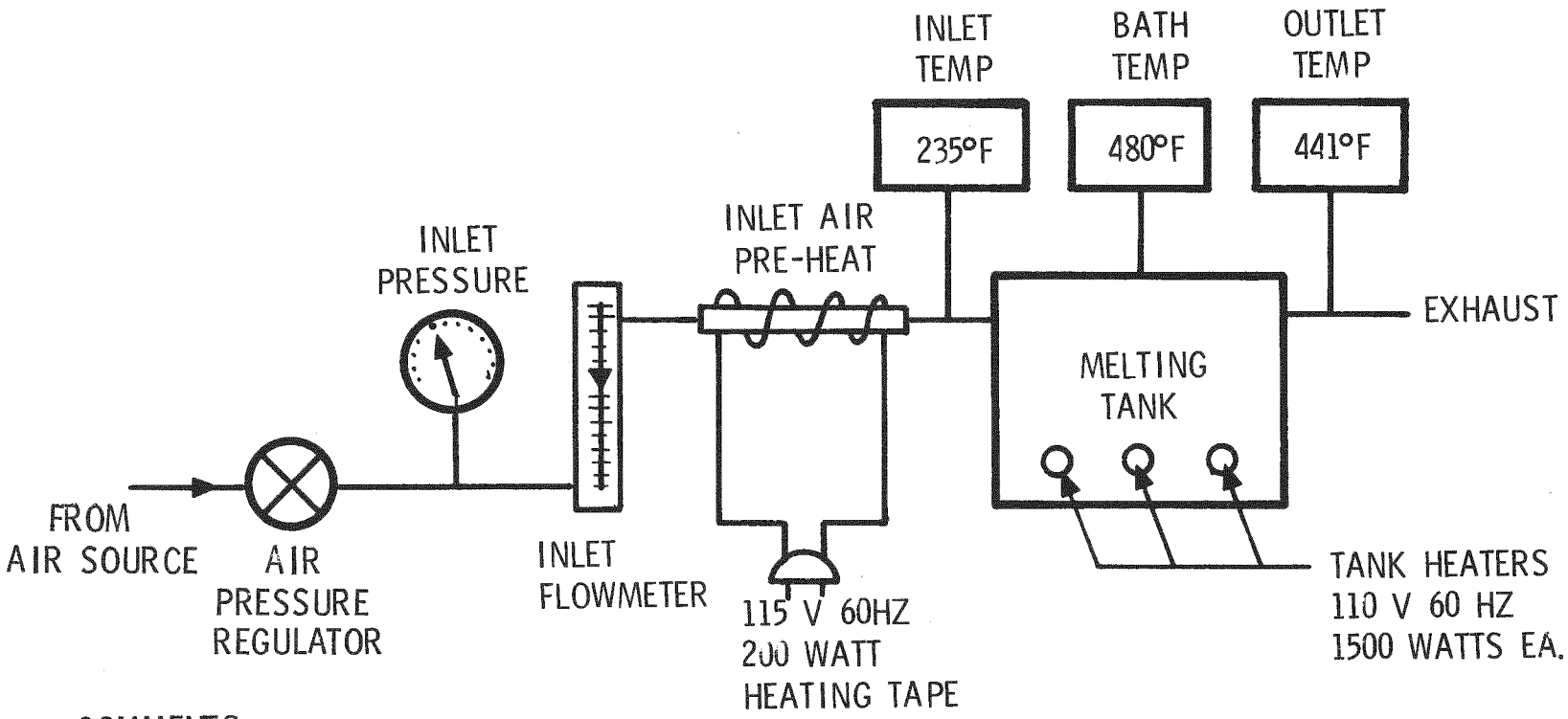

COMMENTS

1. THERMOCOUPLES ARE 1/16 IN. DIAMETER TYPE K CHROME-ALUMEL MATERIAL
2. MELTING TANK HAS 5 1/2 IN. DIAMETER STEEL TUBES USED AS A HEAT EXCHANGER
3. INITIAL SALT SOLUTION IS 83% $NaNO_3$ AND 17% NaOH
4. INLET AIR LINE IS 1/4 IN. O.D. TUBING

INLET AND OUTLET THERMOCOUPLE CONFIGURATION

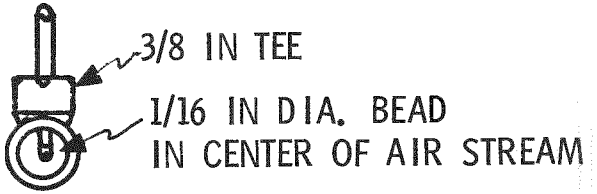

Figure C-1. Initial Experimental Salt Melt Test Setup

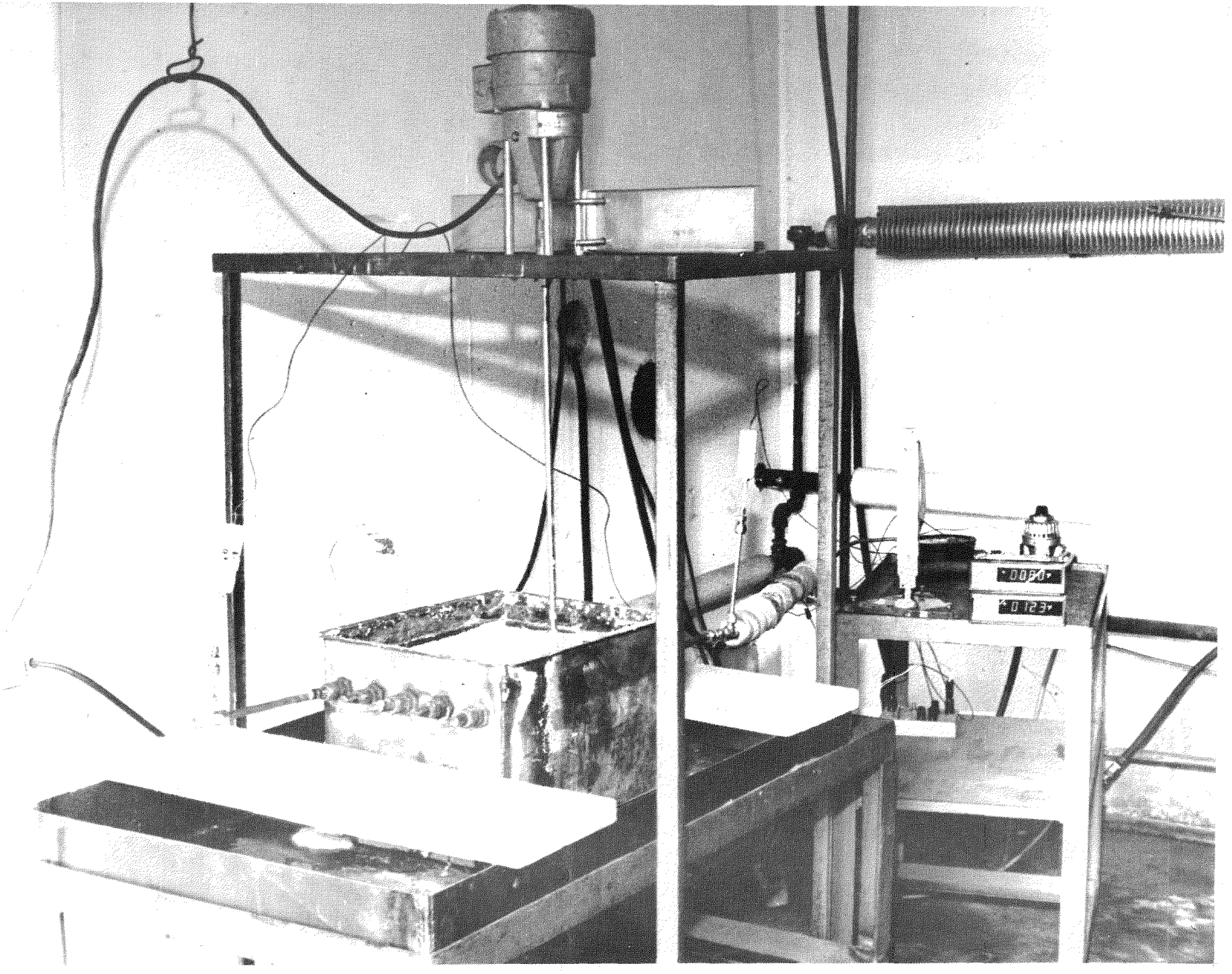

Figure C-3. Preliminary Test Facility

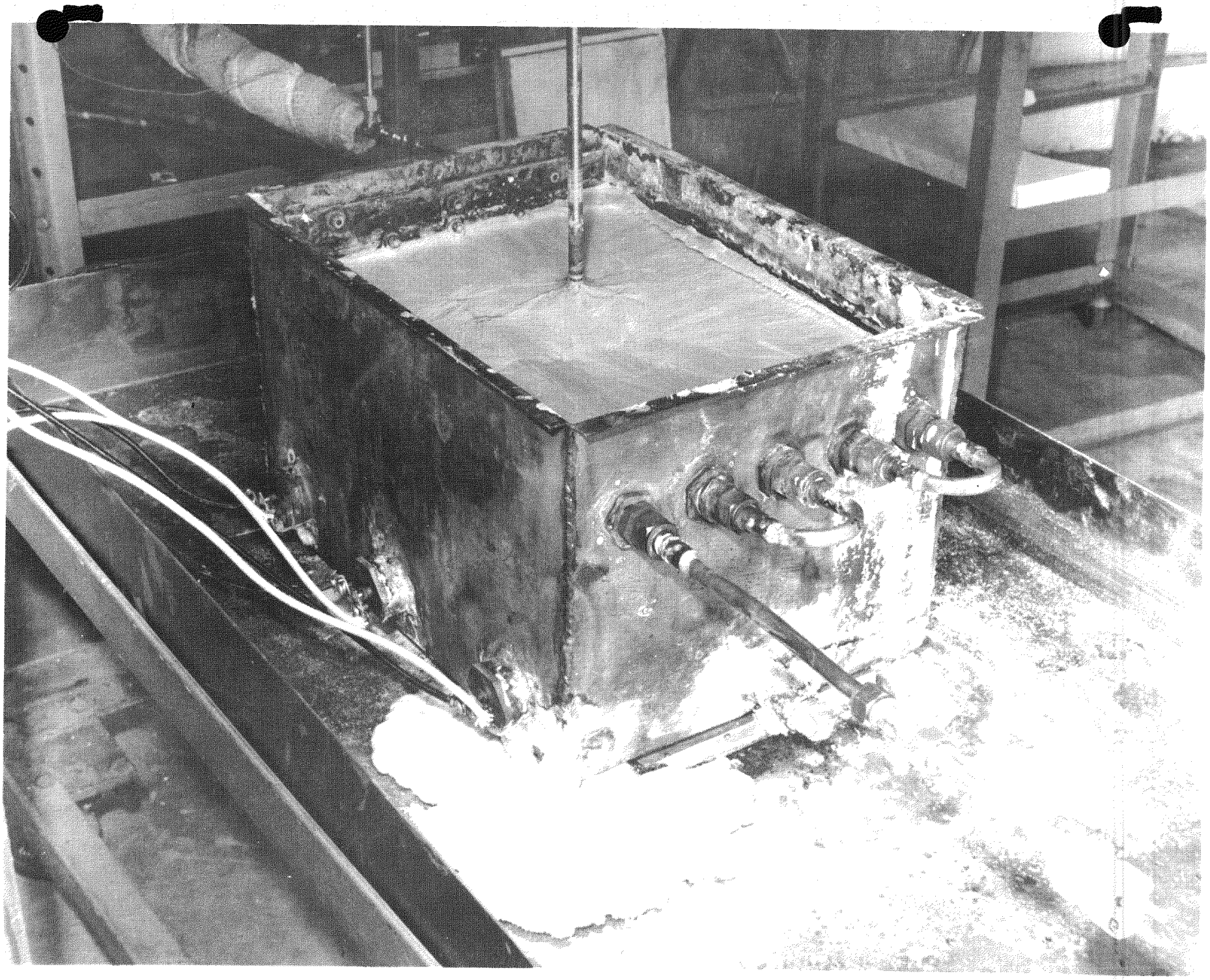

Figure C-3. Preliminary Test Tank with Frozen Charge

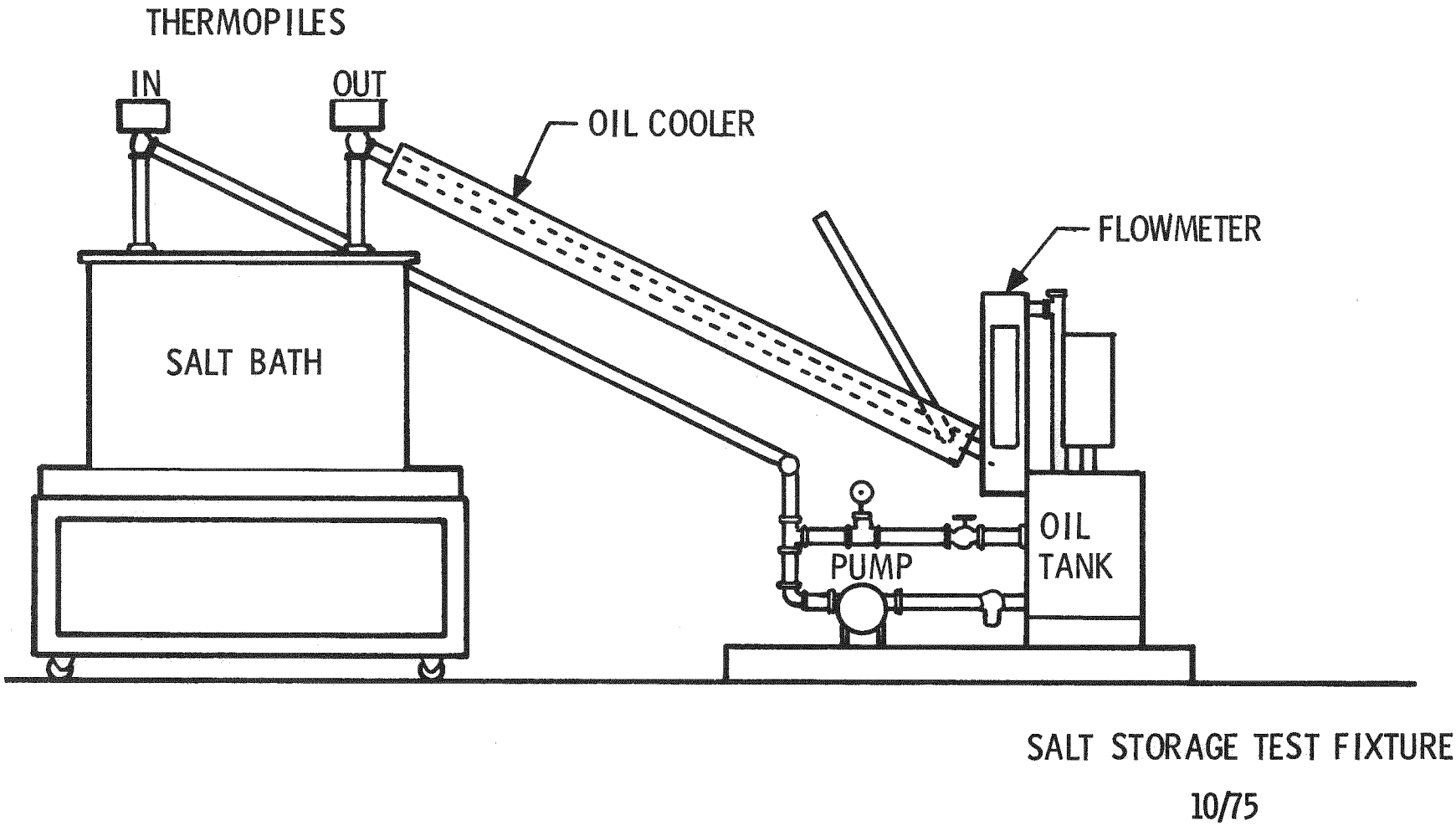

Figure C-4. Phase Change Heat Transfer Test Apparatus Engineering Model

The system was charged with five gallons of Mobiltherm 603, a hydrocarbon-type high temperature oil.

Oil flow was measured with a Rotometer equipped with a Pyrex tube and special stainless steel float.

After preliminary tests with the scrapers shown in Figure C-5, a full set of scrapers similar to the straight bar scraper were installed on the heat exchanger tubes.

These scrapers were rather loosely fitted to the tubes, having clearances about 1 mm (0.04 in.). Heat transfer coefficients were relatively low and improved models were made by applying sharp cutting edges to the blading and decreasing clearances to approximately 0.25 mm. Experiments were then conducted on a near eutectic composition of NaOH and $NaNO_2$ (83 percent $NaNO_3$ and 17 percent NaOH).

The 107 kg (411-lb) eutectic charge was then shifted to an "off" eutectic by the addition of 18.2 kg (50 lb) of NaNO . Further tests were made with the sharp-edged straight scrapers on this composition.

Problems with unscraped area salt buildup and drive chains and sprockets let to replacement of the five scrapers with a single improved zig-zag scraper. This scraper has very close clearances (approximately 0.12 mm (0.005 in.) and completely scraped the tube leaving only a very thin film.

Tests were generally run after the salt was completely melted and raised above the eutectic freezing poing of 247°C (476°F) by using immersion heaters. The cooling oil was then heated to the desired temperature, 232°C (450°F). Scrapers were activated and the cooling oil pumped through the system. Oil temperature rise, flow rates and salt temperature data were recorded at fixed intervals. Scraping was continued until the scrapers became frozen to the tubes.

Hand scraping of the system was carried out for periods up to one hour. Data on heat transfer was taken for further reduction. In all cases, the salt bath temperature fell slowly and eventually the scrapers became firmly frozen to the tubes. Experiments with improved scrapers with sharper edges improved heat transfer but did not permit continued scraping.

The addition of mechanical drives improved operation but the same problem occurred. After a period of time, generally about 1 hour, the scrapers froze. Scrapers were closely examined but no mechanical damage was found.

The zig-zag version single scraper worked at periods up to nearly 3 hours before freezing. An interesting feature of all these tests was that the salt bath temperature always kept dropping never reaching a fixed temperature. In all freeze-ups, the temperature curve would become nearly flat just before the end.

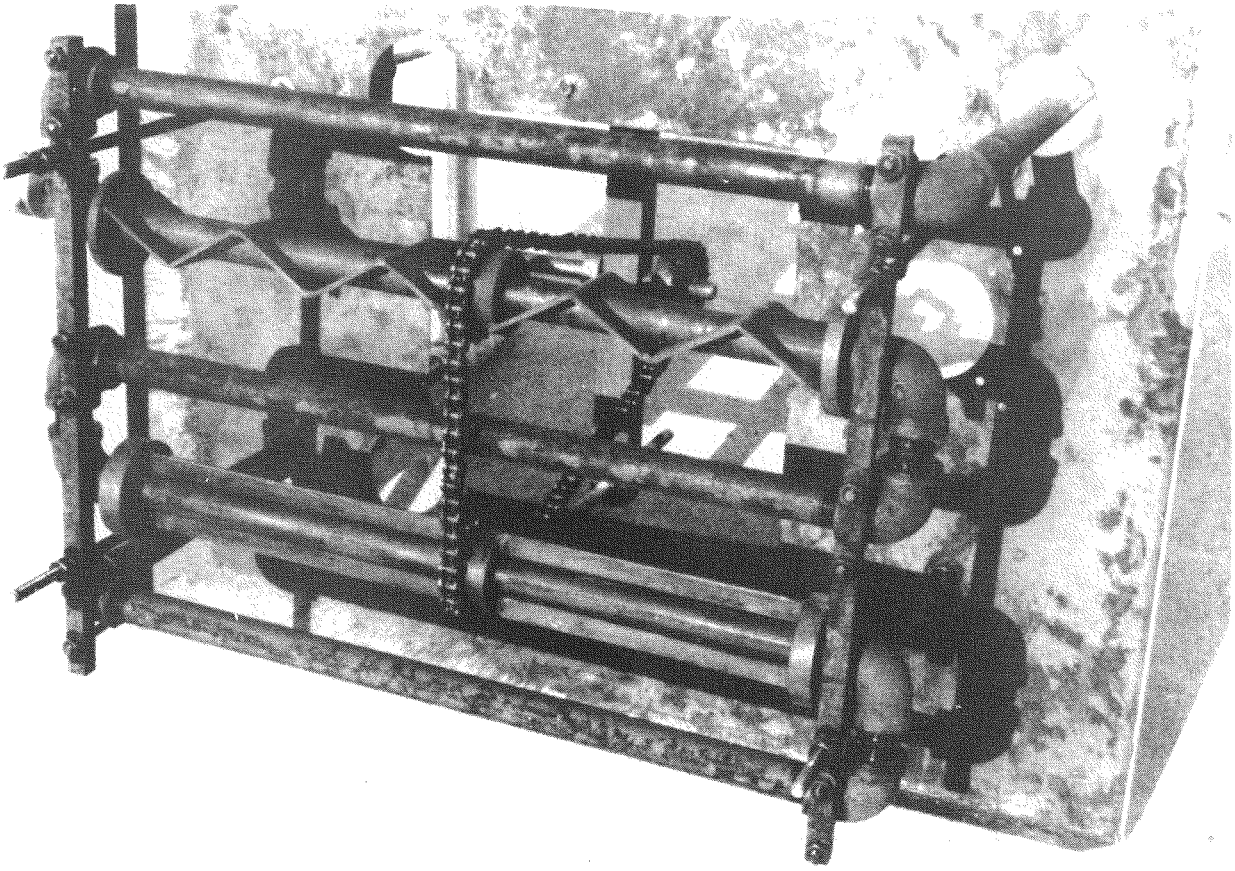

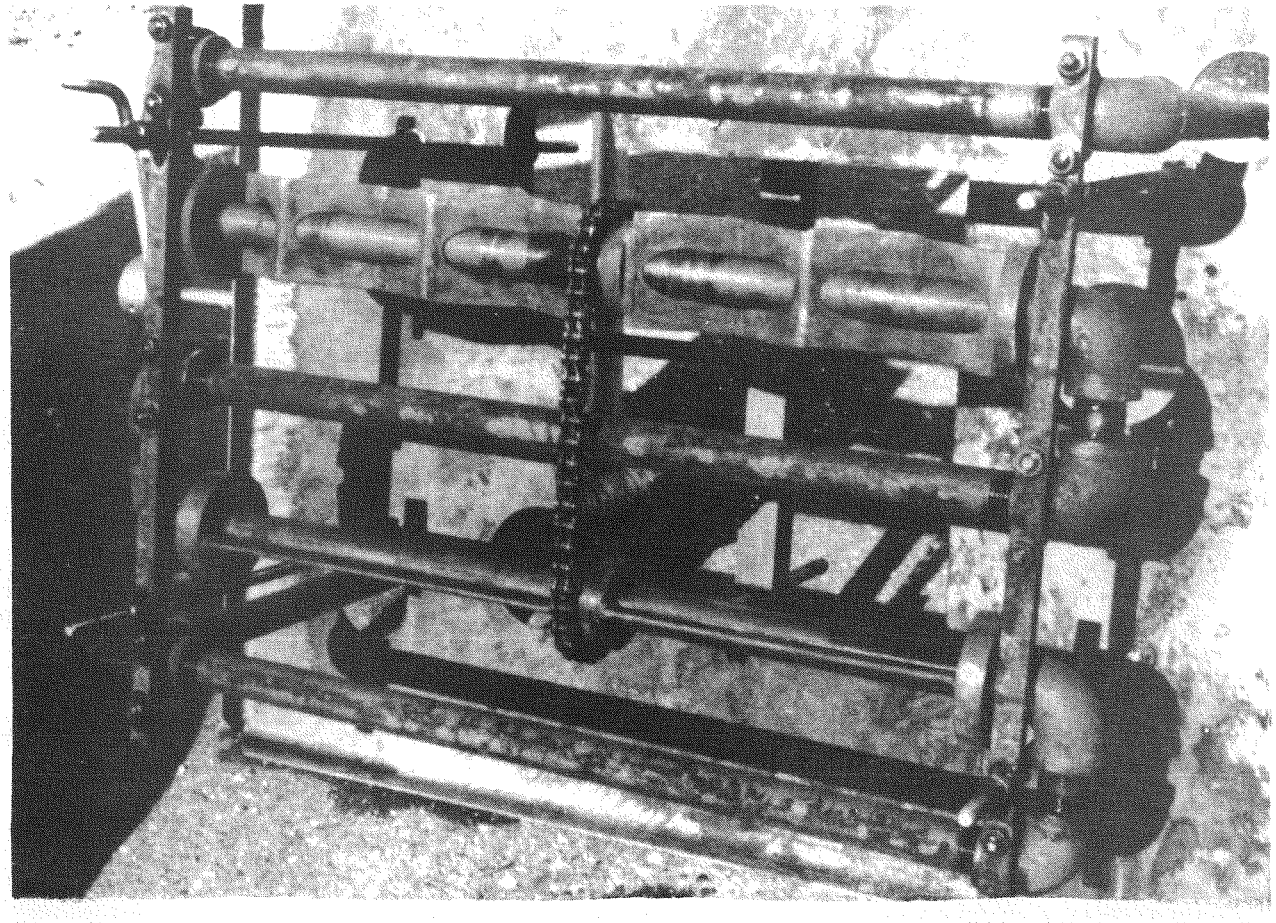

It appears that the "off" eutectic compositions were rejecting the excess component until the true eutectic was reached. At that point, the eutectic, when cooled a short distance below the freezing point, becomes hard and strong, freezing the scrapers.

A special test fixture built to measure shear strength showed that the shearing strength of the NaOH - $NaNO_3$ eutectic was about 551 kPg (80 psi) about 1/4°C (1/2°F) below the melting point.

A series of photographs, Figures C-6 and C-7, taken after a run with the five element scrapers indicates the effectiveness of the scrapers. The end tubing connections are heavily encrusted with salt. The tubes have a small layer of salt clinging to the heat transfer surfaces. Later designs scraped better and maintained better heat transfer rates.

An improved scraper design has been developed to permit easy installation and removal. Figure C-8 shows the three elements of the new inclined scraper drive installed on a three-element test heat exchanger. This scraper will be tried on $NaNO_3$, NaCl and Na_2SO_4 eutectic and off eutectic salt combinations.

Figure C-9 shows an additional high temperature test facility that is being constructed for the salt thermal storage test program.

The test tanks presently are being heated by external electric range top-type heaters clamped tightly to the outside bottom of the tanks. High-temperature insulation around these heaters and tanks conserves energy and helps maintain the tanks at 316°C (600°F).

The oil loop is equipped with four 2400 w immersion heaters installed in the oil sump. The oil may be heated above the temperatures needed for charging the tank. An extended surface heat exchanger consisting of three 45.7 cm (18 in.) finned heat transfer tubes is being constructed for installation at the bottom of the tank. This will permit a test program involving both charging and discharging of the salt storage system.

PART II - ENGINEERING MODEL TEST ANALYSIS

Phase change heat transfer experiments were conducted on engineering models of the tube scraper concept. The test instrumentation is noted in Table C-1, and the experimental parameters in Table C-2. Major performance parameters of interest were heat transfer coefficients, scraping force and percent heat recovery. Heat transfer coefficients of salt resistance have been measured up to 5.67 kw/M^2-°C (1000 Btu/hr ft^2 °F). Table 5-1 summarizes the results. Scraping force and heat recovery performance has been impaired due to scraper freeze-up. Scraper freeze-up is apparently caused by the strength of the eutectic solid and solid buildup around portions of the scraper which are not cutting edges. Heat recoveries of 30 percent with an oil

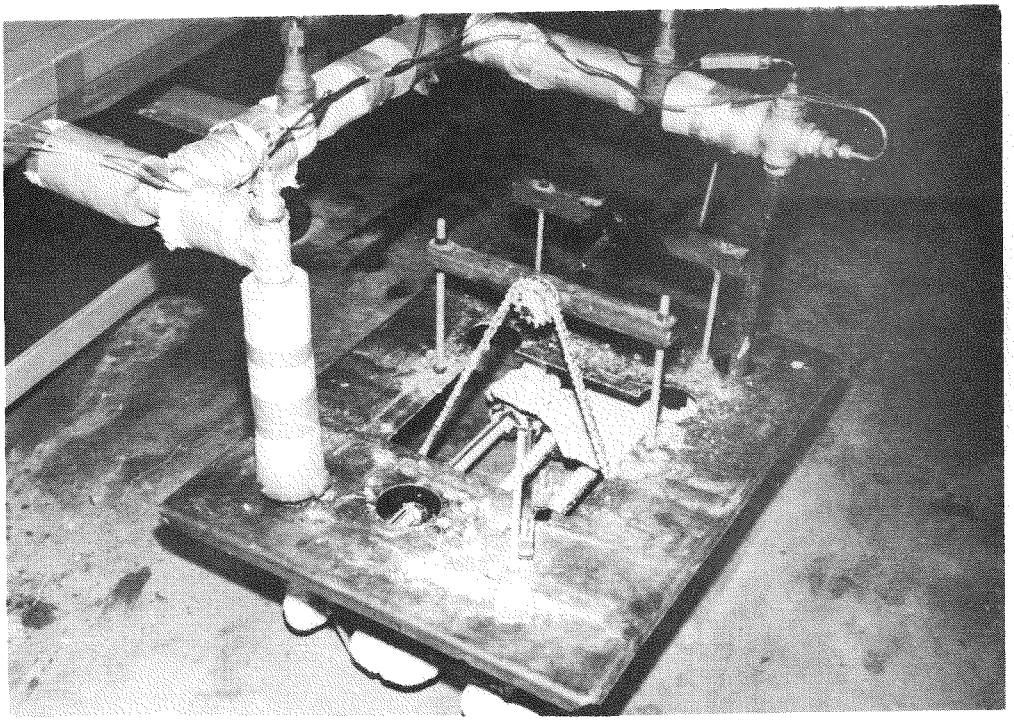

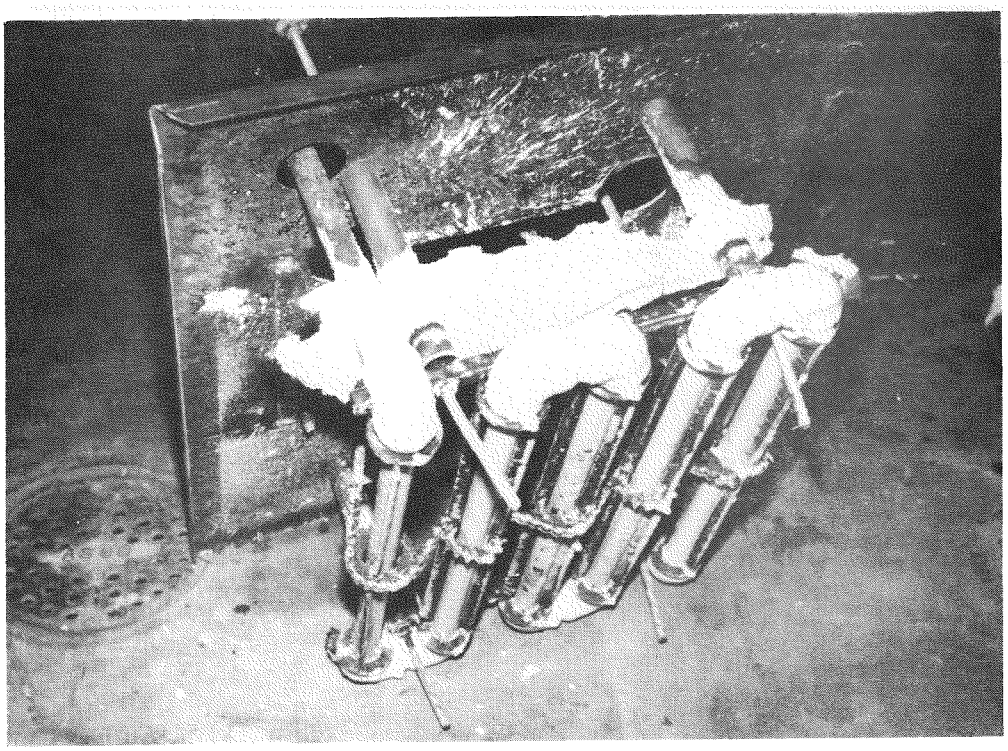

Figure [illegible] - Straight Line 2-Story Scraper After Operation

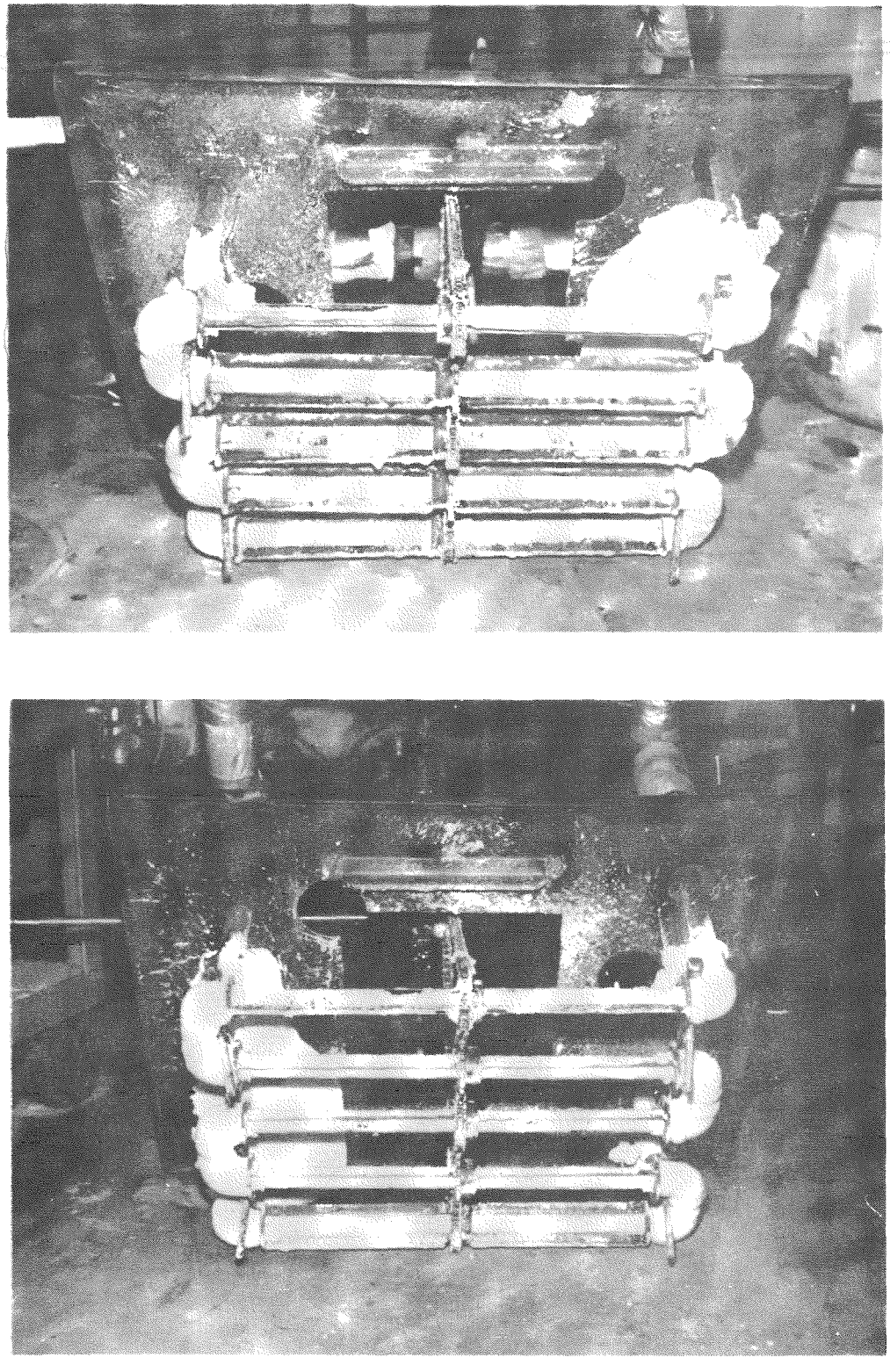

Figure C-7. Bottom View Straight Bar Rotary Scrapers After Operation

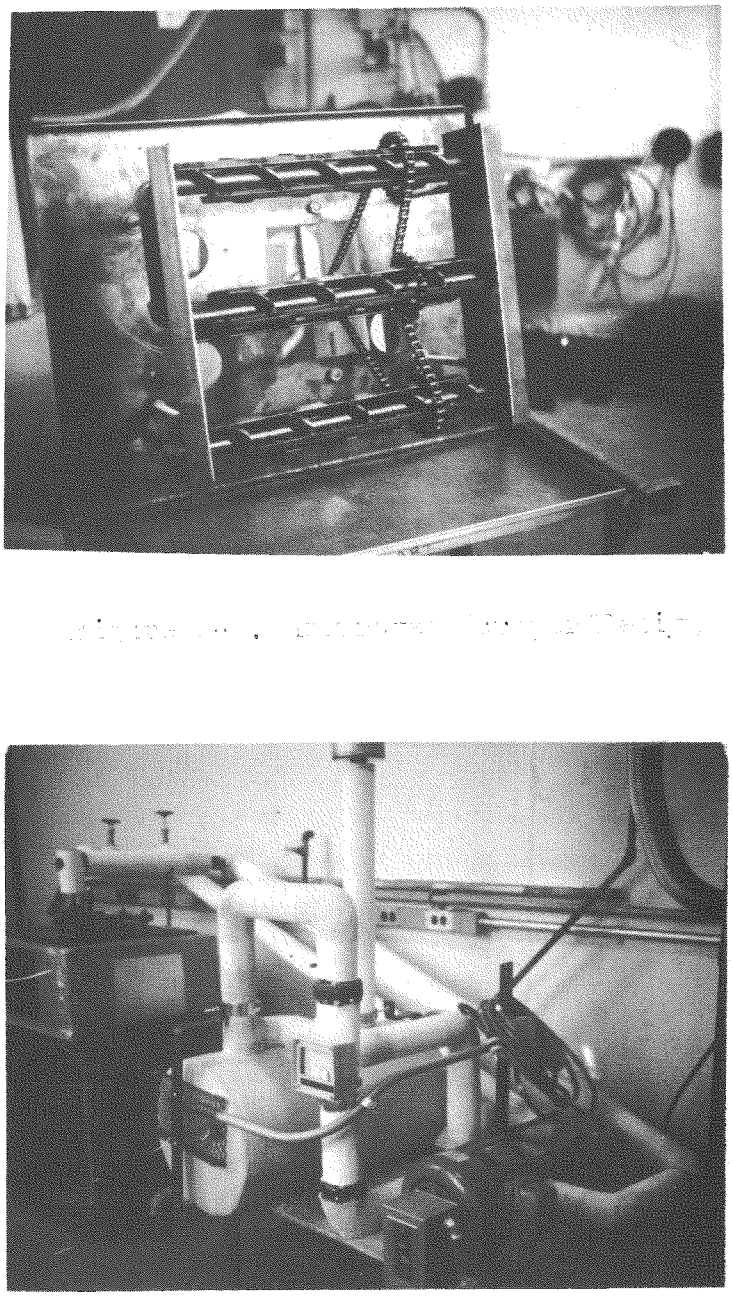

Figure C-9. High Temperature Salt Storage Test Facility

Table C-1. Test Instrumentation

Instrument	Data Measured
Brown Rubicon Potentiometer)2)	Thermopile Output (μv)
Ircon Digital Thermo-couple Indicator	Thermocouple Output (mv)
Brown Recorder	Salt Bath Temperature
Brooks Rotometer	Oil Flow Rate (gpm)

Table C-2. Experiment Parameters

• Salt Composition	$NaNO_3$-NaOH (83% - 17%)
• Vaporizer Configuration	
Tube Length	7.5 ft scraped (2.28×10^2 cm)
Tube Size	0.622 ID/0.840OD(1.58 cm ID/2.13 cm OD)
Material	Steel
Scraped Area	1.52 ft^2 (~.412 x 10^3 cm^2)
• Internal Heat Transfer Fluid	Mobiltherm 603
Thermodynamic Properties at 450°F	(232°C)
Specific Gravity	0.73
Kinematic Viscosity	1.0 cps (1.0×10^{-3} N sec/m^2)
Specific Heat	0.68 BTU/lb °F [6.8×10^{-1} g cal/ (g°C)]
Thermal Conductivity	0.068 BTU/hr ft °F [2.82×10^{-4} cal/(sec cm °C)]
Oil Flow Rate	8.24 gpm (5.198×10^{-1} l/sec)
Internal Heat Transfer	474 BTU/hr ft^2 °F(6.44×10^{-2} cal/sec cm^2 °C)
• Tank Size	24" x 18" x 18" (60.96 cm x 45.72 cm x 45.72 cm)
• Salt Depth	14" (35.56 cm)
• Salt Weight	411 lb (eutectic)(1.8643×10^2 kg)
• Thermal Capacity ($NaNO_3$-NaOH)	9.4 KWH(t)

temperature of -6.67°C (20°F) below eutectic have been measured. This performance was achieved with a salt composition with 10 percent extra weight of the $NAN0_3$ from the eutectic mixture of $NaN0_3$-NaOH.

Heat Transfer Coefficients

The objective of these engineering model tests was to determine the heat transfer coefficients and heat recovery performance of tube scrapers. The first quantitative data taken demonstrated poor heat transfer coefficients, as seen in Figure C-10. This was caused by a large clearance of 1.016×10^{-1} cm (0.040 in.) between the scrapers and the tubes. The large variation in coefficients was caused by variations in solid film thickeness as salt froze under the scrapers. Note also in Figure C-10 the change in coefficient when the scrapers were turned on. The local turbulence caused by the scrapers is important for reducing thermal resistance in the liquid salt. Figures C-11 and C-12 show more precisely the same data as Figure C-10. The scrapers provide high coefficients when the tubes are bare, but the coefficients drop off as the solid builds up under the scraper.

During these tests, a slushy solid was being removed from the tubes due to the slightly off eutectic salt mixture. The off-eutectic composition is evident by the continuous drop in the liquid temperature. As the external resistance increased, the temperature gradient increased, causing the solid material to become colder and harder. This hard material slowly developed until it froze the scrapers.

Sharp liners were added to the scrapers to reduce the clearance and increase their ability to scrape hard material. A 75 percent increase in heat transfer to coefficients was achieved (see Figure C-13).

The next step taken was to move the salt composition farther from the eutectic by adding 22.68 kg (50 lb) of $NaNO_3$. As seen in Figure C-14 the high initial coefficients lasted longer in time, but the coefficient at freeze-up was about the same. The scrapers keep the tubes cleaner when the material is slushy. But after the extra nitrate freezes out of solution, the resultant eutectic material builds up.

The last step was to install a scraper with very close fit and sharp edges. A 300 percent increase in coefficient was achieved. As shown in Figure C-15, the total elapsed time was considerably greater. This was primarily due to the fact that only one of the five serpentine legs was being scraped. The heat transfer coefficient was calculated by measuring the heat flow through the unscraped tubes on a separate run and subtracting it from the scraping run. Note, however, that a considerable amount of eutectic material must have been formed, as 45.36 kg (100 lb) of solid was formed, although the bath never reached the eutectic temperature.

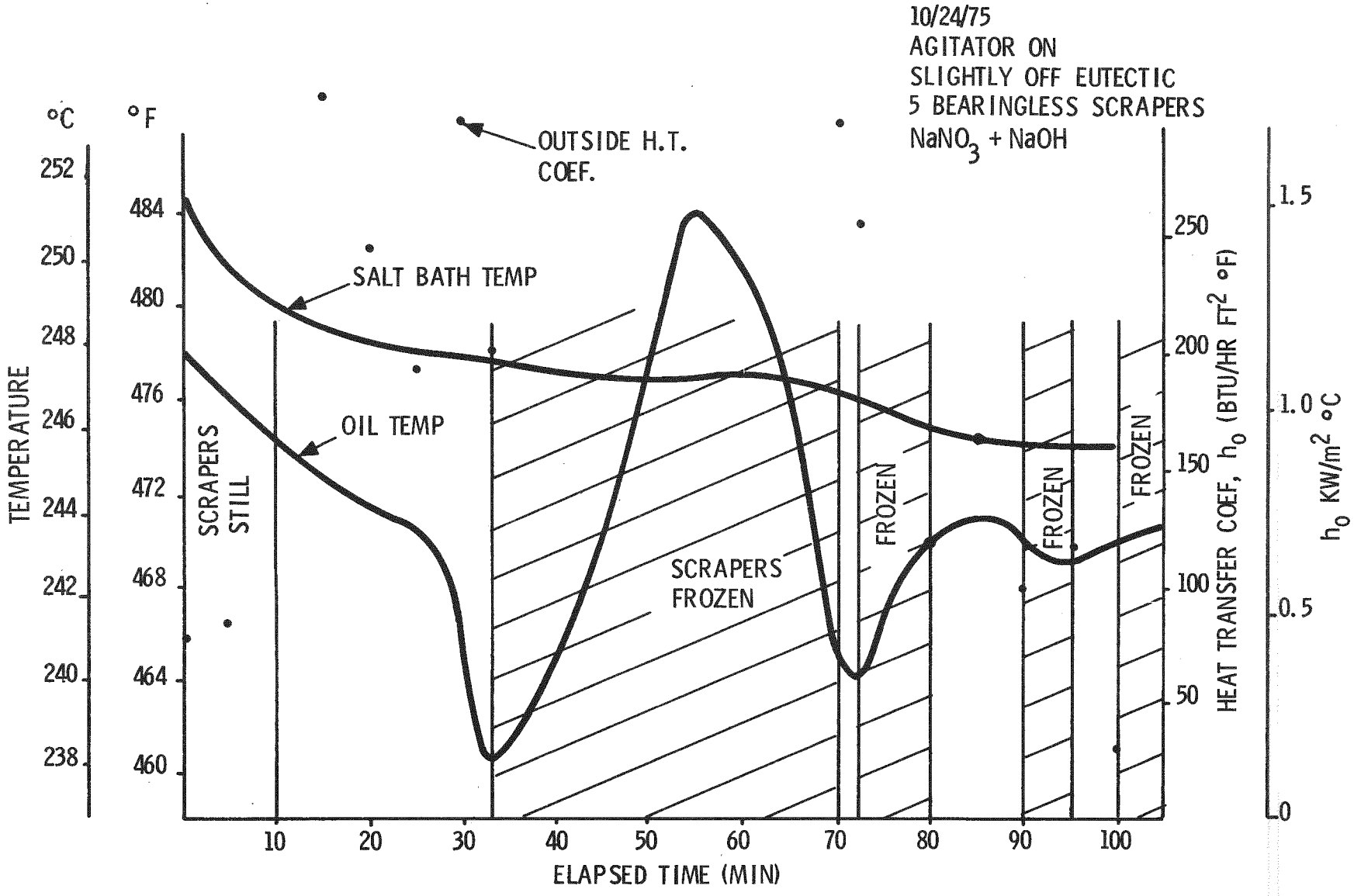

Figure C-10. Loose Tolerance Scraper - Slightly Off Eutectic

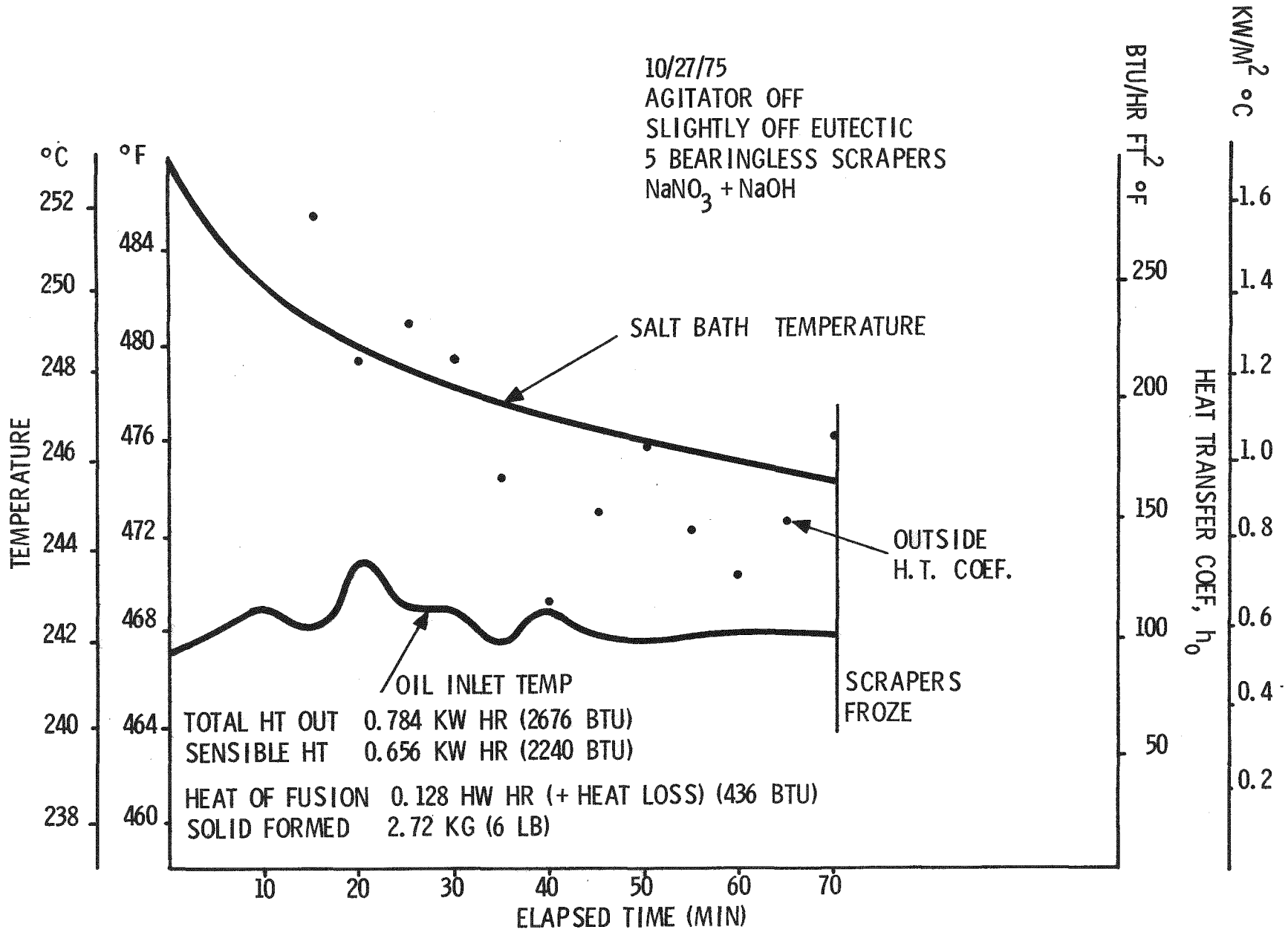

Figure C-11. Loose Tolerance Scraper - Slightly Off Eutectic

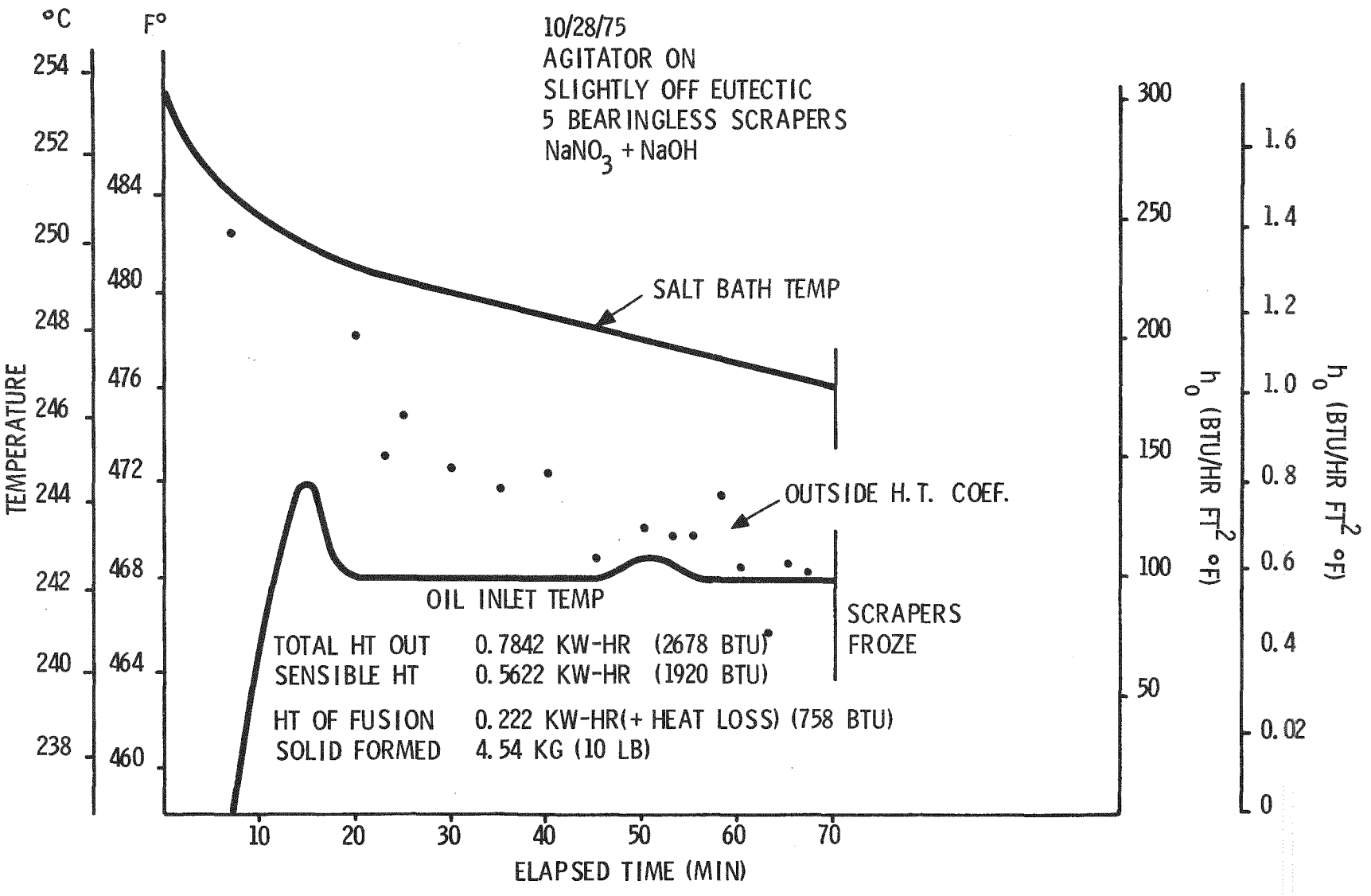

Figure C-12. Loose Tolerance Scraper - Slightly Off Eutectic

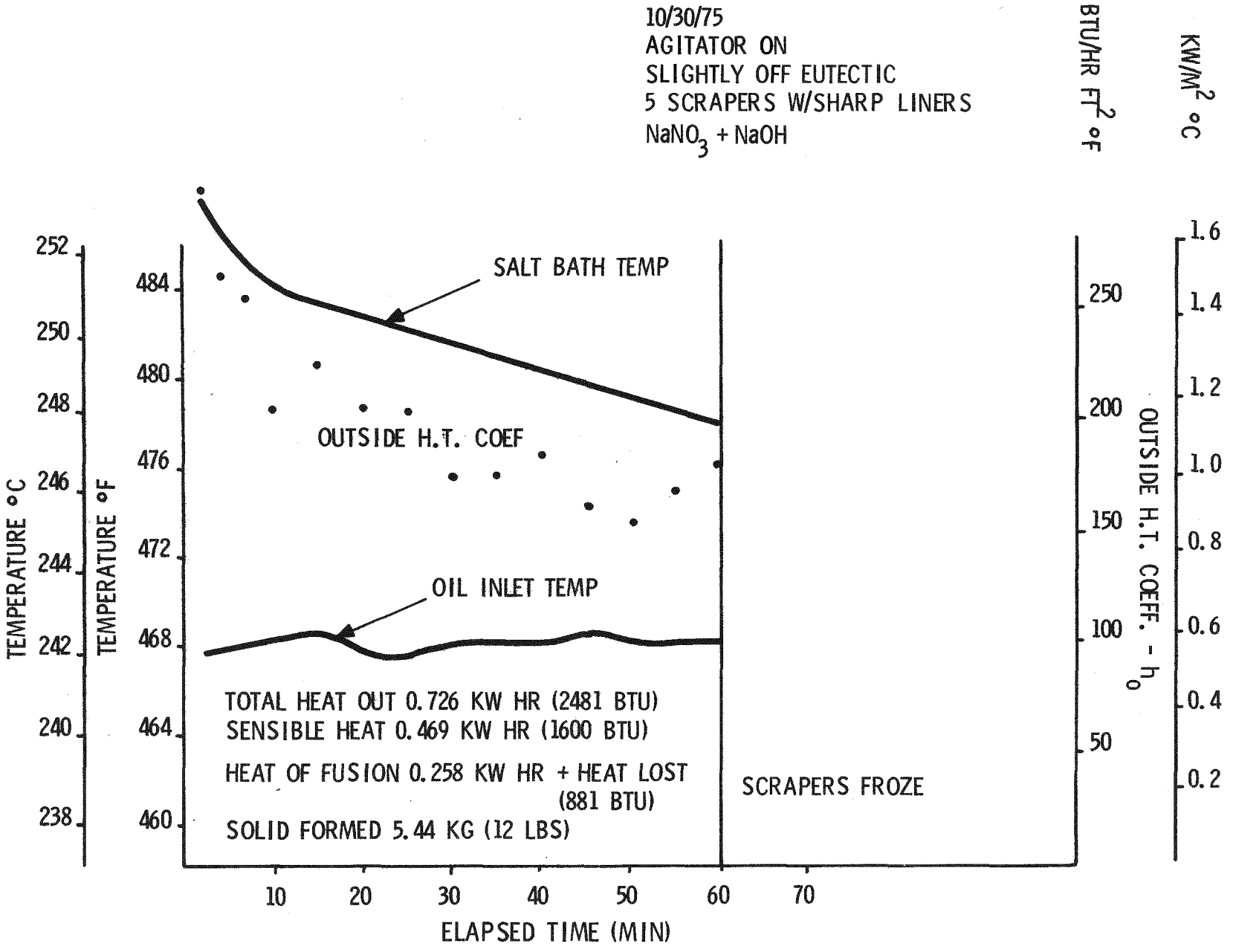

Figure C-13. Medium Tolerance Scraper - Slightly Off Eutectic

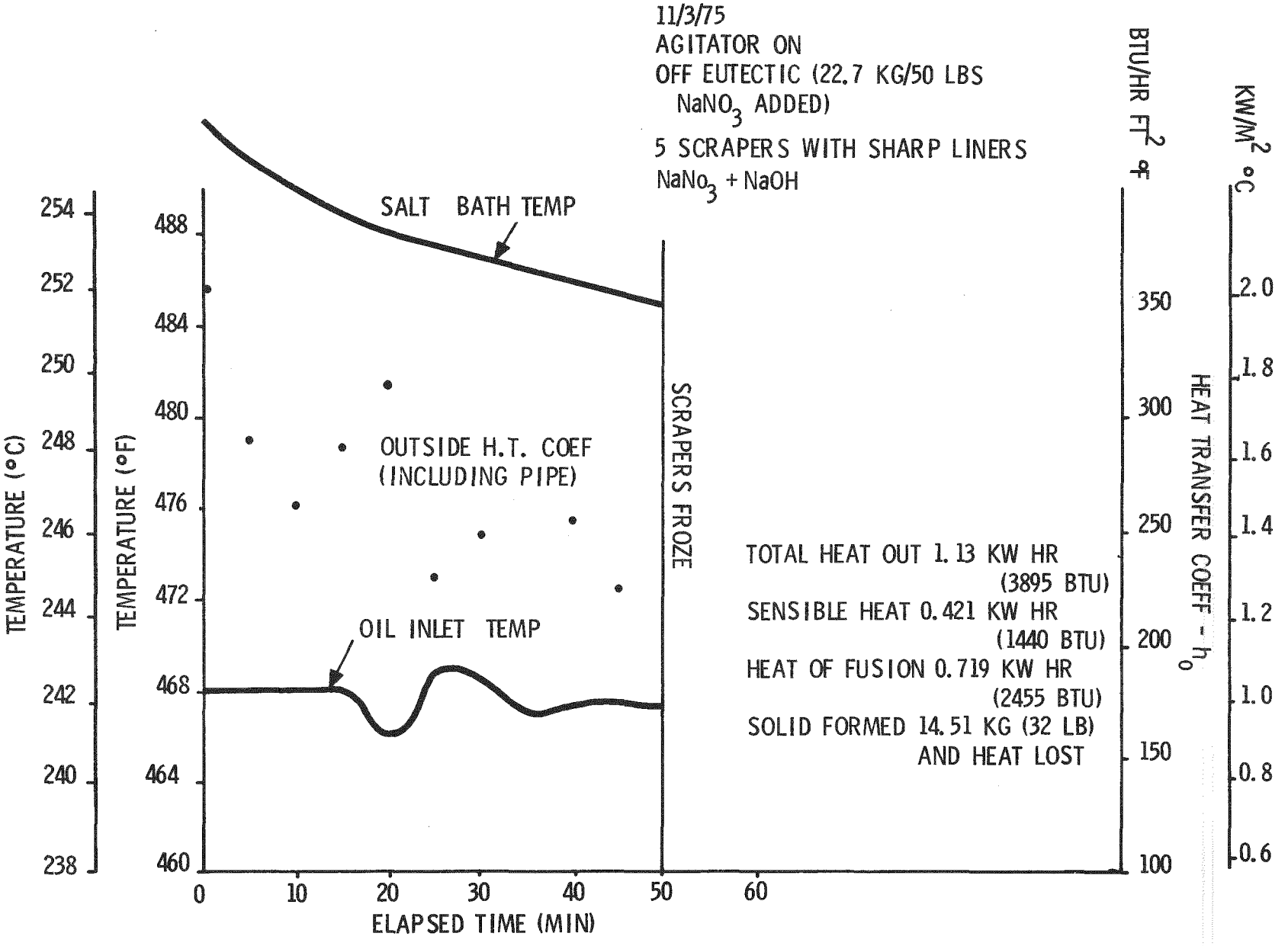

Figure C-14. Medium Tolerance Scraper - Off Eutectic

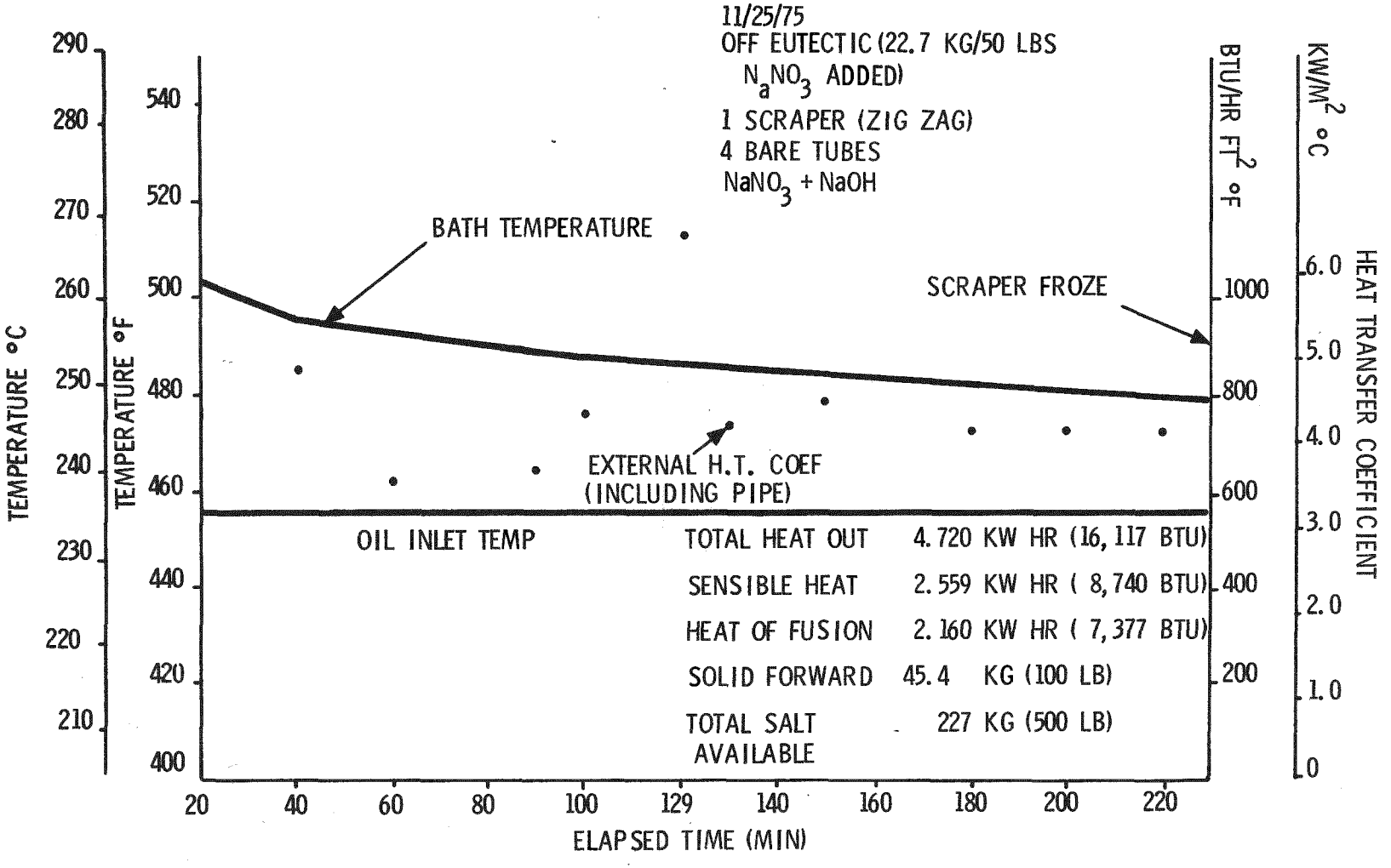

Figure C-15. Close Tolerance Scraper - Off Eutectic

Scraper Freeze-Up

The most obvious factor depicted in the experimental data is that the scrapers freeze before the heat is recovered from the salt bath. The experimental parameters (Table C-3) affecting freeze-up are: salt composition, oil temperature, scraper clearance and unscraped scraper boundaries. The first three of these factors cause eutectic solids to come in contact with the scrapers. This material apparently has strong mechanical properties.

Figure C-10 shows that the scrapers freeze very quickly with an oil temperature -12.22°C (10°F) below the eutectic temperature when the salt composition is near eutectic. Figures C-11 and C-12 show that about 2 percent of the salt was solidified with the oil temperature -13.33°C (8°F) below eutectic. Improving the scraper clearance in Figure C-13 did not improve heat recovery.

When the composition was moved off eutectic, the heat recovery was increased to about 6 percent, as shown in Figure C-14. Then a new scraper was installed with small clearance 0.01016 cm = 1.016×10^{-2} cm (0.004 in.), sharp edges and all boundaries scraped. The small clearance keeps the solid on the tubes near the bath temperature. The sharp edges allow cutting harder material. The scraped ends and self-scraping bearing surface prevents a solid buildup on boundaries which can prevent scraper motion. As shown in Figure C-15, this scraper was able to recover 30 percent of the tank heat with the oil temperature -6.67°C (20°F) below eutectic.

Computation of Heat Transfer Coefficient

Energy Balance Across the Tube Wall --

$$q = \dot{m} C_p (T_{out} - T_{in})_{oil} = U_o A_o (T_{salt} - T_{oil})$$

$$U_o = \frac{\dot{m} c_p \Delta T_1}{A_o \Delta T_2}$$

where,

$$\Delta T_1 = (T_{out} - T_{in})_{oil}$$

$$\Delta T_2 = T_{salt} - T_{oil} .$$

Separating the conductance of the internal fluid from the pipe and salt

$$h_o = \frac{1}{1/U_o - 1/h_i \, A_o/A_i}$$

Table C-3. Summary of Results

Date	Scraper Type	Salt Composition	$T_{oil} - T_{EU}$ (°F)	(°C)	Final H. T. Coefficient (BTU/hr ft^2 °F)	(cal/sec cm^2 °C)	Total Heat Out (BTU)	(cal)	Solid Formed (lb)	(kg)
(1) 11/25/75	Tight Zig-Zag	50 lbs. off eutectic	20	-6.67	725	9.85×10^{-2}	16,000	4.03×10^6	100	45.36
(2) 11/03/75	Straight Blades w/liners	50 lbs. off eutectic	8	-13.33	200	2.72×10^{-2}	4,000	1.008×10^6	32	14.52
(3) 10/30/75	Straight Blades with liners	Near Eutectic	8	-13.33	175	2.38×10^{-2}	2,400	6.048×10^5	12	5.44
(4) 10/28/75	Straight Blades	Near Eutectic	8	-13.33	100	1.36×10^{-2}	2,700	6.804×10^5	10	4.536
(5) 10/27/75	Straight Blades	Near Eutectic	8	-13.33	150	2.04×10^{-2}	2,700	6.804×10^5	6	2.72
(6) 10/24/75	Straight Blades	Near Eutectic	5-15	-15 - -9.44	---	---	---	---	---	

Ex. $\dot{m}$ = 2990 lb/hr (1.356×10^3 kg/hr) $\quad \Delta T_1$ = 4.2°F (-15.44°C) h_i = 500

e_p = 0.69 $\quad \Delta T_2$ = 32°F (0°C)

A_o = 1.52 ft^2 (1.412×10^3 cm^2) $\quad A_o/A_i$ = 1.38

U_o = 178

$$h_o = \frac{1}{1/178 - 1.38/500} = 350$$

Internal Oil Heat Transfer Coefficient --

Dittus - Boelter Eqn,

$$h_i = 0.023\,(k/d)\,(Vd/\nu)^{0.8}\,(cp\mu/k)^{0.4}$$

where

k = 0.068 BTU/hr ft °F (2.82×10^{-4} cal/sec cm °C)

d = 0.622 in. (1.58 cm) = 0.052 ft (158 cm)

V = 8.73 ft/sec (2.66×10^2 cm/sec) = 3.14 $(10)^4$ ft/hr (2.659 cm/sec)

ν = 1.0 cps (1.0×10^{-3} N sec/m^2) = 0.386 ft^2/hr (9.96×10^{-3} cm^2/sec

c_p = 0.68 BTU/lb °F [6.8×10^{-1} g cal/(g °C)]

μ = 0.73 cs = 1.76 lb/ft hr (2.619 kg s/m hr)

h = $(0.023)\,(1.31)\,(42,300)^{.8}\,\Delta 17.6)^{.4}$

= 474 BTU/hr ft^2 °F (6.44×10^{-2} cal/sec cm^2°C)

APPENDIX D
VAPORIZER DESIGN/HEAT TRANSFER ANALYSIS

APPENDIX D

PART I

DESIGN ANALYSIS FOR PILOT PLANT VAPORIZER

The design begins with an energy balance on the thermal output which determines the total tube surface area.

$$q = X_e \dot{m} h_{fg} = U_i A_i \Delta T$$

$$A_i = \frac{x_e \, m \, h_{fg}}{U_i \, \Delta T} = 418 \text{ ft}^2 \, (38.8 \text{ m}^2)$$

where

x_e = 0.4

$\dot{m}$ = 32,500 lb/hr (14,740 Kg/hr)

U_i = 550 Btu/hr ft^2 °F (11.24 x 10^7 j/hr-m^2-°C)

ΔT = 40°F (22.2 °C)

h_{fg} = 710 Btu/lb (1.65 x 10^6 j/Kg)

Total tube length,

$$L_{tube} = \frac{A_i}{\pi D_i} = 1837 \text{ ft. } (560 \text{ m})$$

where

D_i = 0.870 in. (2.21 cm) (ASTM A214)

D_o = 1.00 in. (2.54 cm)

The number of parallel lines is determined by assuming an inlet water velocity of 10 ft/sec. This velocity was chosen for proper flow distribution in the feedwater headers. The total flow area is then determined.

$$A_f = \frac{\dot{m}}{\rho V_i} = 0.0184 \text{ ft}^2 \, (1.71 \times 10^{-3} \text{ m}^2)$$

where ρ = 49 lb/ft^3 (30.8 Kg/m^3)

$$N_{tube} = \frac{A_f}{A_{tube}} = 4.45$$

rounding N_{tube} to 4 gives an inlet velocity of 11 ft/sec (3.35 m/s)

$$L_{tube} = \frac{\text{Total } L_{tube}}{N_{tube}} = 459 \text{ ft. } (140 \text{ m})$$

$$N_{legs} = \frac{L_{tube}}{\text{module width}} = \frac{459}{7} = 42$$

Since the legs are divided into 4 bundles, make $N_{legs} = 44$ and $L_{tube} = 484$ ft.

Heat Transfer Coefficient

The heat transfer coefficient is summarized here. The internal boiling coefficient is derived in Appendix A. The overall heat transfer coefficient is determined from the scraper clearance, tube wall thickness, and an average boiling coefficient.

$$U_i = \frac{1}{\frac{1}{h} + \frac{r_i}{k_t} \text{ hr } \frac{r_o}{r_i} + \frac{r_i}{k_s} \text{ hr } \frac{r_s}{r_o}}$$

$$= \frac{1}{\frac{1}{6500} + \frac{1}{4900} + \frac{1}{693}}$$

$$= 550 \text{ Btu/hr - ft}^2 \text{ - °F } (3.12 \text{ kW/m}^2 \text{ - °C})$$

where

h_i = 6500 Btu/hr ft^2 °F (36.9 kW/m^2 - °C) (average of 2000 to 11,000, (11.3 to 62.4 kW/m^2 - °C))

r_i = 0.435" (1.10 cm)

r_o = 0.500" (1.27 cm)

r_s = 0.506" (0.006" salt film (0.015 cm))

k_t = 25 Btu/hr ft°F (43 W/m - °C)

k_s = 0.3 Btu/hr ft °F (0.519 W/m - °C)

Note that no fouling factor was included in the thermal resistance because of the difficulty in simulating it in the SRE.

ANSI Pressure Code

The following is an analysis of the ANSI pressure pipe code from section 104. The 1.0 inch (2.54 cm) tube is analyzed for required wall thickness.

$$t_m = \frac{PD_o}{2\,(SE + P_y)} + C$$

t_m = wall thickness (in)

P = internal design pressure (psig)

D_o = outside diameter (in)

SE = max allowable stress in material (psi)

C = additional thickness to compensate for corrosion (in)

y = empirical coefficient from Table = 0.4

For ASTM A214 welded carbon steel tubing:

$T \leq 650^{\circ}F$ (343 °C)

SE = 9900 psi (68.3 M Pa)

For Corrosion 0.8 mils/yr for 20 years:

C = .016" (.406 cm)

P = 700 X 1.10 = 770 psi (5.31 M Pa)

$$t_m = \frac{(770)\,(1.00)}{2\,[9900 + (770)\,(.4)]} + 0.016 \text{ in.}$$

$$= .0377 + .016 = 0.054\ (0.137 \text{ cm})$$

Use standard size .065 wall (0.165 cm)

For Scaled SRE:

OD = 0.625" (1.588 cm), ID = .548" (1.392 cm),

Wall = .041" (0.104 cm)

Maximum allowable pressure will be:

$$P = \frac{2(SE = P_y)\,tm}{D_o}$$

= 1390 psi (9.58 M Pa)

APPENDIX D
PART II
VAPORIZER HEAT TRANSFER ANALYSIS

SUMMARY

This literature survey is to evaluate the qualitative and quantitative aspects of the two-phase forced convection heat transfer.

Chen's correlation is used to evaluate the inside heat transfer coefficients for qualities between 0.01 to dryout pt (~0.6). Rohsenow's relation is used for qualities below 0.01. The inside coefficient increases with quality.

Salt thickness as a function of time is evaluated using the energy conservation equation. Assuming a clearance between scraper blades and vaporizer tubes, outside heat transfer coefficients as a function of time are evaluated for clearances between 0 to 2.54×10^{-2} cm (0 to 10 mils). The overall coefficient is calculated as a function of both time and quality. Simpson's rule of integration is used to calculate the time-averaged coefficients. The outside coefficient is found to be controlling.

Trial and error calculations were done to estimate temperature drops and heat fluxes at different qualities and time. In thermal storage, boiler heat fluxes vary between 39.7 to 96.5 $kW/m^2\ ^\circ C$ (7000 to 17,000 $B/hr\text{-}ft^2\ -\ F^\circ$).

Macbeth's correlation for critical heat flux is used to determine the exit steam quality. For design, 40 percent quality at the vaporizer exit was chosen.

QUALITATIVE DESCRIPTION OF THE PROCESS:

In the vaporization of a liquid stream flowing through a closed channel, essentially three regimes of heat transfer can occur (see Figures D-1 and D-2):

1) Nucleate boiling regime
2) Forced convection controlled heat transfer regime
3) Regime of liquid deficiency

The first regime is characterized by bubble growth and nucleation at the heat transfer surface, and the heat transfer coefficient is a function of heat flux. In the convection controlled regime, the heat transfer coefficient is independent of the heat flux and is given by a modified form of the Dittus-Boelter-type equation (Reference 2) as for single phase convection heat transfer. The

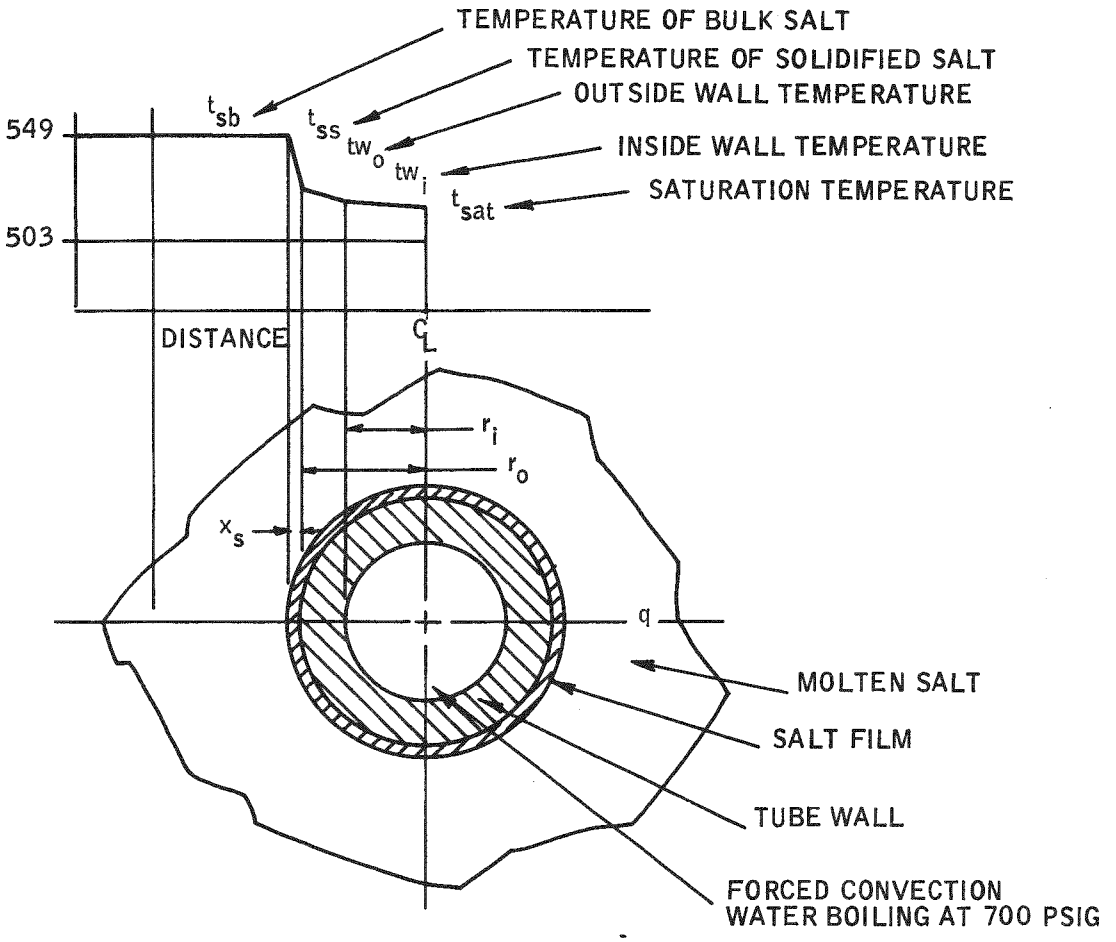

$$\frac{U_i A_i}{L} = \frac{1}{\frac{1}{h_i A_i /} + \frac{\ell n \frac{D_o}{D_i}}{2\pi k_s} + \frac{1}{h_o A_o /}}$$

Figure D-1. Boiler Tube Heat Transfer

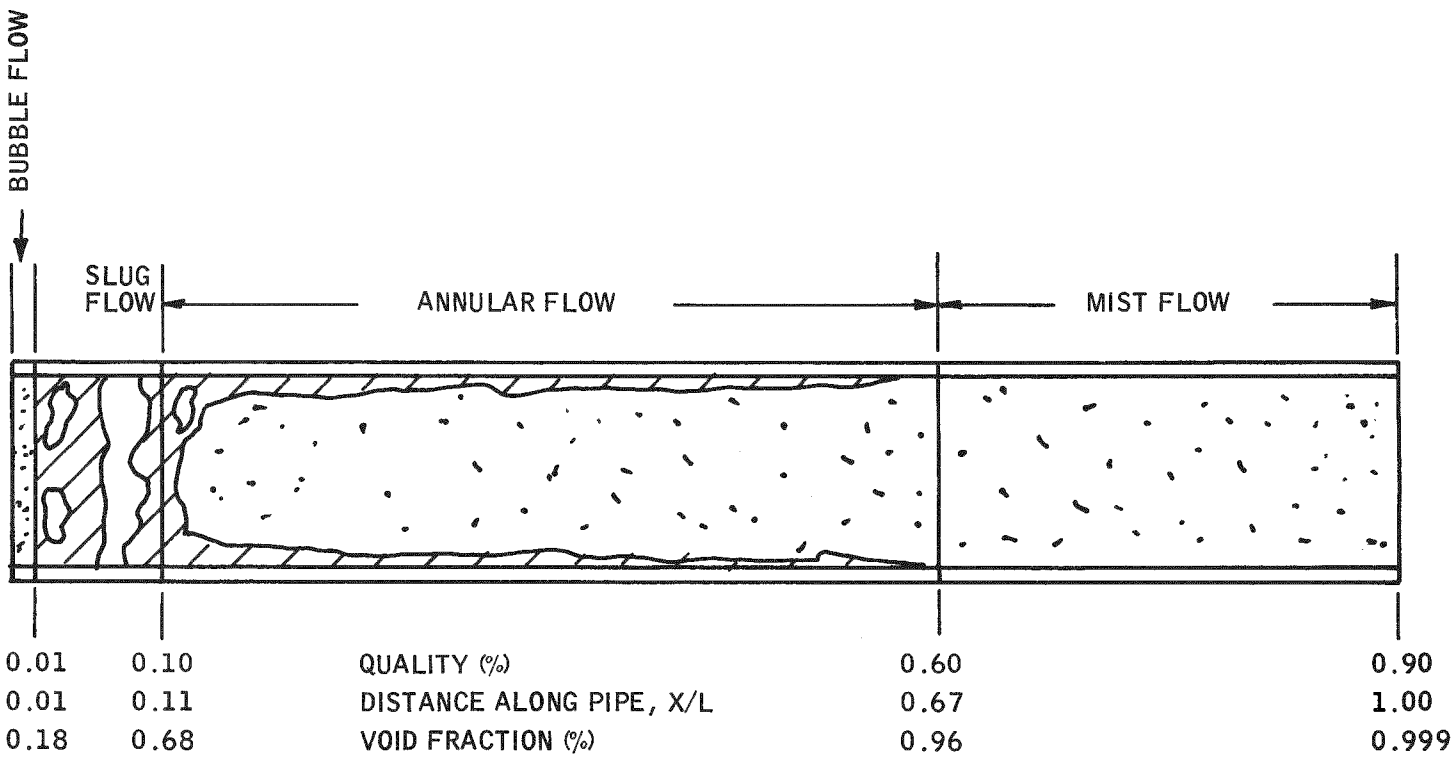

NOTE: CONSTANT HEAT FLUX MAKES QUALITY PROPORTIONAL TO PIPE LENGTH.

Figure D-2. Boiling Flow Regimes

third regime is characterized by a liquid deficient condition at the wall and occurs at high vapor mass fractions. It is in this regime the heat transfer coefficient experience a sharp decrease. Experimental studies for each case were done by various authors and the heat transfer relations were correlated.

EMPIRICAL CORRELATION FOR TWO-PHASE COEFFICIENTS:

Table D-1 lists the authors and the correlating equations and Table D-2 gives the variables studied by investigators. Of the equations listed, Chen's correlation had received much of our attention. Contacts were made to specialists in the area of forced-convection two-phase boiling heat transfer. It was established that Chen's correlation ought to be satisfactory.

Chen's (Reference 1) correlation for heat transfer coefficients is based upon macroconvective and microconvective effects. The macroconvective term is the modified Dittus Boelter equation and the microconvective term is based on the Forster-Zuber (Reference 4) formulation for pool boiling. Table D-3 gives the variables and system conditions and the ranges for which Chen's correlation is applicable. The conditions fall within or close to the specified range. However, Chen's correlation is for vertical flow, but at the high velocities of 3.05 m/s (10 ft/sec), the correlation could satisfactorily be applied to horizontal boilers (Reference 2).

Besides Chen's correlation, other correlations considered were those of Rohsenow (Reference 3) for low-quality regimes, and of David and Davis for annular flow regime. The heat transfer coefficients calculated as a function of quality are shown in Figure D-5 for each of the correlations.

Chen's Correlation: (Ref. Table D-4 for definition of terms)

Quality range used $0.01 < X < 0.7$ (or dryout pt.)

$$h = h_{mic} + h_{mac}$$

$$h_{mac} = 0.023\, F\, (R_e)^{0.8}\, (Pr)^{0.4}\, \frac{k_L}{D}$$

$$h_{mic} = 0.00122 S\, K_C\, (\Delta T)^{0.24}\, (\Delta P)^{0.75}$$

where

$$R_e = \frac{G(1-x)D}{\mu}$$

$F = F(\tilde{X})$ and

$$X = \left(\frac{X}{1-X}\right)^{0.9} \left(\frac{\rho_L}{\rho_g}\right)^{0.5} \left(\frac{\mu_g}{\mu_L}\right)^{0.1}$$

Table D-1. Proposed Correlating Equations

Authors	Correlating Equations*
David, et al. (Ref. 4)	$\frac{hD}{k_L} = 0.06C\left(\frac{PL}{P_g}\right)^{0.28}\left(\frac{DG_tX}{\mu L}\right)^{0.87}\left(\frac{C_p}{k}\right)_L^{0.4}$
Bennett, et al. (Refs. 3, 13)	$\frac{h_{TP}}{h_L}\left(\frac{q}{A}\right)^{0.11} = 0.64\left(\frac{1}{X_u}\right)^{0.74}$
Chen (Ref. 1)	$h = h_{mac} + h_{mic}$ $h_{mac} = 0.023\,(Re_L)^{0.8}\,(Pr_L)^{0.4}\,\frac{k_L}{D}\,F$ $h_{mic} = 0.00122\,\frac{k_L^{0.79}C_{PL}^{0.45}P_L^{0.49}g_c^{0.25}}{\sigma^{0.5}\mu_L^{0.29}h_{fg}^{0.24}\rho_v^{0.24}}\,(\Delta t)^{0.24}\,X\,(\Delta P)^{0.75}\,S$ where F and S are empirically correlated factors. (S = 0 when nucleate boiling is totally suppressed)
Dengler (Ref. 5)	$\frac{h_{TP}}{h_L} = 3.5\left(\frac{1}{X_u}\right)^{0.5}$
Fikry (Ref. 6)	$\frac{hD}{k_g} = \left(\frac{D\rho_g' U_c}{\mu g}\right)^{0.8}$ where C = 0.84 0.4 x 0.5 C = 0.887 0.55 x 0.65 C = 0.904 0.70 x 0.80
Guerrieri and Talty (Ref. 7)	$\frac{h_{TP}}{h_L} = 3.4\left(\frac{1}{X_u}\right)^{0.45}$
Groothuis and Hendal (Ref. 8)	$\frac{hD}{k_L} = 0.029\left(\frac{P_L u_L D}{\mu_L} + \frac{p_g u_g D}{\mu g}\right)^{0.87}\left(\frac{C_p u}{\left(\frac{\mu b}{\mu w}\right)^{0.14}}\right)^{0.33}\,X$

Table D-1. Proposed Correlating Equations (Concluded)

Authors	Correlating Equations*
Kvamme (Ref. 9)	$\frac{h_{TP}}{h_L} = 1.5\left(\frac{1 - X}{1 - R_g}\right)^{0.8}$ where R_g = steam void fraction calculated from Martinelli-Lockhart correlation
Mumm (Ref. 10)	$\frac{hD}{K} = \left[4.3 + 5.0 \times 10^{-4}\left(\frac{V_{Lg}}{V_L}\right)^{1.64}_{0.464} X\right] X \left(\frac{q}{G\lambda}\right) \left(\frac{DG}{\mu L}\right)^{0.808}$ where V_{Lg} = specific volume increase upon vaporization
Shrock and Grossman (Ref. 11)	$\frac{hD}{k_L} = 170\left[B_o + 1.5 \times 10^{-4}\left(\frac{1}{X_u}\right)^{2/3}_{R_e}\right] X\ 0.8\ Pr^{1/3}$ where $B_o = \left(\frac{q}{A}\right)\left(\frac{1}{G\lambda}\right)$
Silvestri, et al. (Ref. 12)	Graphical correlation of $\frac{h}{\Delta\pi/\Delta T} \times \frac{\pi/T^{3/2}}{R_e 0.8}$ vs. $\frac{DG_t}{\mu TP}$ where $\mu TP = X_{\mu g} + (1 - x)\,\mu_L$

*These empirical equations were obtained under specific flow conditions and may not be applicable to other configurations and fluids. However, these typify the manner of analyzing and predicting the behavior of two-phase forced-convection systems.) Note, the correlating equations are in English units. See references for definition of terms.

Table D-2. Variables Studied by Investigators of Two-Phase Convection Heat Transfer

Investigator	System	Pressure, PSIA	Mass Flow Rate, lb/hr-sq ft x 10-3	Vapor Mass Fraction	Heat Flux, Btu/hr-sq ft x 10-3	Tube Dia., ft	Tube Orientation
Anderson, et al.	Steam-water	20-120	32.8-656	0.01-0.60	3.7-97.0	0.0387	Vertical
Bennett, et al.	Steam-water	15-35	51.5-217	0-0.546	63-138	0.0203 (equiv. diam.)	Vertical (annulus)
Davis	Steam-water	25-150	50-600	0.30-0.90	50-260	0.0324 (equivl diam.)	Horizontal (rectangular duct)
Dengler and Lee	Steam-water	7-40	44-1010	0.07-0.90	0-200	0.0833	Vertical
Fikry	Steam-water	15-25	41.4-74.7	0.02-0.82	6.0-30	0.0208	Horizontal
Groothuis and Hendal	Air-water	14.7	112-621	0-0.20	Not reported	0.0460	Vertical
Kvamme	Steam-water	18-87	52-182	0-1.00	9.4-50.2	0.0208	Horizontal
Mumm	Steam-water	45-200	252-1008	0-0.60	50-250	0.0387	Horizontal
Parker and Grosh	Steam-water	49-61	37-73	0.89-0.99	3.0-20.7	0.0833	Vertical
Silvestri, et al.	Steam-water	15-75	73.6-162 (steam) 51.5-332 (water)	0.25-1.00	0-1427	0.0164	Vertical

Table D-3. High-Quality, Forced-Convection Evaporation Correlations (Yadigaroglu and Bergles)*

AUTHOR	CHEN (97)
FLUID	WATER, METHANOL, CYCLOHEXANE, PENTANE, HEPTANE, BENZENE
DIRECTION OF FLOW	UP AND DOWN
CHANNEL GEOMETRY	CIRCULAR AND ANNULAR
DIAMETER, D (IN.)	LARGE RANGE
LENGTH, L (FT)	LARGE RANGE
PRESSURE LEVEL, p (psia)	8-505
MAX FLUX, $G/10^5$ (LB/HR-FT^2)	LARGE RANGE
HEAT FLUX, q" (Btu/HR-FT^2)	2000-760,000
QUALITY RANGE, x	0-0.71
RECOMMENDED CORRELATION	$h = h_{mic} + h_{mac}$ $= 0.00122 \frac{k_\ell^{0.79} c_\ell^{0.45} \rho_\ell^{0.49} g_c^{0.25}}{\sigma^{0.5} \mu_\ell^{0.29} h_{fg}^{0.24} \rho_v^{0.24}}$ $(\Delta T)^{0.24} (\Delta p)^{0.75} S + h_{LP} F$ WITH: $\Delta p = \frac{\Delta T h_{fg}}{T_{sat} v_{fg}}$ diff. in sat. vap. press. corr. TO $\Delta T = T_w - T_{sat}$ $g_c = 32.2(3600)^2$, S and F given in comp. vugraph
PROPERTIES EVALUATED AT	T_{sat}
NO. OF DATA POINTS/RUNS	DATA OF MANY INVESTIGATORS
ERROR IN CORRELATING DATA	85% WITHIN ± 15.1%
EQUATION	38

* REF. HANDBOOK OF HEAT TRANSFER, P 13-40

$$K_c = \frac{k_L^{0.79} C_L^{0.45} \rho_L^{0.49} g_0^{0.25}}{\sigma^{0.5} \mu_L^{0.29} h_{fg}^{0.24} \rho_g^{0.24}}$$

$S = S(y)$ and

$$y = R_e' F^{1.25} \times 10^{-5}$$

the functions for F and S used were,

$$\log F = 0.447 + 0.57 \log \tilde{X} \; 0.1056 \log^2 \tilde{X} - 0.0176 \log^3 \tilde{X}$$

$$S = 0.0962 + 0.786\, e^{-0.9405y} - 0.9405y.$$

Using these relations with the fluid properties given in Table D-4, parameters F and S were calculated and plotted as shown in Figures D-3 and D-4, while Figure D-5 gives a plot of heat transfer coefficient versus quality. Chen's equation for the specified conditions is,

$$h_i = 0.0962(F)(R_e')^{0.8} + 782(S)(\Delta T)^{0.99}$$

Rohsenow's Relation:

Quality: $0 < x < 0.01$ (used)

$$h_i = (q/A)^{0.67}/(0.014)K_R$$

where

$$K_R = \frac{(h_{fg}\mu_L)^{0.67}}{k\rho}\left(\sqrt{\frac{(\sigma g_o)}{g(\rho_L - \rho_g)}}\right)^{0.33}$$

For case at hand,

$$h_i = 4.48\,(q/A)^{0.67},$$

substituting for $q/A = h_i \Delta t_i$

$$h_i = 90\,(\Delta t_i)^2 \; (B/hr - ft^2 - F^\circ)$$

where $\Delta t_i = t_w - t_{sat}$. (F°)

40284

Table D-4. Properties of Saturated Liquid Water

At P = 700 psia		English	SI
Density,	ρ_L	49.06 lb/ft^3	785.9 kg/m^3
Heat Capacity,	C_{pL}	1.182 Btu/lb-°F	3.496 j/kg-°C
Viscosity,	μ_L	0.26139 lb/hr-ft	0.3889 kg/m-hr
Thermal Conductivity,	kL	0.353 B/hr-ft-°F	0.611 W/m-°C
Prandt 1 No.,	Npr_L	0.874	
Heat of Vaporization,	h_{fg}	708 Btu/lbm	1.65 x 10^6 j/kg
Gravity Acceleration,	g_o	32.2 (3600)^{2}ft/hr^2	9.81 m/s^2
*Surface Tension,	ρ	1.042 x 10^{-3} lbs/ft	1.55 x 10^{-3} kg/m
Properties of Saturated Vapor			
Density,	ρ	1.53 lb/ft^3	24.5 kg/m^3
Viscosity,	μ_g	0.05 lb/hr-ft	7.44 x 10^{-2} kg/hr-m

* $\sigma = \dfrac{h_{fg}\, L}{364}$ (Walden's Rule)

40284

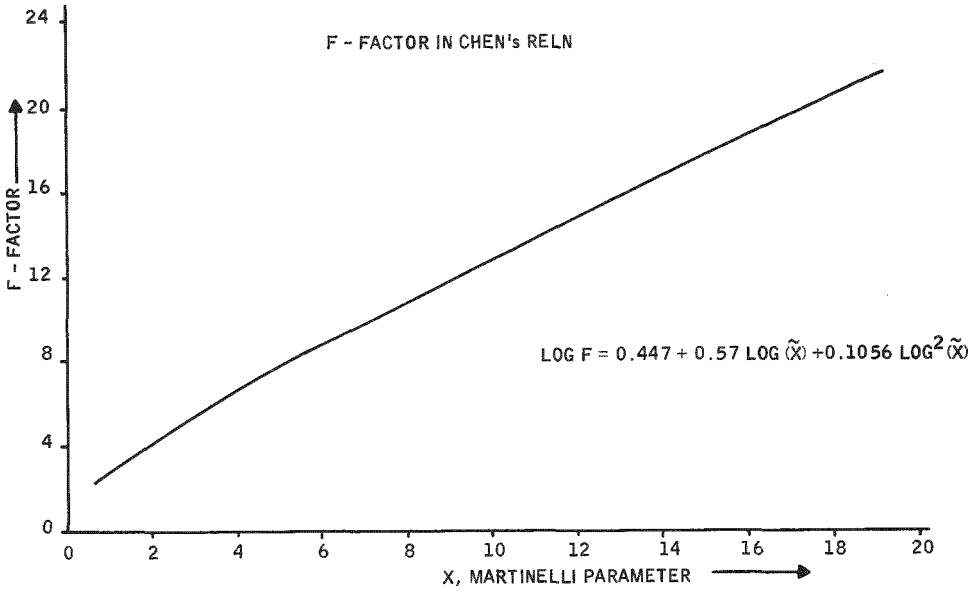

Figure D-3. F-Factor in Chen's Correlation

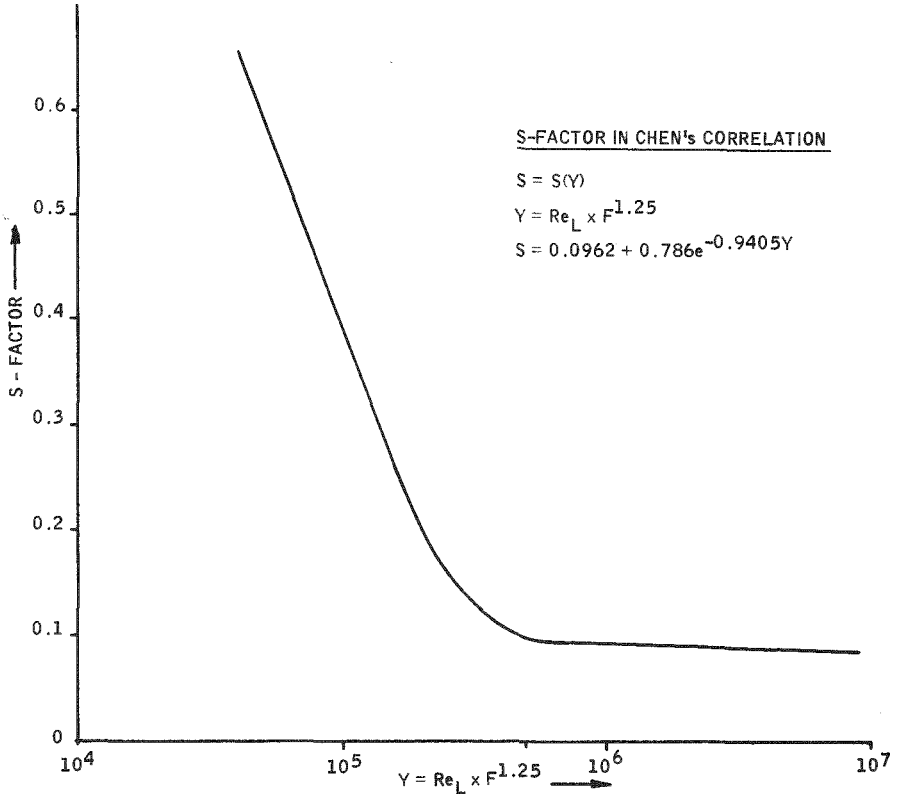

Figure D-4. S-Factor in Chen's Correlation

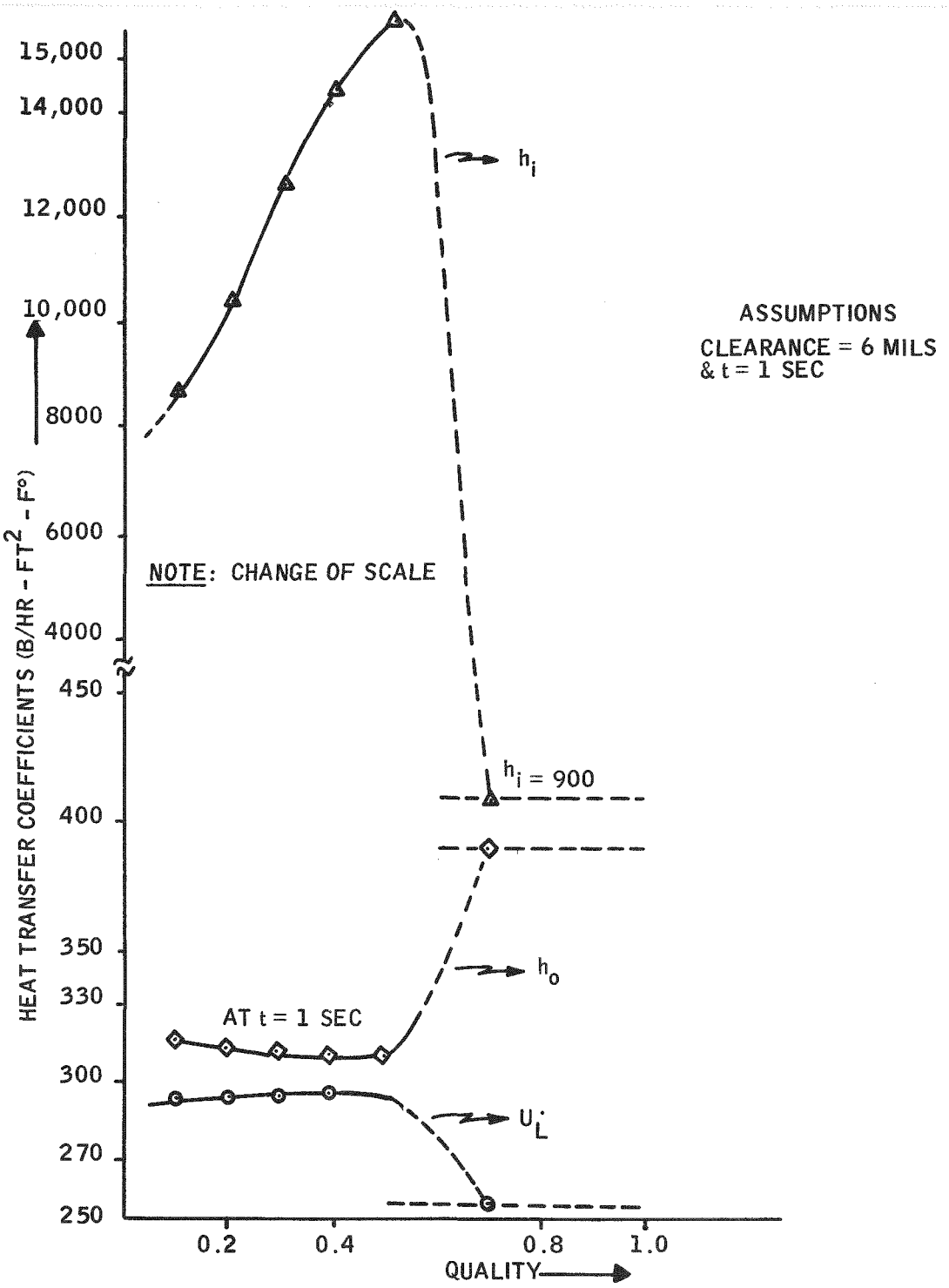

Figure D-5. Heat Transfer Coefficients versus Quality

In the high quality ($X > 0.1$) the S factor in Chen's correlation is of the order of 0.01 and h_{mic} is relatively small compared to h_{mac}. However, for low qualities, heat transfer coefficient is a function of heat flux and, hence, Δt_i. To calculate h_i; Δt_i has to be estimated by trial and error for which outside coefficients are required.

OUTSIDE HEAT TRANSFER COEFFICIENTS:

Outside the vaporizer tubes, solid salt builds up, resulting in a decrease in the heat transfer coefficient. The outside coefficient is a function of time and, hence, Δt_i will be a function of time.

To estimate the outside coefficient, the salt thickness is expressed as a function of time from the salt growth rate equation or the conservation of energy equation:

$$\rho Q_L \frac{d}{dt}(\pi D_0 X_s) = U_i A_i \Delta T$$

and

$$U_i = \frac{1}{\frac{1}{h_i} + \frac{D_i \ln(\frac{D_0}{D_i})}{2k_p} + \frac{D_i \ln(\frac{D_0 + 2Xs}{D_0})}{2k_s}}$$

where,

X_s = salt thickness
k_p = thermal conductivity of pipe material
Q_L = heat of fusion of salt
ρ = density of salt
D_i, D_0 = inside and outside pipe diameters
k_s = salt conductivity
h_i = inside heat transfer coeff.
U_i = overall coeff. based on inside area.

$$\ln\left(\frac{D_0 + 2Xs}{D_0}\right) \approx \frac{2Xs}{D_0}$$

$$\therefore \quad U_i = \frac{1}{\frac{1}{h_i} + \frac{D_i \ln(\frac{D_0}{D_i})}{2k_p} + \frac{Xs}{k_s} \cdot \frac{D_i}{D_0}}$$

Solving,

$$X_s = \frac{-B + \sqrt{B^2 + 2ACt}}{C}$$

where

$$B = \frac{D_0}{D_i h_i} + \frac{r_o \ln \frac{D_0}{Di}}{k_p}$$

$$A = \frac{\Delta T}{\rho_L}, \text{ and}$$

$$C = \frac{1}{k_s} .$$

The heat transfer coefficient is

$$h_o(t) = \frac{k_s}{X_s(t)} ,$$

where X_S as a function of 't' (see Figures D-6 and D-7) was calculated for h_i values of 11.3 kw/m^2-°C (2000 B/hr-ft^2-°F) and 22.7 kw/m^2-°C (4000 B/hr ft^2 °F). From h_o values, a time averaged value for heat transfer coefficient was calculated from,

$$h_{o,ave} = \frac{\int_0^t h_o(t)\, dt}{\int_0^t dt}$$

where h_o was integrated over the scraping time. A computer program was prepared and runs made for different scraping times and assuming a clearance between the scraper blades and types of 0 to 2.54 x 10^{-2} cm (0 to 10 mils). The overall coefficient was similarily calculated. The effect of inside coefficient on the overall coefficient was almost negligible. Table D-5 gives typical values for X_s, h_o, U_i versus 't' for a clearance of 1.27 x 10^{-2} cm (5 mils). The calculations were made for Sch 80 pipes.

ESTIMATION OF TEMPERATURE DROP:

Using h_o as calculated above, temperature drops were estimated and the inside h_i was calculated for low qualities (Table D-6). However, Δt's change with time and, hence, h_i changes with time in the low-quality regime. Table D-6 gives values of h_1, h_o, U, Δt's and heat flux at t = 0 secs, t = 1 sec and average values, at different qualities.

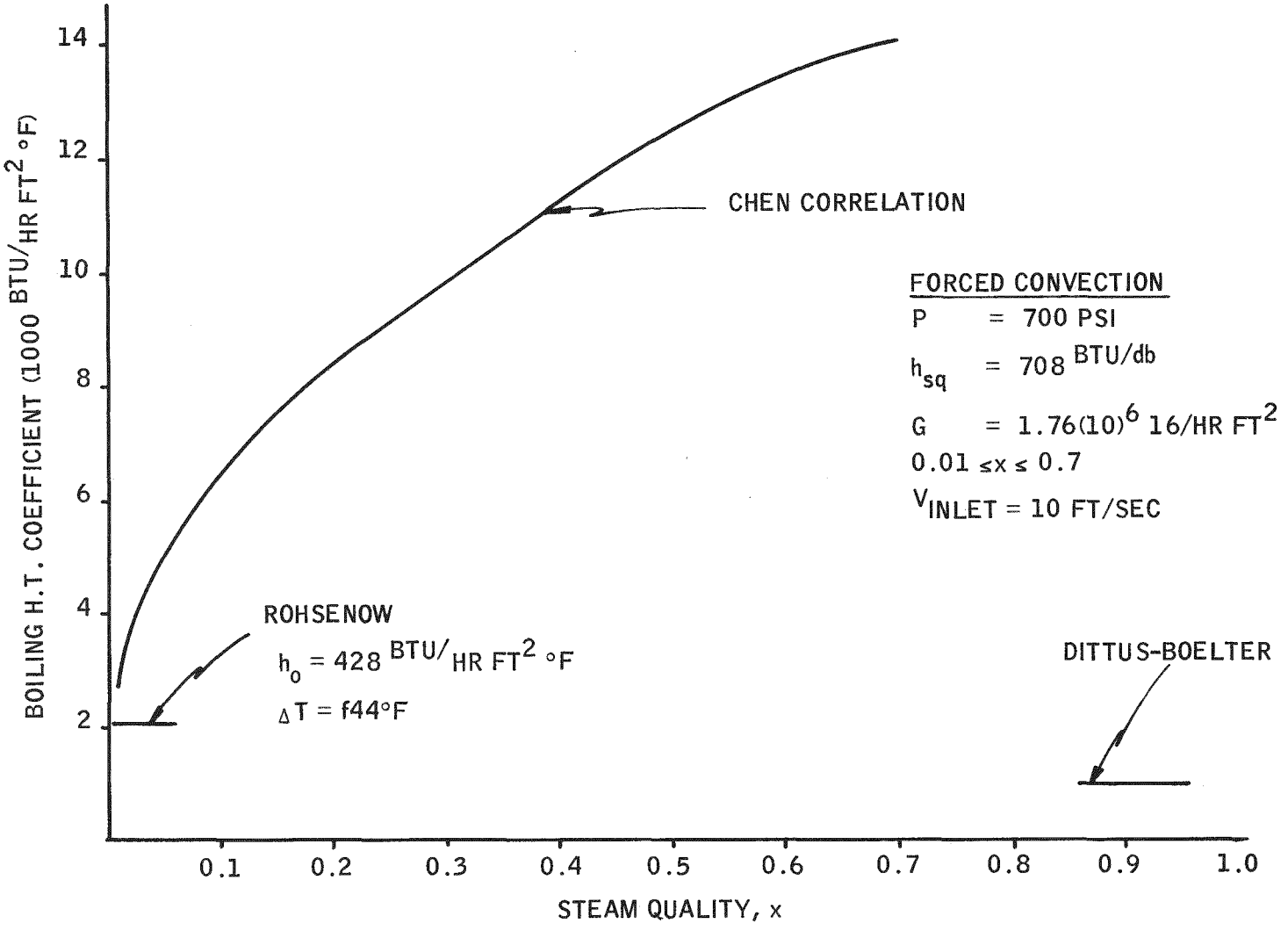

Figure D-6. Two-Phase Heat Transfer Correlation

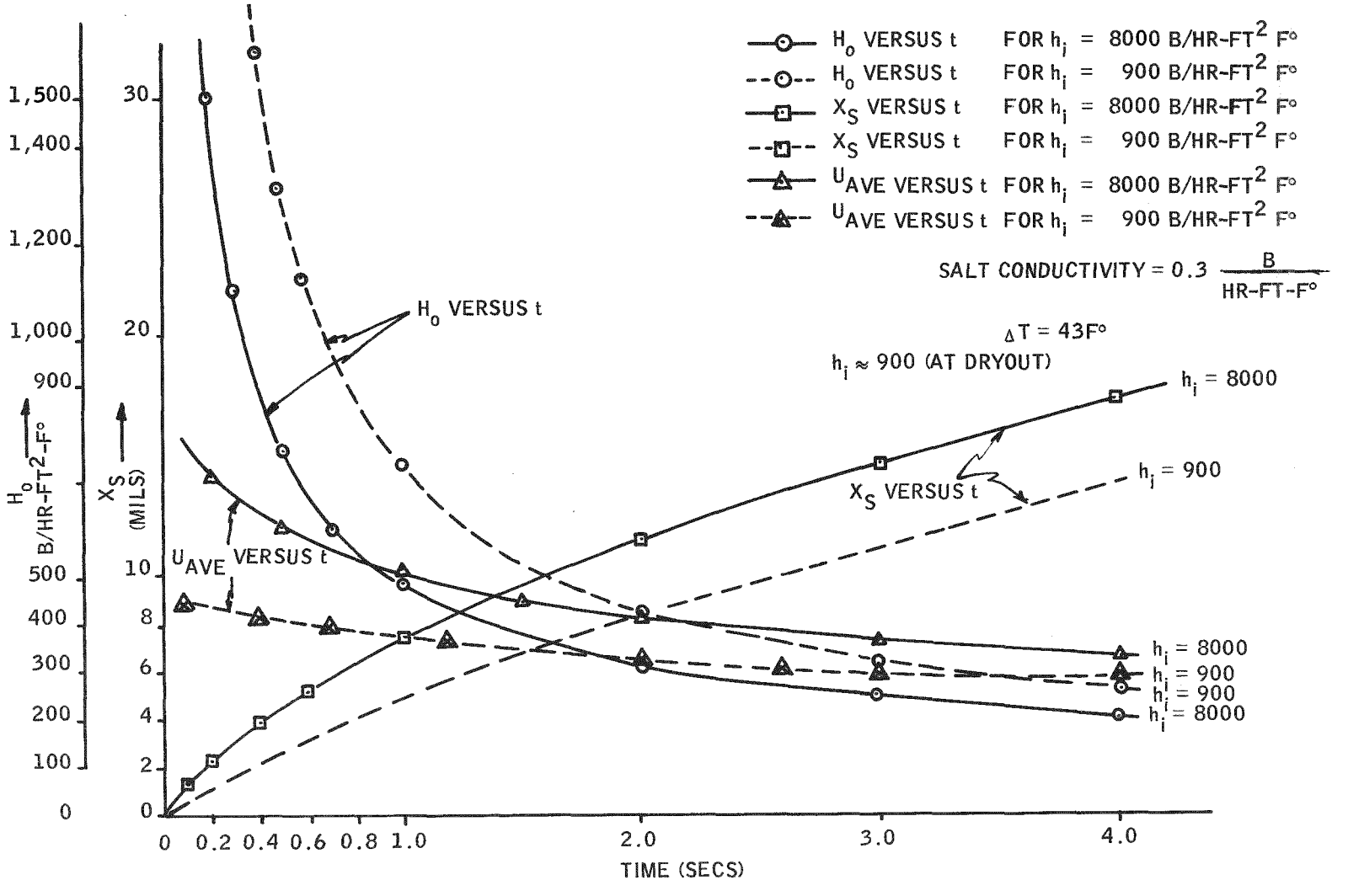

Figure D-7. Salt Thickness as a Function of Time

Table D-5. Typical Values for X_s, h_o, U_i versus 't' for a Clearance of 1.27×10^{-2} cm (5 mils)

Quality	Rey Number	HMAC or HI	CMIC	(G), Mass Velocity
0.200	4.3108375E 05	1.0414783E 04	7.0380005E 01	2.8170250E 06

Clearance = 0.00600 inches

SCR Time (Secs)	X_S Thickness (Inches)	Ho (B/Hr-Ft^2-F)	Ui (B/Hr-Ft^2-F)	(H_oA_o) avg (B/Hr-F)	U (Avg) (B/Hr-Ft^2-F)	Hi (B/Hr-Ft^2-F)
0.100	0.00774	469.578	411.234	114.450	433.156	10414.7
0.200	0.00890	408.705	377.072	104.994	410.488	10414.7
0.300	0.00984	370.087	353.548	98.400	393.668	10414.7
0.400	0.01065	342.278	335.619	93.351	380.212	10414.7
0.500	0.01137	320.811	321.168	89.276	368.970	10414.7
0.600	0.01203	303.493	309.099	85.871	359.306	10414.7
0.700	0.01264	289.084	298.764	82.955	350.830	10414.7
0.800	0.01321	276.818	289.747	80.412	343.284	10414.7
0.900	0.01375	266.190	281.766	78.162	336.485	10414.7
1.000	0.01426	256.850	274.620	76.149	330.302	10414.7
2.000	0.01839	200.090	228.312	63.128	287.929	10414.7
3.000	0.02158	171.137	202.606	55.919	262.562	10414.7
4.000	0.02427	152.601	185.330	51.078	244.697	10414.7
5.000	0.02665	139.361	172.575	47.503	231.054	10414.7
6.000	0.02881	129.265	162.608	44.708	220.106	10414.7

SCR Time = Scraping time

X_S = Salt thickness

H_o = Outside heat transfer coefficient at time 't'

G = Mass velocity = Vel x ρ

U_i = Overall coefficient based on inside area

(H_oA_o) avg = (Outside coefficient x Area) averaged over the Scraping time

H_i = Inside heat transfer coefficient calculated from Chen's Equation

40284

Table D-6. Outside Coefficients, Assumptions:

NOTES:

1. 6 mils clearance between scraper blades and pipes.

2. Salt thermal conductivity, K_s = 0.2 Btu/hr-ft-°F (0.35 w/m °C)

3. Outside coefficient, h_o:

at t = 0 secs, X_s = 6 mils (1.524×10^{-2} cm), h_o = 500 B/hr-ft^2-°F (2.84 kW/m^2-°C)

at t = 1 sec, X_s = 12.31 mils (3.127×10^{-2} cm), h_o = 244 B/hr-ft^2-°F (1.38 kW/m^2-°C)

$0 < t < 1$, h_o(avg) = 330 B/hr-ft^2-°F (1.87 kW/m^2-°C) $h'_o = h_o(A_o/A_i) = 1.4\, h_o$

4. h_w = 1973 Btu/hr-ft^2-°F (11.20 kW/m^2-°C)
   $h_{fouling}$ = 2000 Btu/hr-ft^2-°F (11.35 kW/m^2-°C)

5. $h_i = h_{mac} + h_{mic}(\Delta t_i)^{0.99}$ for $0.01 < x <$ dryout (Ref. Chen's eqn.)
   and
   $h_i = 90\,(\Delta t_i)^2$ for $0 < x < 0.01$ (Ref. Rohsenow eqn.)

	$X < 0.01$, $h_i = 90\,(\Delta t_i)^2$			$X = 0.01$, $h_i = 1886 + 140\,\Delta t_i$		
t(secs)	0	1	Avg.	0	1	Avg.
Δt_i, °F	5.5	4.7	5.1	5.6	4.2	4.0
h_i	2,722	1,988	2,340	2,660	2,475	2,572
$h_i \Delta t_i$	14,974	9350	11,940	14,800	10,390	12,603
Δt_w, °F	15.3	9.7	12.1	15.1	10.6	12.9
Δt_o, °F	22.2	28.8	25.7	20.7	28.2	25.2
$h'_o\ \Delta t_o$	15,550	9840	11,880	14,544	9,650	11,660
$U_i \approx$	355	233	277	342	233	279
$(q/A) \approx$	15,250	9594	11,990	14,700	10,000	12,000

Table D-6. Outside Coefficients, Assumptions: (Concluded)

X = 0.05, h_i = 4520+71 (Δt_i)				X = 0.1, h_i = 6750+70 (Δt_i)		
t(secs)	0	1	Avg.	0	1	Avg.
Δt_i, °F	3.4	2.4	2.8	2.4	1.5	1.9
h_i	4770	4700	4720	6920	6855	6880
$h_i \Delta t_i$	16,220	11,280	13,200	16,600	10,280	13,077
Δt_w	16.5	11.5	13.5	16.9	10.5	13.3
Δt_o	23.1	29.1	26.7	23.6	31	27.8
$h'_o \Delta t_o$ A_o/A_i	16,135	9950	12,350	16,560	10,600	12,823
U_i ~	375	247	297	386	243	301
q/A ~	16,150	10,600	12,750	16,580	10,400	12,950

X = 0.3, h_i = 9820 + 70 (Δt_i)				X > 0.5 (dryout)		
t(secs)	0	1	Avg.	0	1	Avg.
Δt_i, °F	1.65	1.1	1.3	14	10	12
h_i	9930	9900	9915	900	900	900
$h_i \Delta t_i$	16,380	10,890	12,890	12,600	9000	10,800
Δt_w	16.62	11.1	13.15	12.8	9.2	11
Δt_o	24.63	30.8	28.55	16.2	24	20
$h_o t_o$ A_o/A_i	17,200	10,530	13,190	11,500	9200	10,000
U_i ~	391	249	303	280	214	240
q/A ~	16,800	10,700	13,040	12,000	9100	10,000

$\Delta t_i = t_{wi} - t_{sat}$

$\Delta t_w = t_{wo} - t_{wi}$

$\Delta t_o = t_{salt} - t_{wo}$

$\frac{q}{A_i} = h_i \Delta t_i = h_o \frac{A_o}{A_i} \Delta t_o = U_i \Delta t$

$\Delta t = t_{salt} - t_{sat} = 43F° \ (6.11°C)$

$h'_o = h_o \frac{A_o}{A_i}$

CRITICAL HEAT FLUX (MACBETH[17] CORRELATION)

To determine the critical heat flux (i. e., the point where the liquid disengages from the wall) or the dryout point, Macbeth's correlation for high flow regimes was used (Journal o f Heat Transfer).

$$\left(\frac{q}{A}\right)t \times 10^{-6} = A - \frac{1}{4} \times CD(G \times 10^{-6})\, h_{fg}\, X_e,$$

where $A = y_0 D^{y1} (G \times 10^{-6})^{y2}$

$C = y_3 D^{y4} (G \times 10^{-6})^{y5}$.

At 700 psia the y values given are:

y_0	= 1.25	y_3	= 0.0106
y_1	= -0.522	y_4	= -1.4
y_2	= -0.255	y_5	= -0.646 .

Now,

$G = 1.766 \times 10^6$ lb/hr-ft^2 (8.62×10^6 kgs/hr-m^2)

D = 0.957 inches (2.431 cm)

h_{fg} = 7.08 Btu/lb (1.65×10^4 j/kg)

A = 1.107

C = 0.00781

$$\left(\frac{q}{A}\right)_{CRIT} x10^{-6} = 1.107 - 2.335\, X_e$$

Figure D-8 is a plot of $(q/A)_{crit}$ versus X_e, which shows that at qualities of about 45 percent and above, a small amount of heat flux would cause a dry wall.

The heat fluxes in the thermal storage vaporizer are in the range of 45.4 to 113 kw/m^2°C (8000 to 20,000 Btu/hr-ft^2). Thus, according to plot the dryout point will be at X_e = 0.46. However, the critical flux is not quite critical in our case, since we have a constant temperature environment. But since the heat transfer coefficient decreases sharply above this quality, economics dictate that the design point be chosen a little below the critical point.

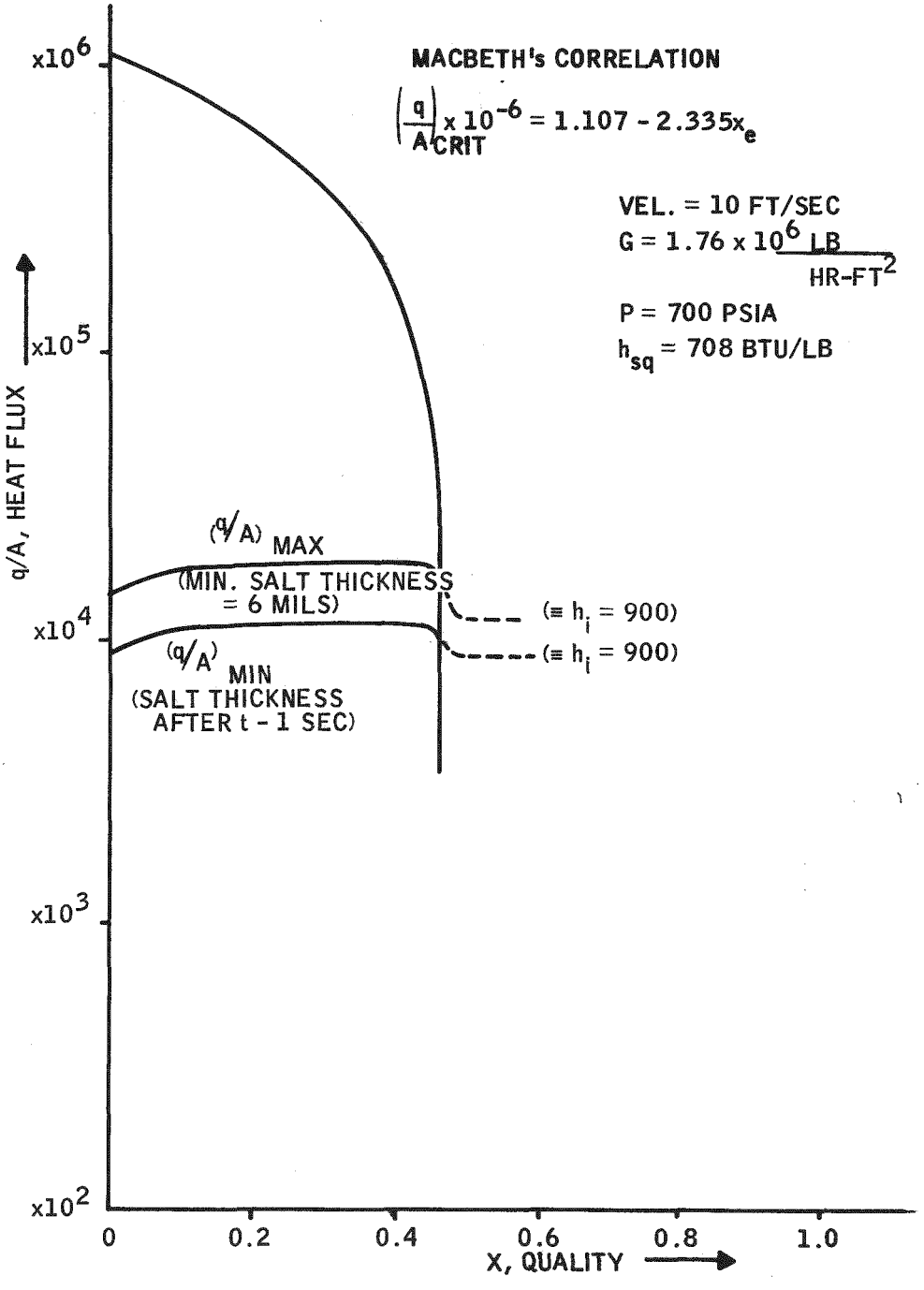

Figure D-8. Heat Flux versus Steam Quality

The design point chosen is 40 percent quality at the pipe exit: which means an operating recirculation ratio of 5 to 2.

BIBLIOGRAPHY:

1. Chen, J.C., "Correlation for Boiling Heat Transfer to Saturated Fluids in Convective Flow", A.S.M.E.-A.I. Ch.E. Heat Transfer Conference, Boston - 1963.

2. Art Bergles, Private Communication

3. Handbook of Heat Transfer, Rohsenow W.M. and Martinett, J.P., pp 13-28.

4. David, E.J., Davis, M.M., "Two-phase Gas-Liquid Convection Heat Transfer," I and EC Fundamentals, Vo.. 3 (1964), pp 111-118.

5. Dengler, C.E., Addoms, J.N.; Chem. Eng. Prog. Symp., Ser., 52, 95 (1956).

6. Fikry, M.M., PhD. Thesis, Imperial College, London, 1953.

7. Guerrieri, S.A., and Talty, R.D., Chem. Eng. Progr. Symp. Ser., 52, 69, (1956).

8. Groothuis, H., Hendal, W.P., Chem. Eng. Sci., 11, 212, (1959)

9. Kvamme, A., M.S. Thesis, University of Minnesota, 1959.

10. Mumm, J.F., Argonne National Lab Report ANL-5276 (1954).

11. Shrock, V.E., Grossman, L.M., Nuclear Sci. Eng., 12, 474, (1962).

12. Silvestri, M., Finzi, S., Roseo, L., Schiavon, M., Zavattaralli, Z.; Proc. Second UN Intern. Conf. Peaceful Uses At. Energy 7, (1958).

13. Bennett, J.A.R., Collier, J.G., Pratt, H.R.C., Thornton, J.D., Trans. Inst. Chem. Engrs. (London) 39, 113 (1961).

14. Stone, R.A., and Berenson, B.J., "A Photographic Study of the Mechanisms of Forced Convection Vaporization," Ch. Eng. Prog. Symp. Ser., No. 57, p-213.

15. Forster, H.K., Zuber, N., A.I. Ch. E., J, 1, 531, (1955).

16. Handbook of Heat Transfer, Rohsenow and Martinett, pp. 13-57 (1974).

APPENDIX E
SRE CONDENSER DETAIL DESIGN CALCULATIONS

APPENDIX E
SRE CONDENSER DETAIL DESIGN CALCULATIONS

1. Scale Factor = 1/4

Linear scale factor = $3-\sqrt{1/4} = 0.63$

2. Geometric Similarity

All the linear dimensions are scaled down by a factor of 0.63, as given in Table 3-3 (Section III).

Since tubes are not available in a continuum of sizes, exact scaling was not possible. The closest available pipe size was chosen. The pipe dimensions were scaled down by the ratios of pipe O. D. or I. D.

$$\frac{\text{Fin height}}{\text{Pipe O.D.}} \; ; \quad \frac{h_F}{D_o} = \left(\frac{h_F}{D_o}\right)_{\text{model}}$$

$$\frac{\text{Fin thickness}}{\text{Fin height}} \; ; \quad \frac{t_F}{h_F} = \left(\frac{t_F}{h_F}\right)_{\text{model}}$$

$$\frac{\text{Fin pitch}}{\text{Fin height}} \; ; \quad \frac{d_F}{h_F} = \left(\frac{d_F}{h_F}\right)_{\text{model}}$$

3. Fin Efficiency

$$\text{Fin effectiveness, } \eta_F = \frac{\text{Tanh}\,(mh_F)}{mh_F}$$

where

$$m = \sqrt{\frac{2h_o}{kt_F}}$$

h_F = fin height = 0.0114 m (0.0375 ft)

t_F = fin thickness = 7.62×10^{-4} m (0.0025 ft)

k = thermal conductivity of fin material = 43.2 $\frac{W}{m^2\text{-}°C}$ $\left(25 \frac{Btu}{hr\text{-}ft\text{-}°F}\right)$

h_o = outside coeff based on bare tube = 454 $\frac{W}{m^2\ °C}$ $\left(80 \frac{Btu}{hr\text{-}ft^2\text{-}°F}\right)$

m = 51

$\therefore \quad \eta_F = 0.49$

Overall effectiveness, $\eta_o = 1 + (\eta_o - 1) \frac{A_F}{(A_F + A_b)}$

4. Pipe Wall Thickness Calculations

The equation recommended for minimum wall thickness is:

$$t_m = \frac{PD_o}{2(SE + PY)} + C$$

where

P = design pressure

D_o = outside pipe diameter

S = allowable stress

Y = coeff. for steel

E = weld joint factor

t_m = minimum wall required

C = sum of allowances; corrosion, etc.

Now,

P = (1.1) working pressure = 11.0 MPA (1595 psi)

S = 89.3 MPA @ 400°C (12,950 psi @ 750°F)

Y = 0.4, E = 1

D_o = 1.91 cm (0.75 in.)

$C = 0.0762$ cm (0.03 in.)

$$t_m - C = \frac{11,000 \times 1.91}{2(89,284 + 11,000 \times 0.4)} = 0.112 \text{ cm } (0.044 \text{ in.})$$

$$t_m = 0.112 + 0.0762 = 0.188 \text{ cm } (0.074 \text{ in.})$$

A 1.91 cm O.D. by 1.47 cm I.D. (14 gauge, 3/4 in.) tubing is recommended.

HEAT TRANSFER CALCULATIONS

5. Inside Heat Transfer

For condensation inside horizontal tubes, the heat transfer coefficient $\bar{h}_i$ is given as

$$\bar{h}_i = F\left[\frac{\rho_f(\rho_f - \rho_g)\, g\, h_{fg}\, k_f^3}{D_i \mu_f (T_{gi} - T_w)}\right]^{1/4} \qquad \text{(E-1)}$$

(Ref. Handbook of H.T. by John G. Collier, McGraw Hill, 1972)

The factor F depends on the angle 2ϕ subtended from the tube center to the chord forming the liquid level (Figure E-1).

A mean value recommended for 2ϕ is 120 deg and corresponding F value is 0.557.

$F = 0$ @ $2\phi = 360$ deg

$F = 0.725$ @ $2\phi = 0$ deg

$F = 0.557$ (mean value recommended)

The fluid properties at 1450 psi and 592°F are given in Table E-1.

Then,

$$\bar{h}_i = 1520\,(D_i \cdot \Delta t_i)^{-0.25} \qquad \text{(E-2)}$$

where

$\Delta t_i = T_{gi} - T_{wi}$ (°F)

$\bar{h}_i$ is average heat transfer coeff. in B/hr-ft^2-°F

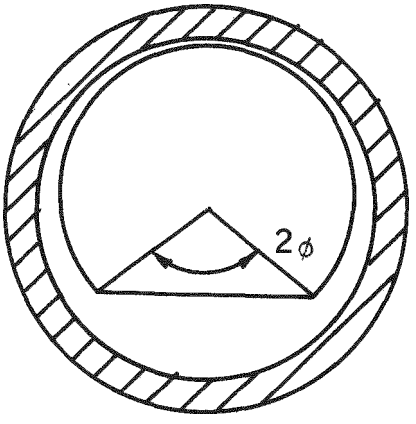

Figure E-1. Laminar Condensation Within a Horizontal Tube

Table E-1

Properties of Saturated Water and Steam at	1450psi / 592°F (10 MPa/311°C)	
Liquid Density, ρ_L	43.1 lb/ft^3	690 kg/m^3
Gas Density, ρ_g	3.46 lb/ft^3	55 kg/m^3
Liquid thermal conductivity, k_L	0.3046 B/hr-ft-°F	0.527 W/m-k°
Liquid viscosity, μ_L	0.225 lb/hr-ft	0.335 kg/m-hr
Evaporation enthalpy, h_{fg}	566 B/lb	1.316 x 10^6 j/kg
Acceleration due to gravity, g	4.18x10^8 ft/hr^2	1.27 x 10^8 m/hr^2

Table E-2

Properties of Molten Nacl-$NaNo_3$ - Na_2So_4 Eutectic		
Density, ρ	122 lb/ft^3	1960 kg/m^3
Coefficient of Expansion, β	2 x 10^{-4}/°F	1.1 x 10^{-4}/°C
Dynamic Viscosity (≈) μ	8.64 lb/hr-ft	12.86 kg/m-hr
Kinematic Viscosity, $v = \mu/\rho$	0.071 ft^2/hr	0.0066 m^2/hr
Thermal Conductivity, k (≈)	0.3 B/hr-ft °F	0.519 W/m-°K

Now, for SRE,

$$D_i = 0.0147 \text{ m } (0.0483 \text{ ft})$$

$$\boxed{h_i = 3242 \, (\Delta t_i)^{-0.25}} \qquad \text{(E-3)}$$

h_i in Btu/hr-ft^2-°F

6. Outside Heat Transfer

Outside the condenser pipe, heat transfer is by free convection in the molten salt. The heat transfer relation for free convection outside horizontal cylinder is

$$Nu = C \, (Gr_D \, Pr)^{0.25}, \quad Gr < 10^7 \qquad \text{(E-4)}$$

$$C = \left(\frac{2/\pi \cdot Pr}{2.435 + 4.884 \, Pr^{1/2} + 4.953 \, Pr} \right)^{0.25}$$

From the fluid properties (NaCl - $NaNO_3$-Na_2SO_4 eutectic) given in Table (E-2)

$$Pr = \frac{C_p \mu}{k} = 8.2$$

$$C = 0.55$$

$$Gr_D = \frac{D_o^3 B^2 g \, \Delta t_o}{\nu^2} = 1.67 \times 10^7 \, D_o^3 \, \Delta t_o$$

where

$$\Delta t_o = t_{wo} - t_{salt}, \ ^\circ F$$

$$Nu_D = \frac{h_o D_o}{k}$$

where h_o is the heat transfer coeff. based on bare tube.

We get,

$$h_o = 17.8 \left(\frac{\Delta t_o}{D_o} \right)^{0.25} \qquad \text{(E-5)}$$

For $D_o = 0.019$ m (0.75 in. or 0.0625 ft)

$$\boxed{h_o = 35.6 \, (\Delta t_o)^{0.25}} \qquad \text{(E-6)}$$

h_o in Btu/hr-ft^2-°F and Δt_o in °F

7. Pipe Wall Coefficient

Wall resistance based on inside area is given as

$$R_{wi} = \frac{X_w \, D_i}{k_w \, \bar{D}_L}$$

where

$$\bar{D}_L = \frac{D_o - D_i}{\ln \left(\frac{D_o}{D_i} \right)} = \frac{2X_w}{\ln \left(\frac{D_o}{D_i} \right)}$$

$$\therefore \text{Pipe wall coeff, } h_{w_i} = \frac{1}{R_{w_i}} = \frac{2kw}{D_i \ln \left(\frac{D_o}{D_i} \right)}$$

$$kw = 43.2 \ \frac{W}{m\text{-}°C} \left(25 \ \frac{B}{hr\text{-}ft\text{-}°F} \right) \text{ (for carbon steel)}$$

$D_o = 1.91$ cm (0.750 in. or 0.0625 ft)

$D_i = 1.47$ cm (0.580 in. or 0.0483 ft)

$$\therefore h_{wi} = 6963 \ \frac{W}{m\text{-}°K} \left(4025 \ \frac{B}{hr\text{-}ft\text{-}°F} \right)$$

8. Heat Rate Equation

Heat rate, q is given by

$$q = W h_{fg} = h_i \Delta_i \Delta t_i = h_o A_o' \Delta t_o = U_i A_i \Delta t_i$$

Consider,

$$W h_{fg} = h_i A_i \Delta t_i$$

Define the condensate loading factor as

$$\boxed{\Gamma = \frac{W}{L}} \qquad \text{(E-8)}$$

$$\Gamma h_{fg} = h_i \pi D_i \Delta t_i$$

$$\Gamma = h_i \frac{\pi D_i \cdot \Delta t_i}{h_{fg}}$$

Substituting h_i from Equation (E-2), we get

$$\Gamma = 1520 \cdot \frac{\pi D_i \Delta t_i}{h_{fg}} (D_i \Delta t_i)^{-0.25}$$

$$\Gamma = 8.44 (D_i \Delta t_i)^{0.73} \qquad \text{(E-9)}$$

For D_i = 1.47 cm (0.58 in, 0.0483 ft)

$$\boxed{\Gamma = 0.87 (\Delta t_i)^{0.75} \quad \frac{lb}{hr\text{-}ft}} \qquad \text{(E-10)}$$

Substituting for Δt_i in Equation (E-3)

$$\boxed{h_i = 3095 (\Gamma)^{-1/3} \quad \frac{B}{hr\text{-}ft^2\text{-}^\circ F}} \qquad \text{(E-11)}$$

CASE I

9. Same Heat Flux (q/A_i) in PP and SRE

$$\left(\frac{q}{A_i}\right)_{PP} = \left(\frac{q}{A_i}\right)_{SRE}$$

$$\left(\frac{q}{A_i}\right)_{PP} = 2.48 \times 10^4 \text{ watts/m}^2 \text{ or } 7870 \frac{B}{\text{hr-ft}^2} \quad \text{(Table 3-2)}$$

Now,

$$q = W\lambda = \Gamma L h_{fg} = h_i (\pi D_i L) \Delta t_i$$

and

$$\frac{q}{A_i} = \frac{\Gamma}{\pi D_i} \cdot h_{fg} = h_i \Delta t_i$$

$$\therefore \quad h_{fg} = 1315 \text{ K-J/kg} \quad (566 \text{ B/lb})$$

The same heat flux condition gives

$$\left(\frac{\Gamma}{D_i}\right)_{PP} = \left(\frac{\Gamma}{D_i}\right)_{SRE}$$

$$\Gamma = 1.56 \times 10^{-3} \text{ kg/sec-m} (3.78 \text{ lb/hr-ft}) \quad \text{(Table 3-2)}$$

$$\therefore \quad \Gamma_m = \Gamma \frac{D_{im}}{D_i}$$

$$= 1.56 \times 10^{-3} \times \frac{0.0147}{0.0264}$$

$$\Gamma_m = 8.52 \times 10^{-4} \text{ kg/sec-m} \quad (2.06 \text{ lb/hr-ft})$$

From Equation (E-11)

$$h_i = 3095\,(\Gamma)^{-1/3}$$

$$= 2415 \text{ B/hr-ft}^2\text{-}^\circ\text{F}$$

$$\text{or } 13,714 \text{ W/m}^2\,^\circ\text{C}$$

From Equation (E-10)

$$\Delta t_i = 1.81^\circ\text{C},\ 3.26^\circ\text{F}$$

Also,

$$q = h_o A_o \Delta t_o$$

and

$$\frac{q}{A_o} = \frac{q}{A_i} \cdot \frac{A_i}{A_o} = h_o \Delta t_o$$

$$= 7870 \times \frac{1}{4.1} = h_o \Delta t_o \quad \frac{\text{Btu}}{\text{hr-ft}^2}$$

Substituting for h_o from Equation (E-6), we get

$$35.6\,(\Delta t_o)^{1.25} = 1920$$

$$\Delta t_o = 24.3^\circ\text{F},\ (13.5^\circ\text{C})$$

and

$$h_o = 449 \ \frac{\text{W}}{\text{m}^2\,^\circ\text{C}} \quad \text{or} \quad 79 \ \frac{\text{Btu}}{\text{hr-ft}^2\text{-}^\circ\text{F}}$$

and

$$h_o' = h_o \ \frac{A_o'}{A_i} = 79 \times 4.1 = 324 \ \frac{\text{Btu}}{\text{hr-ft}^2\text{-}^\circ\text{F}}$$

$$= 1840 \ \frac{\text{W}}{\text{m}^2\text{-}^\circ\text{C}}$$

Assuming a fouling factor of 1500 for SRE,

$$h_{wdi} = \frac{1}{\frac{1}{1500} + \frac{1}{4025}} = 1090 \frac{B}{hr\text{-}ft^2\text{-}°F}, \quad 6190 \frac{W}{m^2\text{-}°C}$$

Then,

$$\Delta t_w = \frac{q/A_i}{h_{wdi}} = \frac{7870}{1090} = 7.2°F, \ 4°C$$

The overall $\Delta t = 3.26 + 24.3 + 7.2 = 34.8°F, \left(19.3°C\right)$.

Therefore, a lower pressure steam should be used. The steam temperature should be

$$T_{sat} = 549 + 34.8 \approx 584°F, \ 307°C$$

Changing the steam temperature changes its properties and hence h_i. Therefore, a trial and error calculation is needed to determine the condensate loading and other parameters. However, since the inside temperature drop is small, steam at 307°C (584°F) could be used.

At 584°F,

$$h_{fg} = 580 \text{ B/lb}$$

$$\therefore \quad \Gamma = \frac{7870 \times \pi D_i}{h_{fg}}$$

$$= 2.06 \frac{lb}{hr\text{-}ft}, \ 8.52 \times 10^{-4} \frac{kg}{sec\text{-}m}$$

This gives,

$$\Delta t_i = 3.2°F \ (1.8°C)$$

$$h_i = 2440 \frac{B}{hr\text{-}ft^2\text{-}°F}, \quad 13,856 \frac{W}{m^2\text{-}°C}$$

$$U_i = 226, \ 1283 \frac{W}{m^2\text{-}°C}$$

$$\text{Steam Rate/Serpentine} = \Gamma \times L = 2.06 \times 202 = 416 \frac{lb}{hr}, \left(187 \frac{kg}{hr}\right)$$

All the other parameters are listed in Table 3-2 (Section III).

CASE II

10. Same Heat Flux (q/A_o)

$$\left(\frac{q}{A_o}\right)_{PP} = \left(\frac{q}{A_o}\right)_{SRE}$$

$$\left(\frac{q}{A_o}\right)_{PP} = 2070 \frac{Btu}{hr\text{-}ft^2}, \left(6526 \frac{W}{m^2}\right)$$

Now,

$$\frac{q}{A_o} = h_o \Delta t_o$$

$$2070 = 35.6 (\Delta t_o)^{1.25}$$

$$\therefore \quad \Delta t_o = 26°F, 14.4°C$$

$$h_o = 80.2 \frac{Btu}{hr\text{-}ft^2\text{-}°F}, \quad 455 \frac{W}{m^2\text{-}°C}$$

and

$$h_o' = 329, \quad 1868 \frac{W}{m^2\text{-}°C}$$

$$\frac{q}{A_i} = \frac{q}{A_o} \cdot \frac{A_o}{A_i} = 2070 \times 4.1 = 8487 \frac{Btu}{hr\text{-}ft^2}, \quad 26,756 \frac{W}{m^2}$$

$$\frac{q}{A_i} = \frac{\Gamma h_{fg}}{\pi D_i}$$

Taking as a first approx. $T_{sat} = 592°F\ (311°C)$

$$h_{fg} = 566 \text{ Btu/lb } (1.32 \times 10^6 \text{ j/kg}$$

Then,

$$\Gamma = 2.28 \text{ lb/hr-ft}, \ 3.39 \text{ kg/hr-m}$$

which gives

$$\Delta t_i = \left(\frac{2.28}{0.87}\right)^{\frac{1}{0.75}} = 3.6°F, \ 2°C$$

and

$$\Delta t_w = \frac{8487}{1090} = 7.8°F, \ 4.3°C$$

and

$$\text{Overall } \Delta t = 26 + 3.6 + 7.8 = 37.4°F, \ 20.8°C$$

$$\therefore \quad T_{sat} = 549 + 37.4 = 586.4°F, \ 308°C$$

The steam temperature to be used to get same (q/A_o) is 586°F, 308°C. Making the corrections, we get

$$\Gamma = 2.22 \text{ lb/hr-ft}, \ 9.18 \times 10^{-4} \ \frac{\text{kg}}{\text{sec-m}}$$

$$\Delta t_i = 3.5°F$$

$$h_i = 2392 \ \frac{\text{Btu}}{\text{hr-ft}^2\text{-°F}}, \ 13,583 \ \frac{\text{W}}{\text{m}^2\text{-°C}}$$

$$U_i = 229 \ \frac{\text{Btu}}{\text{hr-ft}^2\text{-°F}}, \ 1300 \ \frac{\text{W}}{\text{m}^2\text{-°C}}$$

and

$$\text{Steam rate/serpentine} = 449 \ \frac{\text{lb}}{\text{hr}}, \ 204 \ \frac{\text{kg}}{\text{hr}}$$

Thus using the same steam temperature, heat flux conditions can be varied by adjusting the steam rate.

Yet another case would be to look at the same steam temperature as in the pilot plant.